NATIONAL ADVISORY COMMITTEE FOR AERONAUTICS

WARTIME REPORT

ORIGINALLY ISSUED
January 1944 as
Memorandum Report

TESTS OF THE NORTHROP MX-334 GLIDER AIRPLANE

IN THE NACA FULL-SCALE TUNNEL

By Gerald W. Brewer

Langley Memorial Aeronautical Laboratory
Langley Field, Va.

JPL LIBRARY
CALIFORNIA INSTITUTE OF TECHNOLOGY

NACA

WASHINGTON

L-620

MEMORANDUM REPORT

for the

Army Air Forces, Materiel Command

TESTS OF THE NORTHROP MX-334 GLIDER AIRPLANE

IN THE NACA FULL-SCALE TUNNEL

By Gerald W. Brewer

INTRODUCTION

Tests of the Northrop MX-334 airplane have been made in the NACA full-scale tunnel at the request of the Army Air Forces, Materiel Command. The results of this investigation are of particular interest since the MX-334 is an all-wing glider-type airplane having neither a conventional fuselage nor vertical surfaces.

The primary purpose of these tests was to obtain sufficient data with which to determine the longitudinal and lateral stability and control characteristics of the airplane. In addition to the stability and control study, this memorandum report contains the results of tests that were made to (1) determine a suitable wing-tip leading-edge slat arrangement which would improve the static longitudinal stability of the airplane as well as increase the maximum lift coefficient; (2) establish a value of the minimum drag coefficient for the basic wing and determine the additional drag caused by the leading-edge slats; (3) determine the effects on the directional stability characteristics of the airplane of the addition of vertical fins; (4) measure the effectiveness of the air-operated directional control system.

SYMBOLS

C_D drag coefficient (X/q_oS)

C_Y lateral-force coefficient (Y/q_oS)

b_a — aileron span (9.7 feet)

b_t — elevon tab span (2 feet)

$\overline{c}_e$ — root-mean-square elevator chord (0.833 foot)

$\overline{c}_a$ — root-mean-square aileron chord (0.833 foot)

$\overline{c}_t$ — root-mean-square tab chord (0.167 foot)

Q/V_o — relative air-flow quantity

Q — volume rate of air flow

$pb/2V$ — helix angle

p — rolling velocity, radians per second

V — indicated airspeed

F_e — elevator stick force

F_a — aileron stick force

Δp — difference in static pressure between the inside and outside of the rudder bellows

c_{d_o} — section profile-drag coefficient

H_o — free-stream total pressure

H_1 — total pressure in the field of the airfoil

y — vertical distance from the wake center

F — a correction factor, usually about 0.8 to 0.9

α — angle of attack of thrust axis, degrees

ψ — angle of yaw, degrees; positive when the right wing is retarded

δ_e — elevator deflection (with respect to the wing chord), degrees; positive when the trailing edge is deflected downward

δ_a — aileron deflection, degrees; positive when the trailing edge is deflected downward

given in figure 3. It was necessary to install addi-
tional seals at the hinges and at the inboard and out-
board ends of the elevons prior to the tests to obtain a
completely sealed control surface.

The inboard surfaces are the air-operated bellows
type and provide both dive braking and directional con-
trol. Each surface was divided into two parts to simplify
the structure at the joint between the wing and center
section. The mechanical linkage between these two sur-
faces is such that the upper and lower surfaces have
identical angular travel. Neither surface can be oper-
ated individually. The ducting for this system consists
of a passage from a leading-edge inlet through a venturi
section to a trailing-edge outlet and a second duct
leading from the venturi throat to the bellows. The
pressure and air flow for the bellows are regulated by
means of a butterfly control valve placed in the venturi
section.

METHODS AND TESTS

During preliminary tests of the airplane with the
slats removed the wing tips stalled at high angles of
attack. Due to the high sweepback of the wing this tip
stall caused a serious longitudinal instability. The
development was therefore undertaken of a leading-edge
slat configuration that would eliminate the inherent
longitudinal instability of the wing.

The three slat arrangements that were tested in-
clude (1) the original slat (fig. 4), (2) the original
slat moved closer to the wing leading-edge contour
(fig. 4), and (3) a large-span slat with the revised
slot. The original and the large-span slats extended
20 and 36.6 percent of the wing span, respectively
(figs. 1 and 5). Force and moment measurements were
made through a large range of angles of attack for the
basic wing and for the three slat configurations. To
supplement the force tests, tuft observations were made
to determine the stalling characteristics of the wing as
affected by these slat configurations.

In order to provide a check on the force-test re-
sults, the minimum drag of the airplane was also obtained
by measuring the loss of total pressure in the wake behind

RESULTS AND DISCUSSION

Aerodynamic Characteristics of the Airplane

Lift and pitching moments.- The lift and pitching-moment characteristics of the airplane, with the leading-edge wing slat removed and with the original and large-span slats installed, are given in figure 8. The results of tuft observations, which supplement the force test data, are shown in figures 9 and 10. The pitching-moment variation for the basic wing shows approximately neutral stability for lift coefficients up to the stall with the center of gravity located at 27.5 percent mean aerodynamic chord. At the stall the loss of lift at the wing tips increases the positive pitching-moment coefficient and causes serious longitudinal instability. It was evident that, before further investigation of the aerodynamic characteristics of the airplane were justified, improvement of the static longitudinal stability of the wing near the stall was necessary.

The most effective method for eliminating the instability appeared to be the control of the stalling pattern with suitable wing-tip slats and, accordingly, the three slat configurations previously described were tested. Each slat configuration progressively improved the stalling characteristics of the wing, as shown by the continuous decrease in wing-tip stall in the tuft surveys, and by the decrease in positive pitching moments at angles of attack near the stall in figure 8. The large-span slats with the revised slot retarded the flow breakdown at the tip section until after the center section had stalled, thus eliminating the cause of the instability. They also increased the maximum lift coefficient from a value of 1.15 to 1.26. The unstable pitching-moment variation at low lift coefficients for this condition is probably due to the interference effects of the slats on the air flow over the wing at low angles of attack.

Drag.- The drag data from these tests are presented in figure 11. The minimum drag coefficient for the basic wing was 0.0100. The original slats with the revised slot increased this value to 0.0118; the large-span slats with the revised slot, to 0.0146.

In order to determine the section drag coefficients and to check the minimum drag of the basic wing, wake

Static Longitudinal Stability and Control

<u>Elevator effectiveness</u>.- The results of tests made with the sealed elevons operated as elevators are given in figures 13 and 14 which show the variation of C_L, C_m, and C_{h_e} with elevator deflection. The data are presented for the basic wing and for the wing with the large-span slats installed. At low angles of attack the elevator effectiveness $dC_m/d\delta_e$, measured at $C_m = 0$, is -0.0047 with the slats removed and is -0.0041 with the large-span slats installed. Although $dC_m/d\delta_e$ is decreased at high lift coefficients for the slats-removed condition to -0.0034, the value of $dC_m/d\delta_e$ for the slats-installed condition remains unchanged. Similarly, the values of $dC_{h_e}/d\delta_e$, measured at $C_{h_e} = 0$, are lower at low lift coefficients and higher at high lift coefficients with the slats installed than with the slats removed. For the slats-removed condition $dC_{h_e}/d\delta_e$ is -0.0055 at a C_L of 0.34 and -0.0035 at a C_L of 0.90; with the slats installed, $dC_{h_e}/d\delta_e$ is -0.0050 at a C_L of 0.33 and -0.0043 at a C_L of 0.92.

In order to compare the stick-fixed longitudinal stability of the airplane with and without slats, curves showing the variation of elevator deflections for trim with lift coefficient have been obtained from the test results and are given in figure 15. With the slats removed, the airplane is unstable from a C_L of 0.1 to 0.4 and is neutrally stable from a C_L of 0.4 to 0.9. At higher lift coefficients there is a large degree of instability since increases of down-elevator deflections are required to reduce the forward speed of the airplane. With the large-span slats installed, however, the airplane is stable at all lift coefficients above 0.6 but is approximately neutrally stable at lower lift coefficients.

A criterion for satisfactory stability requires a stable stick-free pitching-moment variation. The results in figure 16 show that the airplane with slats removed is very unstable, stick free. With the airplane trimmed at the same lift coefficient, it is shown that the large-span slats decreased this instability slightly and that the large positive pitching-moment variation at high lift coefficients was reduced.

Tab effectiveness.- The results of elevator effectiveness tests made for tab deflections of ±10° and ±20° with the large-span slats installed are given in figure 21. These curves show the variation of C_L, C_m, and C_{h_e} with δ_e for three angles of attack. The values of $dC_m/d\delta_e$ and $dC_{h_e}/d\delta_e$ are both approximately -0.0040 for the range of lift coefficients and tab deflections tested.

The longitudinal stability and control characteristics of the airplane with the tab deflected are compared with the results of the preceding section for the zero tab setting in figures 22 to 25. For the range of lift coefficients tested, the variation of elevator deflection for trim with lift coefficient (fig. 22) is stable for tab deflections of 10° and ±20°. The variation of δ_e for trim with C_L with the tab deflected -10° is approximately the same as that with the tab neutral.

The instability of the airplane, stick free, is generally the same with the tab deflected as with the tab neutral (fig. 23). At the larger positive tab deflection and at high angles of attack the instability increases, probably on account of tab stalling.

It is shown in figure 24 that the elevator with the tab deflected -10° floats about 1° more nose up at a C_L of 0.3 and 3° more at a C_L of 1.2 than with the tab neutral. Above a lift coefficient of 0.6 the nose-up floating angle is less with the tab deflected -20° than for a deflection of -10°. Deflecting the tab 10° and 20° progressively decreased the nose-up floating angle of the elevator.

The curve of elevator stick force for trim against indicated airspeed at sea level (fig. 25) shows that the airplane is trimmed at approximately the same speed, 100 miles per hour, for either -10° or -20° tab settings. For these trim tab settings, however, the airplane is unstable inasmuch as pull forces are required at speeds above the trim speed and push forces below the trim speed.

Although the airplane can be trimmed for zero stick force, it will be unstable for this condition. Also, the stick-free longitudinal instability is decreased very little with the tab deflected. This tab is ineffective at large tab deflections.

Lateral Stability and Control

<u>Aerodynamic characteristics in yaw</u>.- The results of tests made with the airplane yawed $0°$, $2.9°$, $5.6°$, $9.5°$, $14.5°$, and $18.6°$ are presented in figures 33 to 35. The data include the variations of C_l, C_n, C_Y, and C_{h_a} with total aileron deflection for four angles of attack at each angle of yaw. The variations of C_l, C_n, and C_Y with ψ, which were obtained by cross-plotting the original data at zero aileron deflection, are shown in figure 36.

As shown by the low value of $dC_l/d\psi$ at an angle of attack of $3.3°$, the airplane will have practically no effective dihedral in the low angle-of-attack range. It is important to note that $dC_l/d\psi$ increases rapidly with increasing lift coefficient. At an angle of attack of $16.9°$, for example, $dC_l/d\psi$ is approximately 0.0016, which corresponds to an effective dihedral angle of about $8°$. This large increase in effective dihedral with lift coefficient is attributed to the large angle of sweepback of the wing.

The airplane will have almost no weathercock stability at low angles of attack as shown by the small value of $dC_n/d\psi$ (-0.0002) at an angle of attack of $3.3°$. As was the case for the dihedral effect, the weathercock stability increases rapidly with increases in lift coefficient. At an angle of attack of $16.9°$, $dC_n/d\psi$ is approximately -0.0010 per degree.

The variation of lateral-force coefficient with ψ is also very small at low angles of attack. The value of $dC_Y/d\psi$ shows a stable variation for angles of attack below the stall up to a yaw angle of $15°$ where the values of $dC_Y/d\psi$ begin to reverse sign with further increases of ψ. At the stall, there is a reversal in the side force from positive to negative at $\psi = 7°$.

The variation of lift coefficient and pitching-moment coefficient with angle of yaw is shown in figure 37 for four angles of attack. The changes in pitching-moment coefficient with angles of yaw are small and somewhat irregular. The decrease of lift coefficient with angle of yaw was small for the range of yaw angles tested.

change of C_l with $pb/2V$ and is dependent only upon the geometric characteristics of the airplane. The variation of helix angle with total aileron deflection for the two airplane conditions is shown in figure 41. Extrapolation of these results shows that for the maximum aileron deflection of 24° the value of $pb/2V$ is about 0.055 at 248 miles per hour and 0.070 at 70 miles per hour, slats installed, and is approximately 0.065 at 229 miles per hour and 0.068 at 72 miles per hour, slats removed. These values have been calculated from wind-tunnel data, but it should be noted at this point that in flight the adverse yaw at low speeds and the effects of compressibility and wing twist at high speeds would probably lower these values by about 20 percent.

Aileron stick forces for the required $pb/2V$ have been computed for different aileron deflections and flight speeds, and the results are given in figure 42. The forces were obtained from the relation

$$F_a = \frac{q b_a \bar{c}_a^{\,2}}{57.3}\left[-\frac{d\delta_{a_u}}{dx}\left(C_{h_{a_u}} + \frac{dC_{h_{a_u}}}{d\alpha}\,\Delta\alpha\right) - \frac{d\delta_{a_d}}{dx}\left(C_{h_{a_d}} - \frac{dC_{h_{a_d}}}{d\alpha}\,\Delta\alpha\right)\right]$$

where $C_{h_{a_u}}$ and $C_{h_{a_d}}$ are the aileron hinge-moment coefficients for a given up and down aileron deflection, respectively, and $d\delta_{a_u}/dx$ and $d\delta_{a_d}/dx$ are the variation of aileron deflection with stick travel obtained from figure 43. The value $\Delta\alpha$ is the change in effective angle of attack of the down-going wing.

The aileron-control-force variation with aileron deflection shows no reversal of forces and an increase in force with increased aileron deflection. The force for maximum aileron deflection is about 75 pounds at 248 miles per hour with slats installed and 90 pounds at 229 miles per hour, slats removed. Forces of this magnitude will be excessive for a wheel-type control operated from a prone position. At landing speed, the control force is of the order of 3 pounds for maximum aileron deflection.

by (1) reducing the sweepback of the leading-edge inlet to zero degrees and by (2) providing an initial negative angle of attack of about 14° at the face of the inlet (fig. 7).

Results similar to that obtained for the original inlet were obtained for the modified inlet except that greater rudder deflections were obtained and the tendency to stall at the inlet was delayed several degrees (fig. 46). The measurements made to estimate the quantity of air flow through the duct system (fig. 47) show similar characteristics of the effectiveness of the two inlets. Air flowed out of the system at an angle of attack of 15° for the original inlet and at 24° for the modified inlet. In both cases the available quantity decreased rapidly with change in angle of attack from the high-speed attitude.

The variation of deflection of the inboard and outboard sections of the rudder is caused by an uneven distribution of pressure in the two sections of the rudder as shown by the variations of the pressure differential across the bellows with angle of attack in figure 48. The effectiveness of the butterfly valve is shown in figure 49 for each inlet type. It is important to note that the rate of change of valve position with rudder deflection varies considerably and that the valve is most sensitive when about one-half closed. Paralleling the results in the previous figures, it is shown that, when the inlet is stalled, the full range of valve setting will not change the rudder deflection.

The over-all efficiency of the bellows and duct system was determined by measuring the time lag for maximum surface deflection with instantaneous full-rudder control. The minimum time interval for the best condition was about 4 seconds. Since the inlet and duct system do not provide adequate quantity of air flow through the ducts and pressure within the bellows and since the control-valve operation was not effective, the directional control system such as tested in this model is very unsatisfactory.

SUMMARY OF RESULTS

1. At the design center-of-gravity location of 27.5 percent mean aerodynamic chord, the airplane with

10. The method for obtaining directional control is entirely inadequate. The yawing moment developed by maximum rudder deflection will not be sufficient to trim out the total adverse yaw resulting from maximum aileron deflection.

11. If the present directional control system is to be used, the design of the duct system must be revised to obtain satisfactory performance. Modifications to the inlets, the ducting, and the butterfly control valve are required, and, if possible, the control surfaces should not be sectioned.

Langley Memorial Aeronautical Laboratory,
National Advisory Committee for Aeronautics,
Langley Field, Va., January 15, 1944.

TABLE I

EFFECT OF SLATS AND FINS ON THE AERODYNAMIC CHARACTERISTICS OF THE MX-334 AIRPLANE YAWED AT 5.6° AND 18.6°

ψ, deg / α, deg	5.6°				18.6°				Slats	Fins
	3.3	10.6	16.9	21.6	3.3	10.6	16.9	21.6		
C_l	-------	-------	-------	-------	0.0080	0.0200	0.0340	1.0700	Off	Off
	0.0008	0.0002	0.0010	0.0010	.0078	.0180	.0350	.0520	On	Off
	.0015	.0035	.0050	.0065	.0065	.0173	.0258	.0360	On	Full chord
	-------	-------	-------	-------	.0075	.0280	.0450	.0560	On	Half chord
C_n	-------	-------	-------	-------	-0.0023	-0.0068	-0.0146	-0.0075	Off	Off
	-0.0003	-0.0010	-0.0050	-0.0075	-.0027	-.0068	-.0160	-.0230	On	Off
	-.0005	-.0018	-.0035	-.0063	-.0002	-.0050	-.0130	-.0200	On	Full chord
	-------	-------	-------	-------	-.0040	-.0080	-.0160	-.0235	On	Half chord
C_Y	-------	-------	-------	-------	0.0038	-0.0010	-0.0060	-0.0450	Off	Off
	0.0005	0.0015	0.0005	0.0062	.0052	.0027	-.0027	-.0173	On	Off
	.0095	.0095	.0095	.0045	.0460	.0415	.0380	.0360	On	Full chord
	-------	-------	-------	-------	.0500	.0430	.0330	.0220	On	Half chord
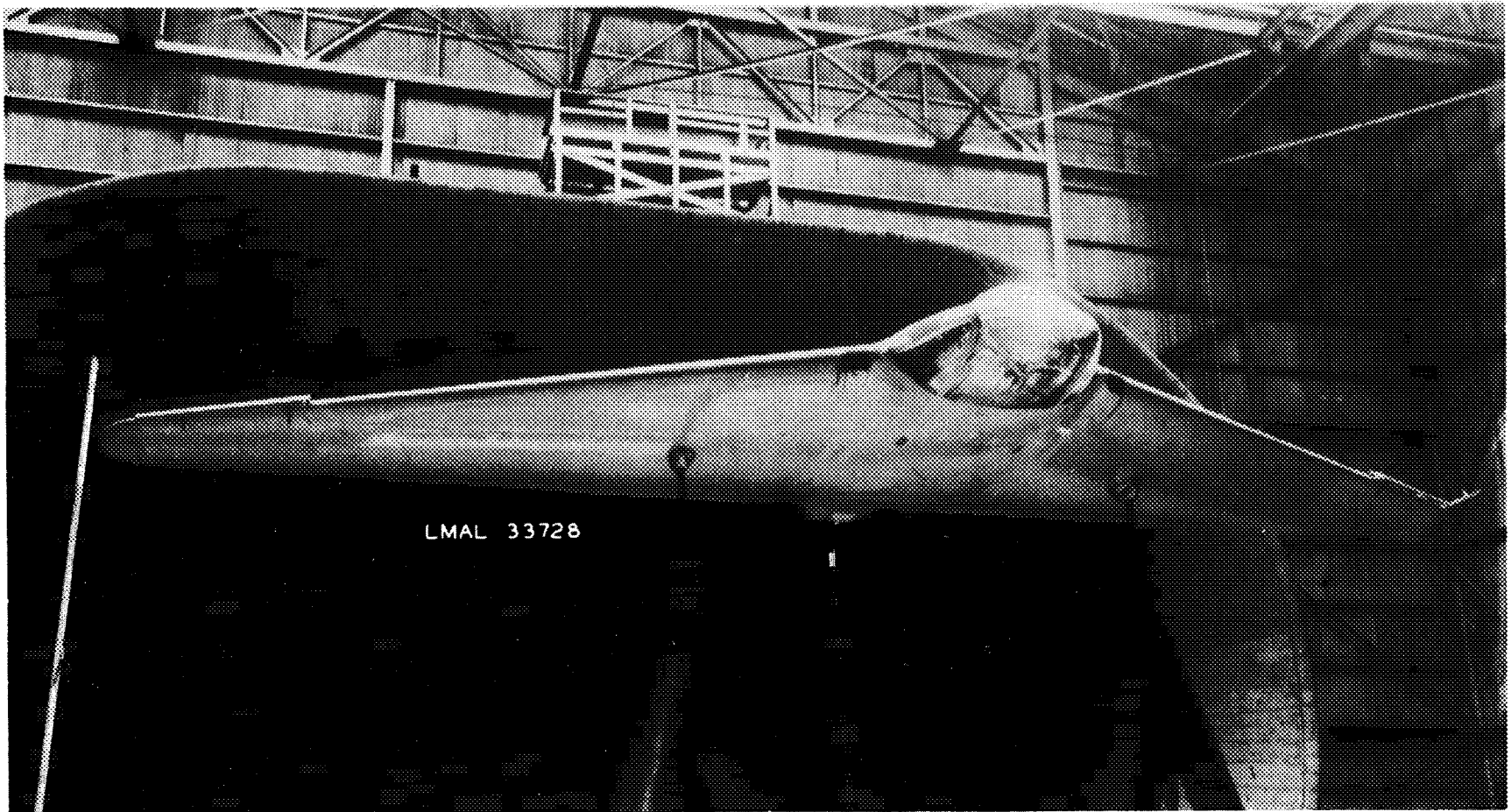
(a) Three-quarter front view.

Figure 1.- The MX-334 airplane mounted for tests in the NACA full-scale tunnel.
Original slats installed.

(b) Rear View.

Figure 1.- Concluded.

36'

$14\frac{1}{4}'$
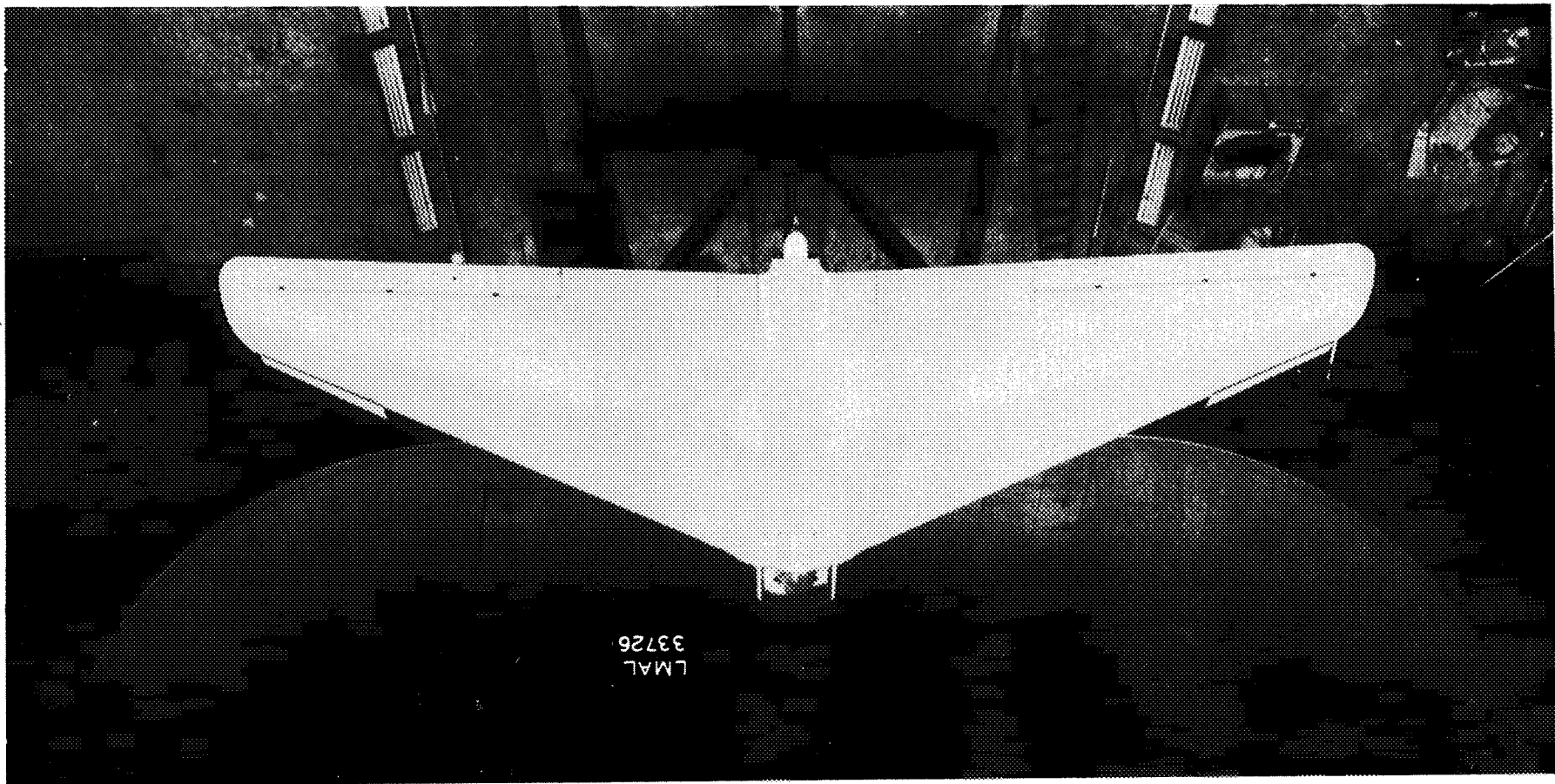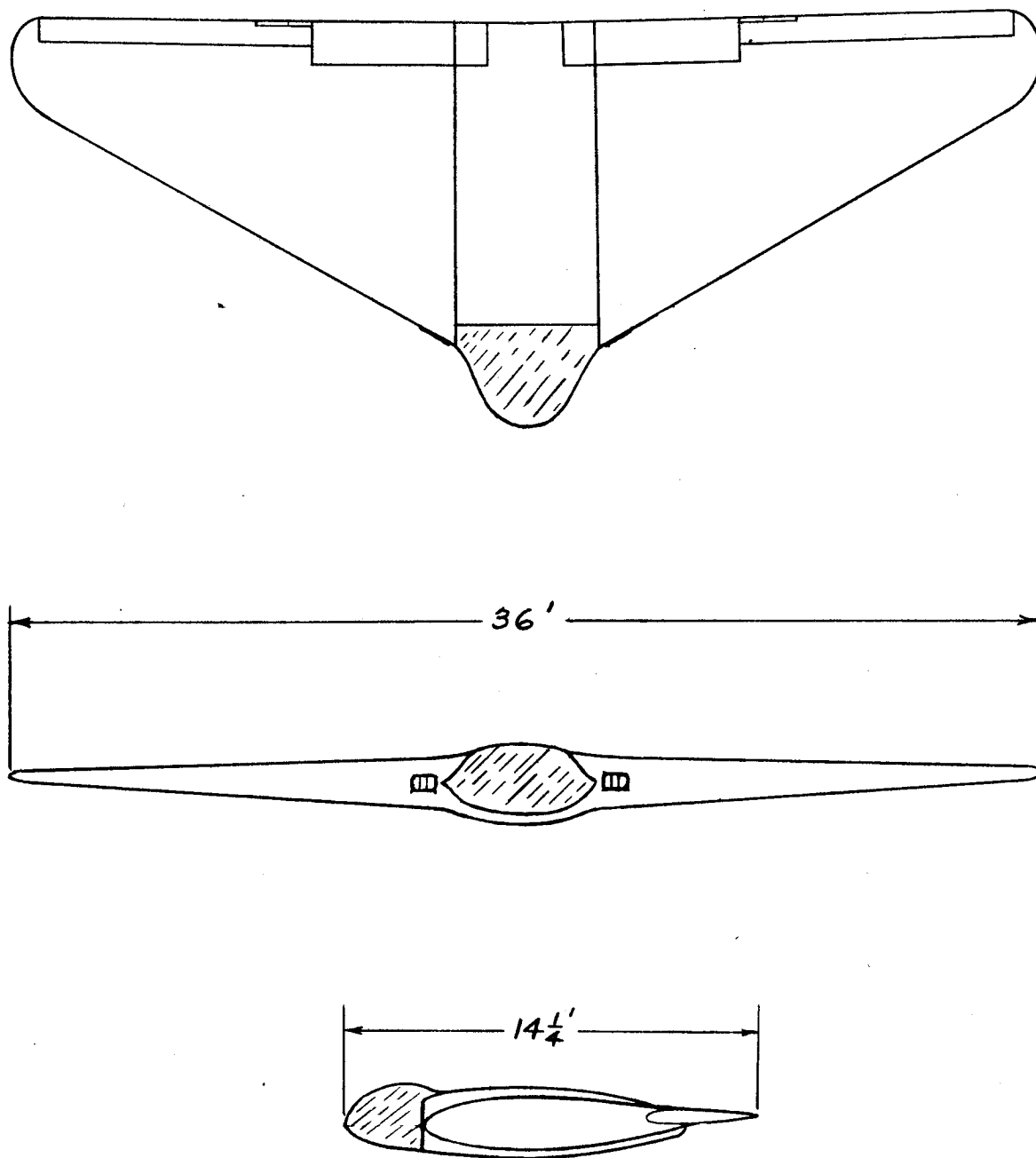
Figure 2 .— Three-view drawing of the MX-334 airplane.
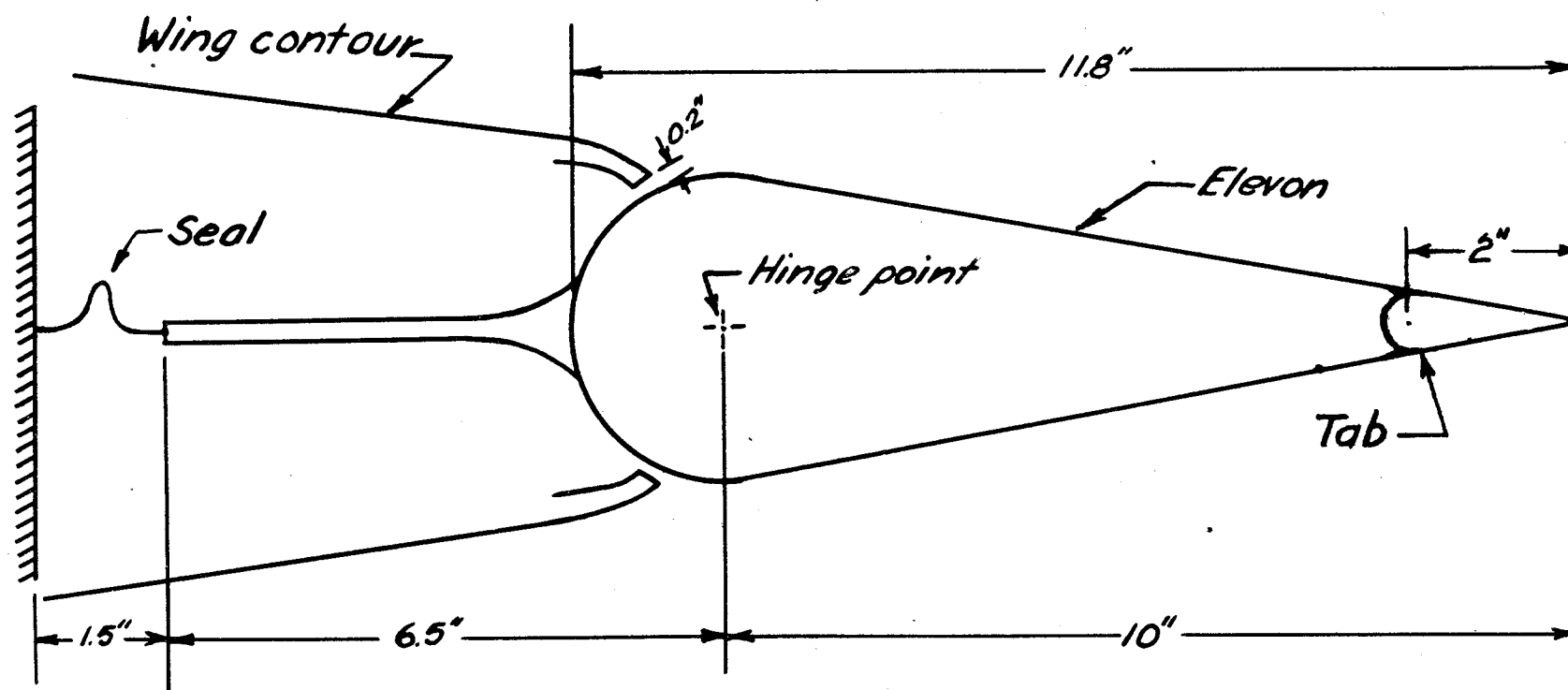
Figure 3: Diagram of internal balance for the elevon of the MX-334 airplane.
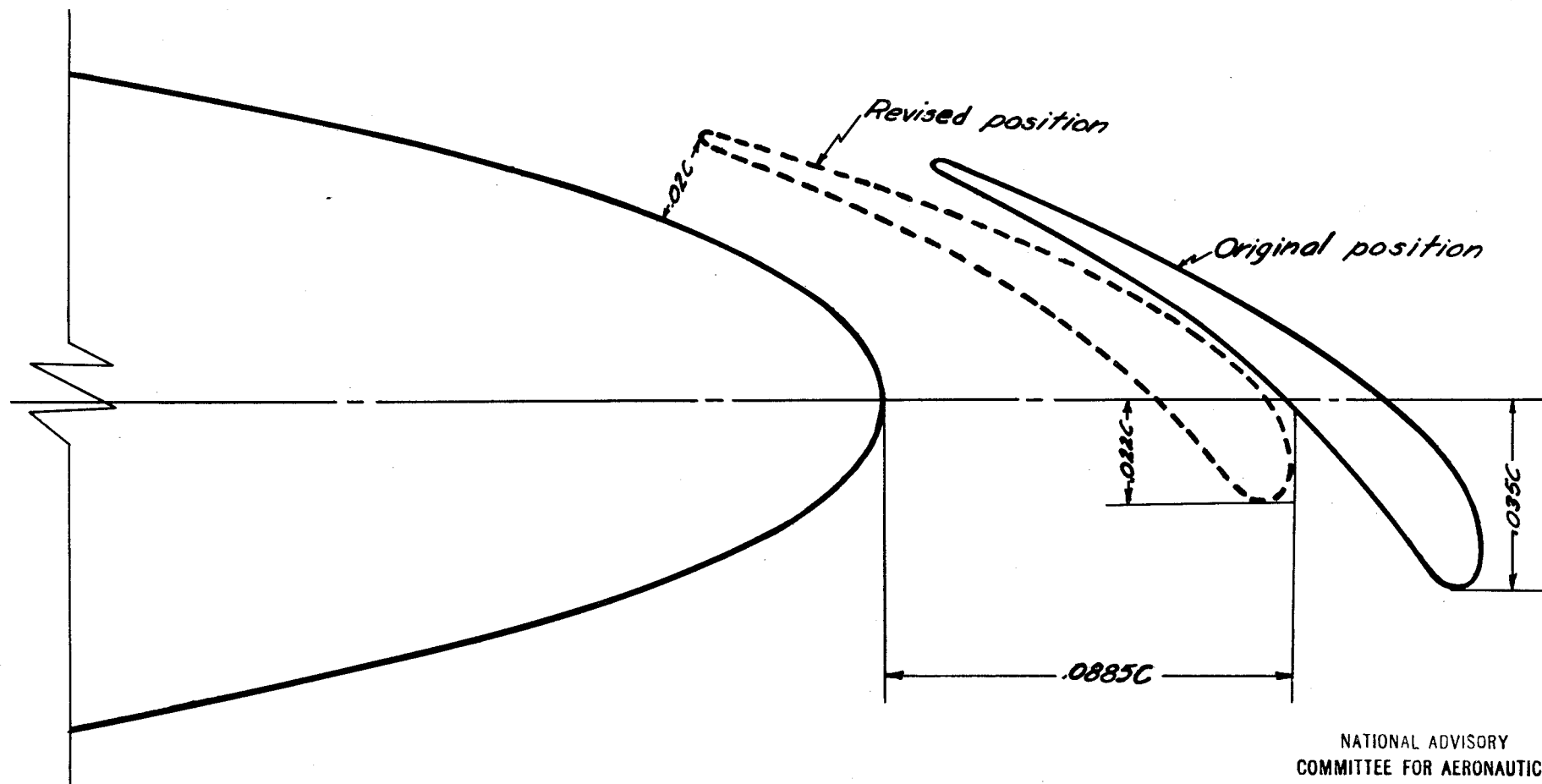
Figure 4.- Final slot configuration for MX-334 glider section at the outboard support station.
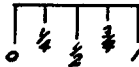
Revised position

Original position

.020c

.022c

.035c

.0885C

Scale

0 ¼ ½ ¾ 1
one inch

8′

4′

Full chord type

Half chord type

1′

2′

CG
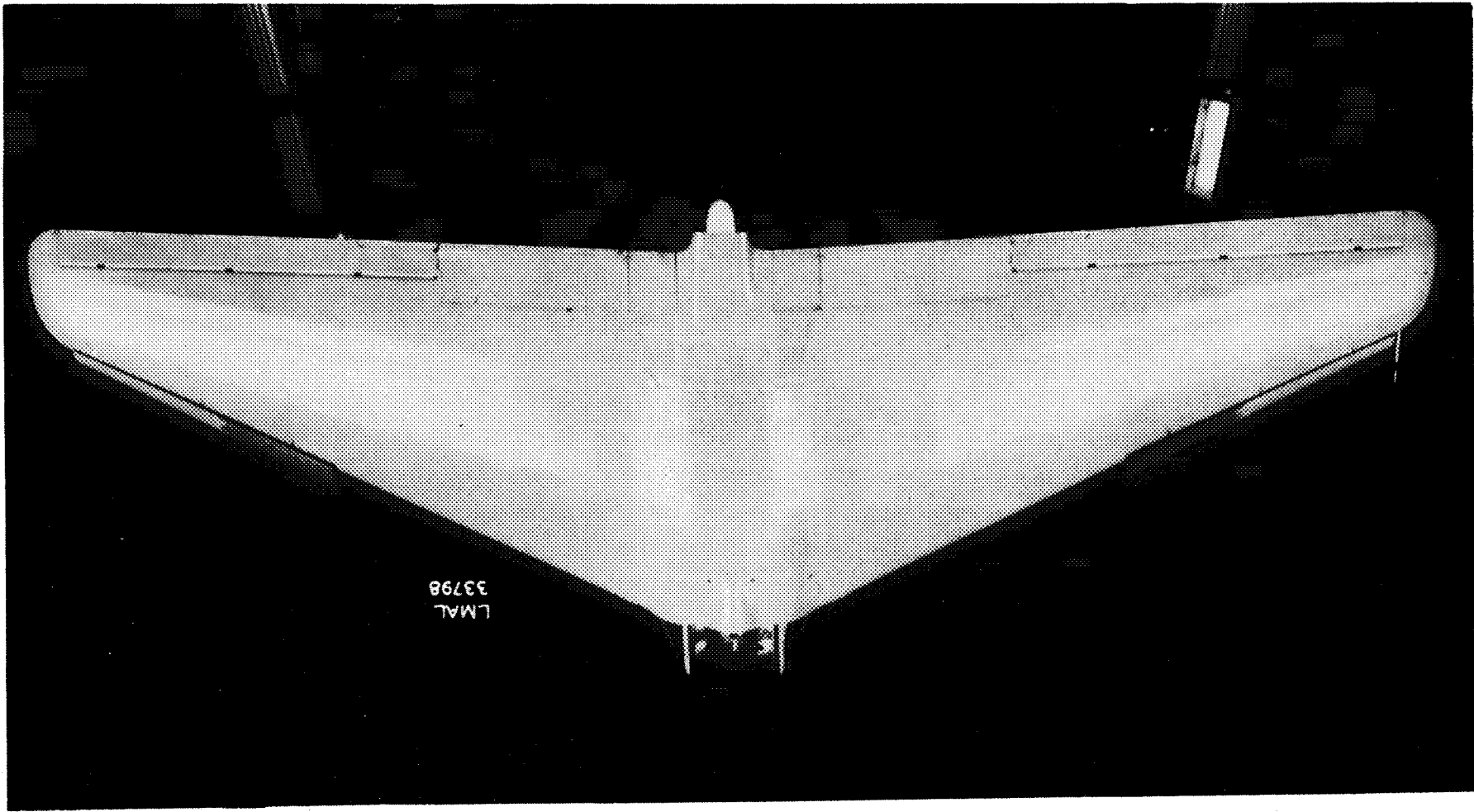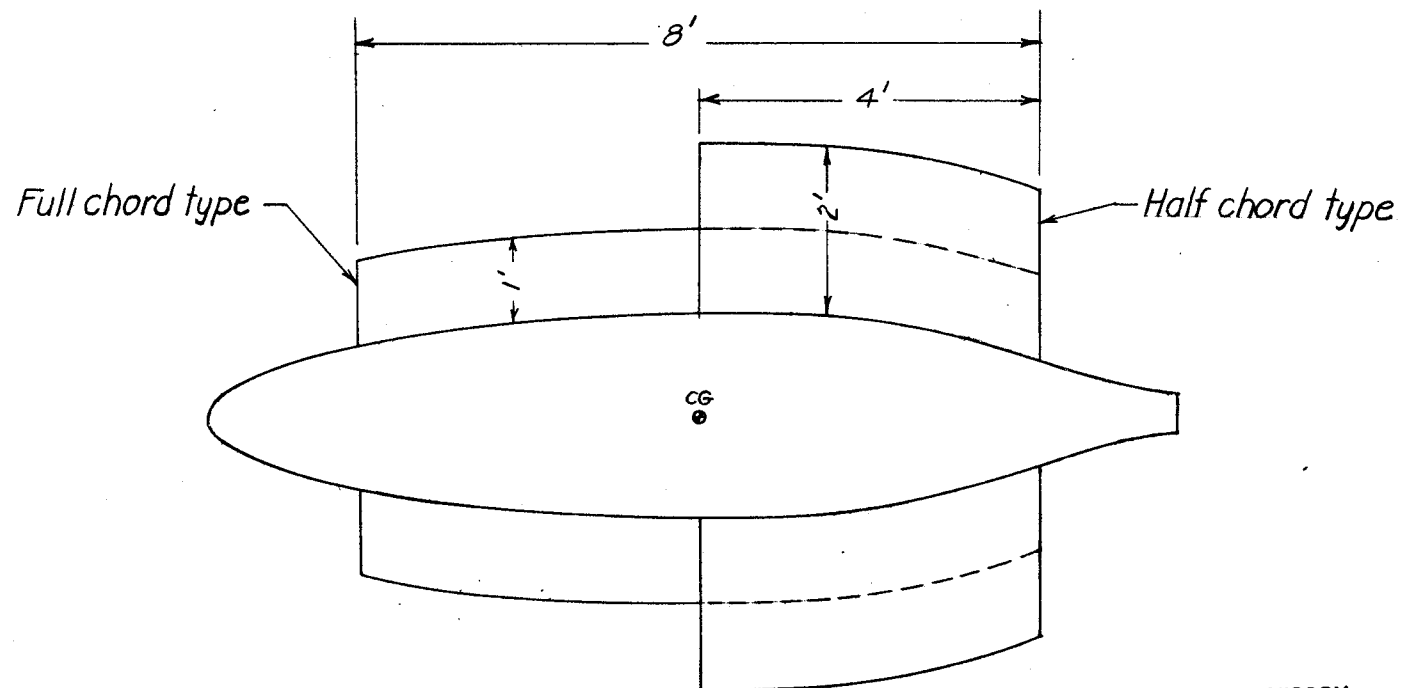
Section at center line of the airplane

Figure 6.- Arrangement of fins on the MX-334 airplane.

Revised inlet face

Airflow Direction

28°

Fairing

Original inlet face

Wing leading edge

Horizontal section through the wing chord line

Original inlet face

14°

Revised inlet face

Vertical section of the duct inlet
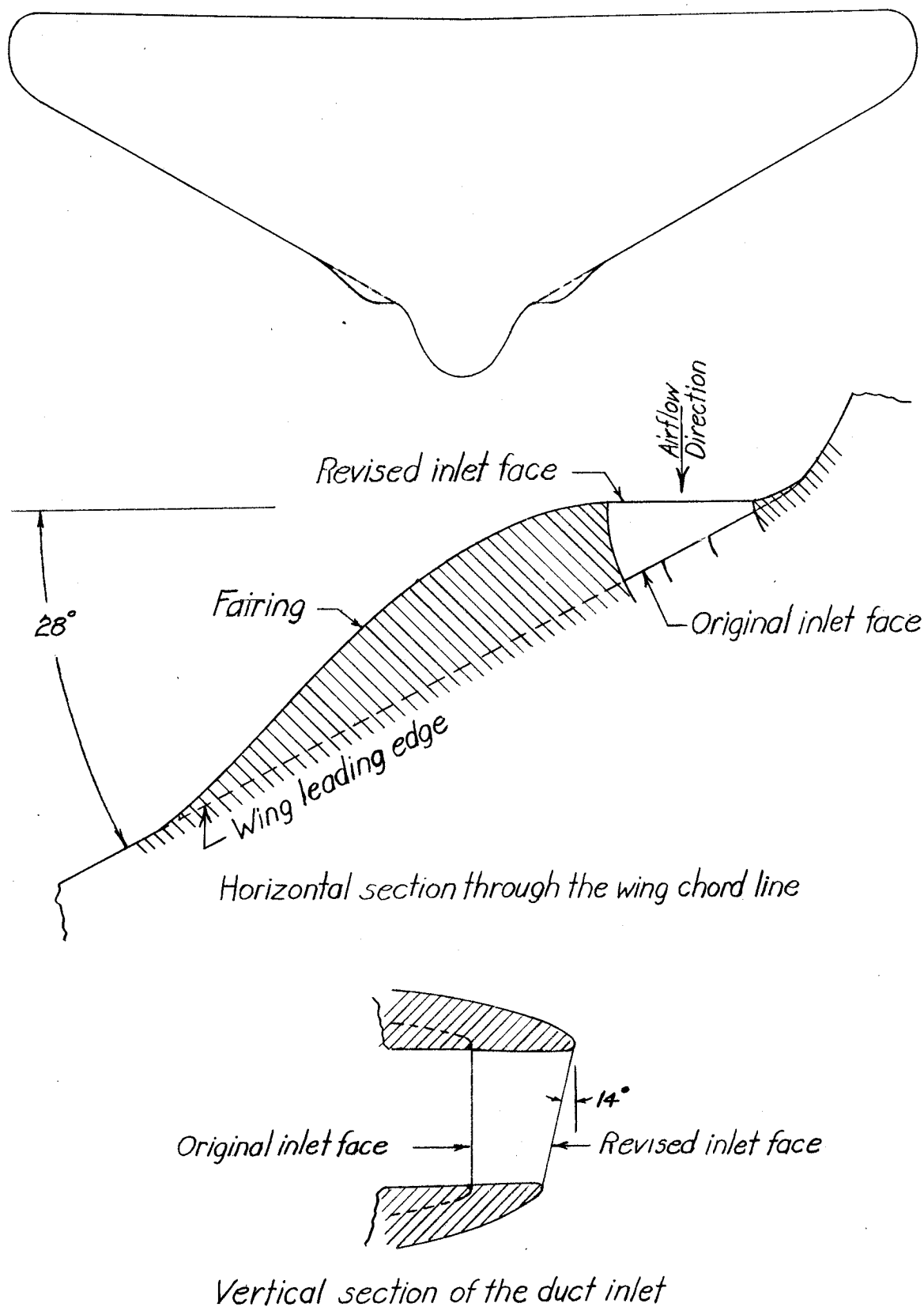
Figure 7.- Inlet modification for the MX-334 airplane.

Lift coefficient, C_L

NATIONAL ADVISORY
COMMITTEE FOR AERONAUTICS

Angle of attack α, deg

Pitching-moment coefficient, C_m

○ Slots removed
+ Original slots, raised slot
× Large-span slots, raised slot
● Original slot

C_m

L-628

$\alpha, 10.5°$

$\alpha, 10.5°$

$\alpha, 17.9°$

$\alpha, 18.7°$

$\alpha, 19.8°$

$\alpha, 20.5°$

$\alpha, 21.6°$

$\alpha, 21.6°$

$\alpha, 23.8°$

$\alpha, 23.8°$
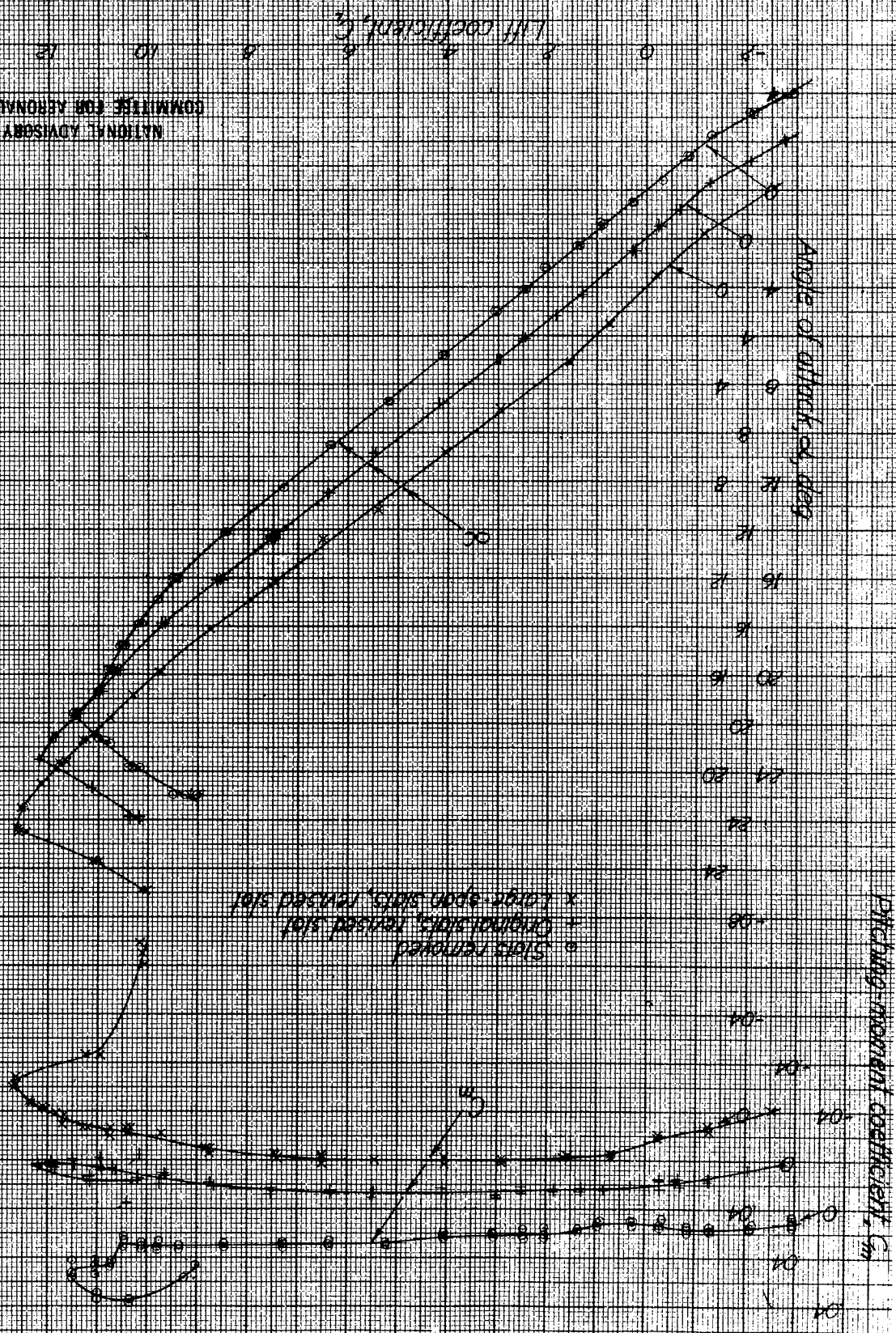
⬡ Disturbed flow
⬡ Stall
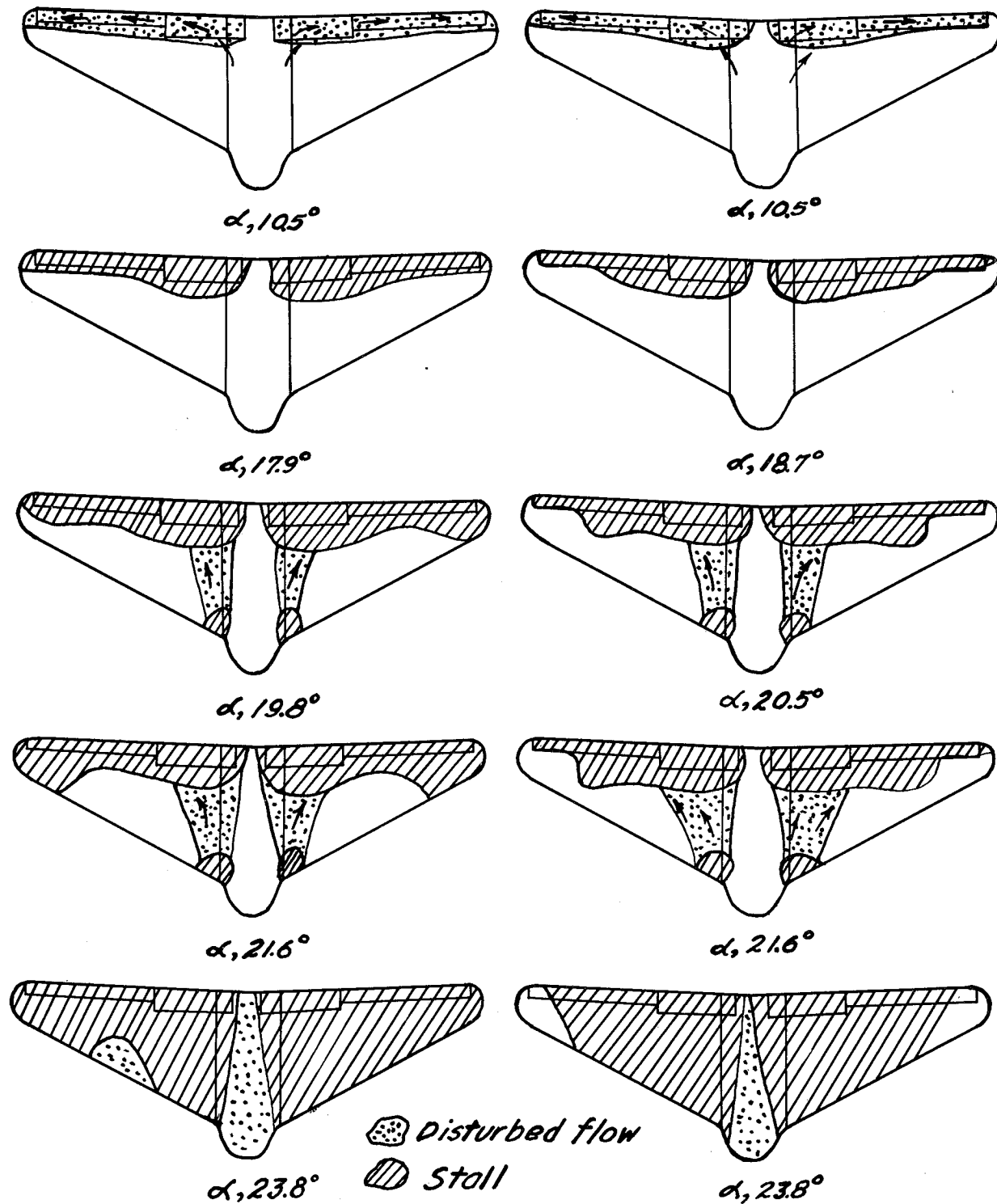
(a) Slots removed

(b) Original slots

Figure 9.-Flow characteristics over the MX-334
glider airplane; V, approximately 63 mph.

L-628
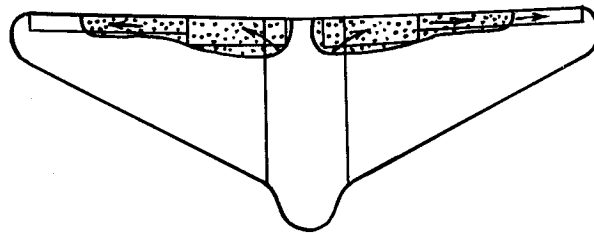
$\alpha, 10.5°$
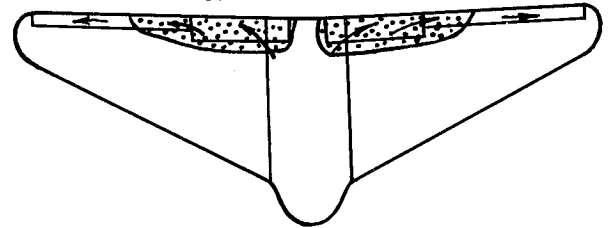
$\alpha, 10.4°$
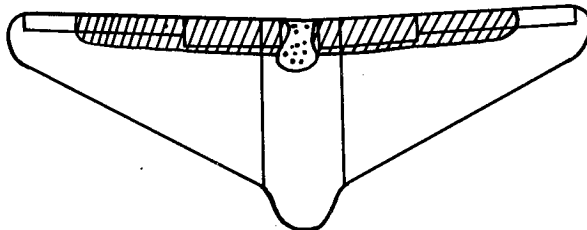
$\alpha, 18.7°$

$\alpha, 18.7°$

$\alpha, 20.6°$

$\alpha, 20.5°$

$\alpha, 21.5°$

$\alpha, 22.5°$
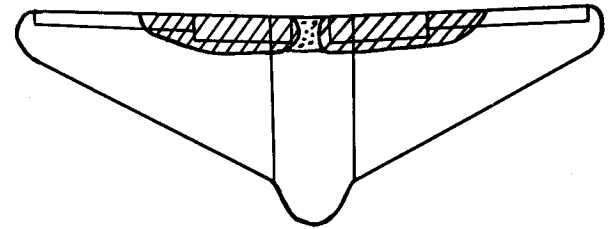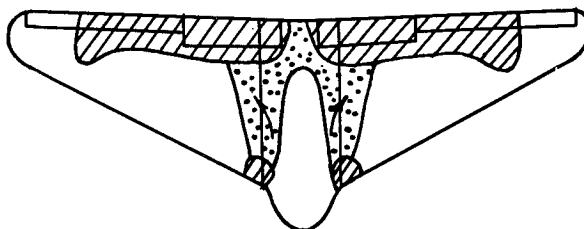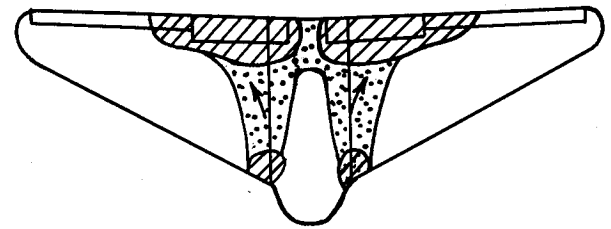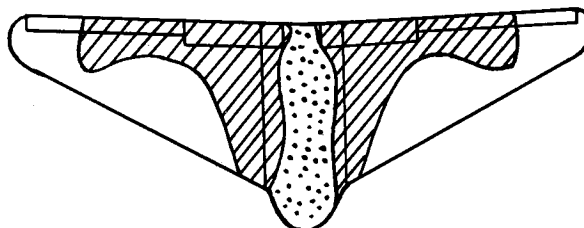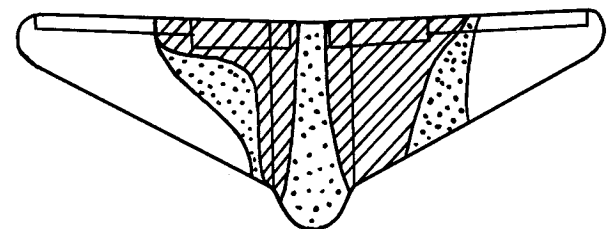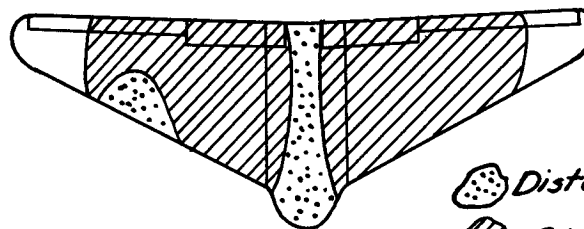
Disturbed flow

Stall

$\alpha, 23.9°$
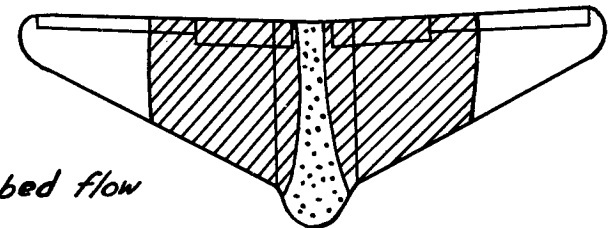
$\alpha, 23.7°$

(a) Original slats
     Revised slots

(b) Large-span slats
     Revised slots

Figure 10.-Flow characteristics over the MX-334 glider
airplane, V, approximately 63 mph.

Spanwise station, in.

Right

Left

240   200   160   120   80   40   0   40   80   120   160   200   240

2

4

6

8

10

12

14

16

$c_{d_0}c$ (in.)

Drag of support strut
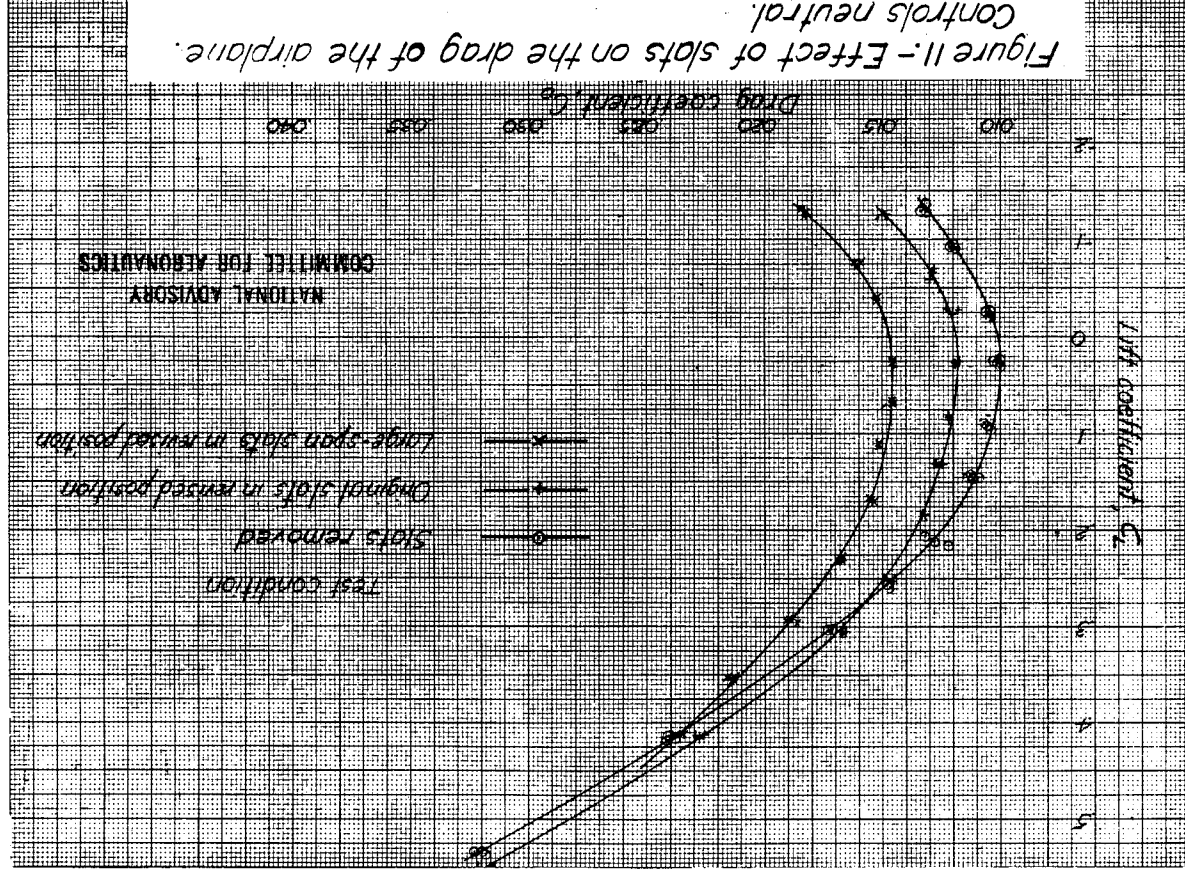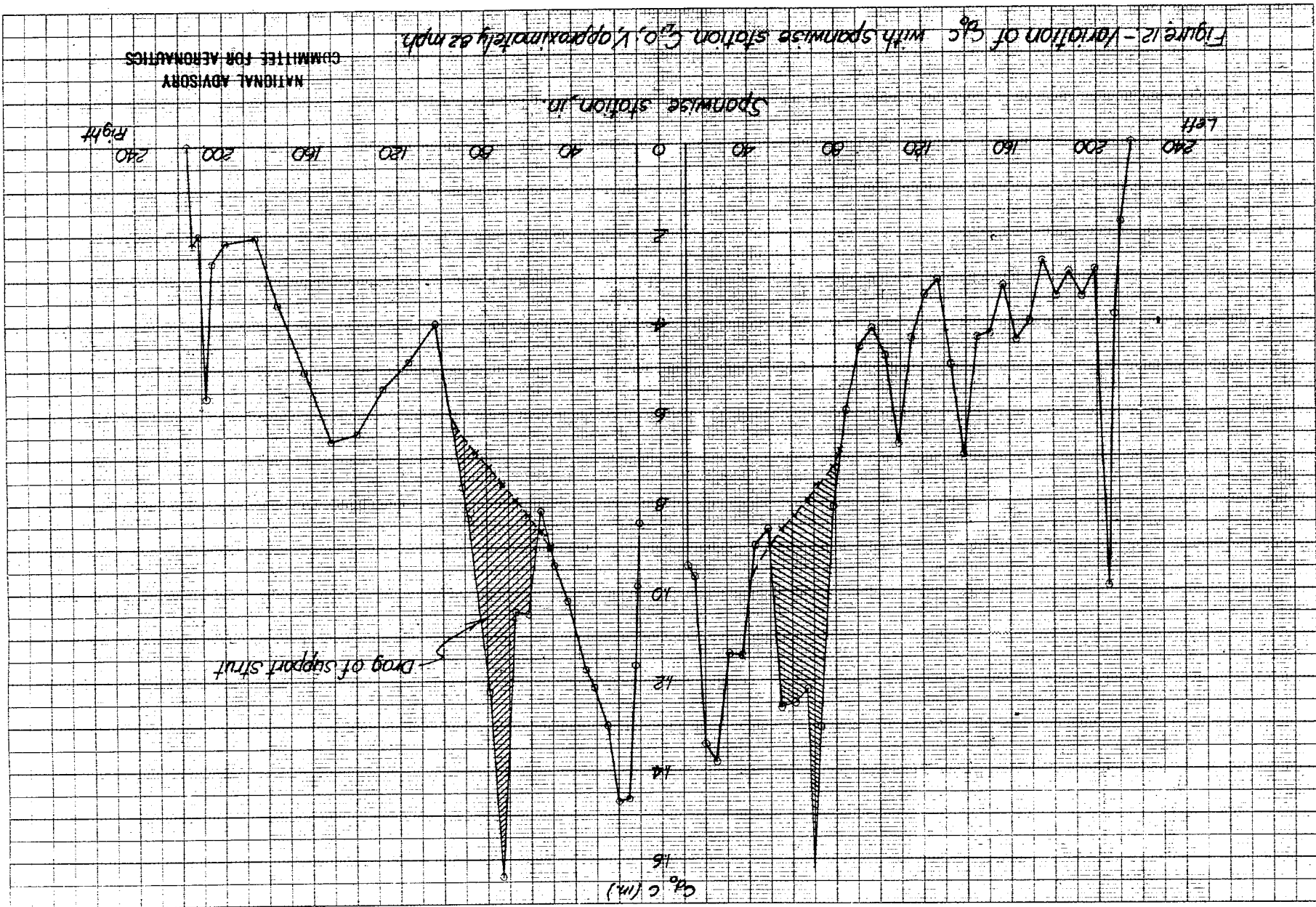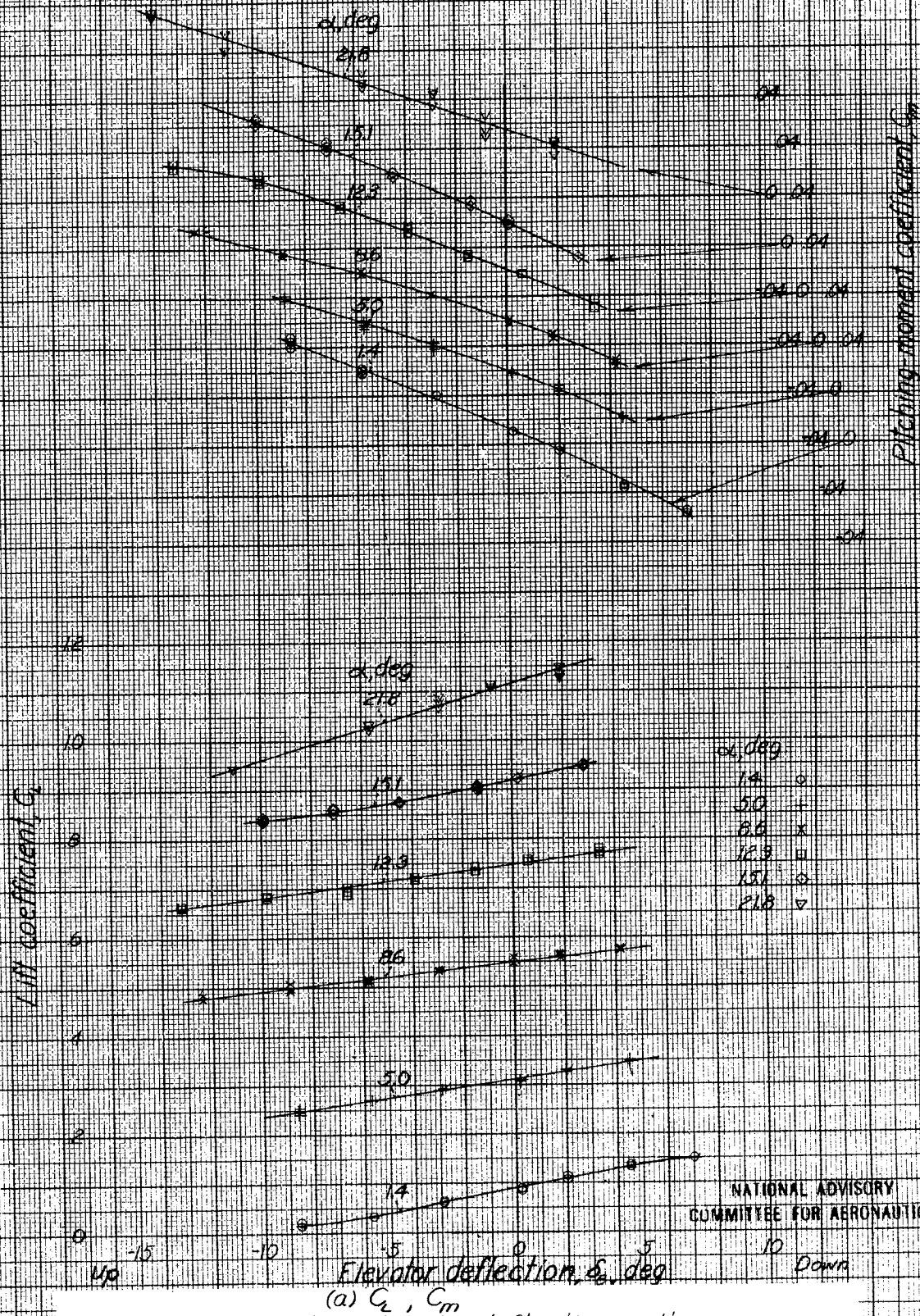
Figure 13.- Effect of elevator deflection on the aero-
dynamic characteristics of the airplane. Slots
removed; elevon sealed; tab neutral.
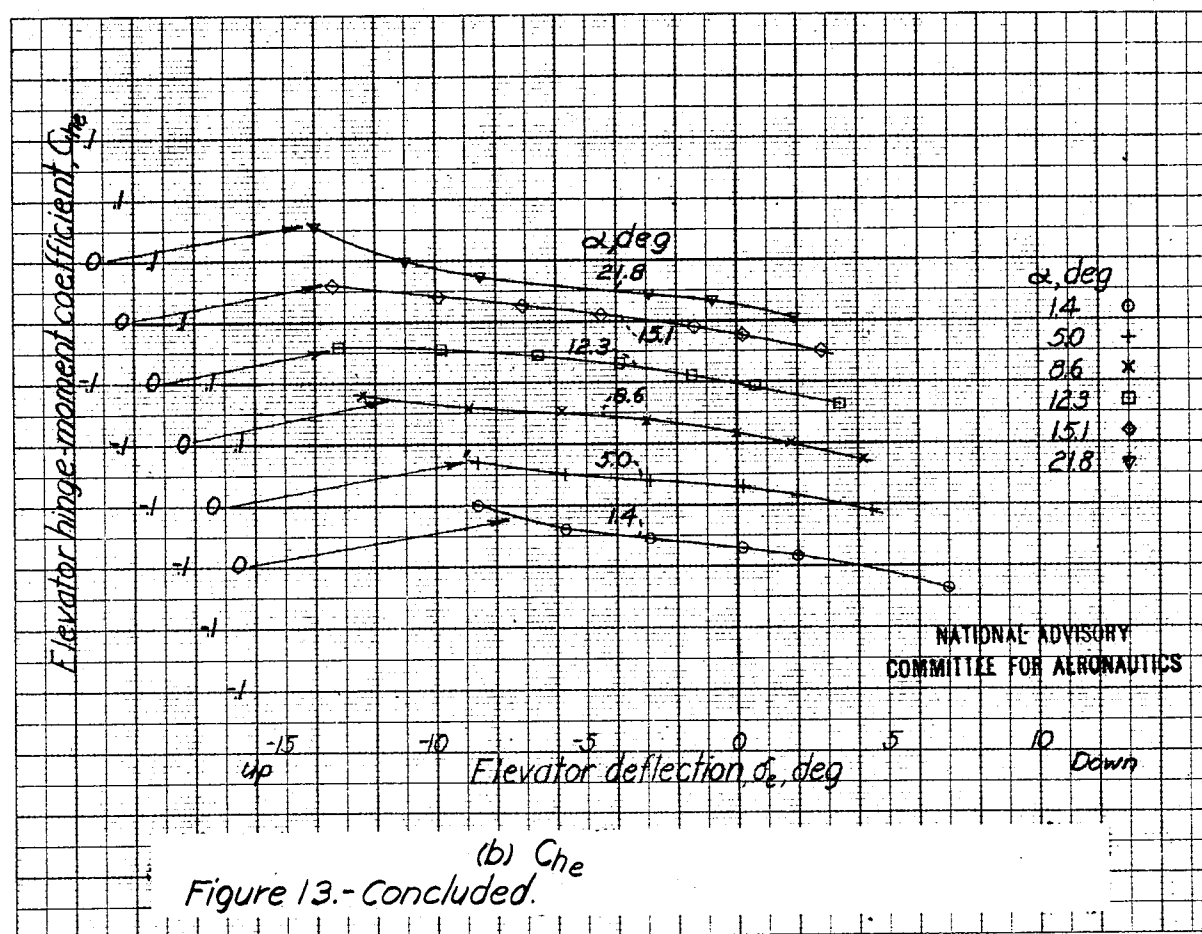
(b) C_{h_e}

Figure 13.- Concluded.

(b) C_{h_e}

Figure 14.- Concluded.

Figure 15.- Effect of slats on the variation of elevator trim angle with lift coefficient. Tab neutral; center of gravity at 27.5 percent MAC.
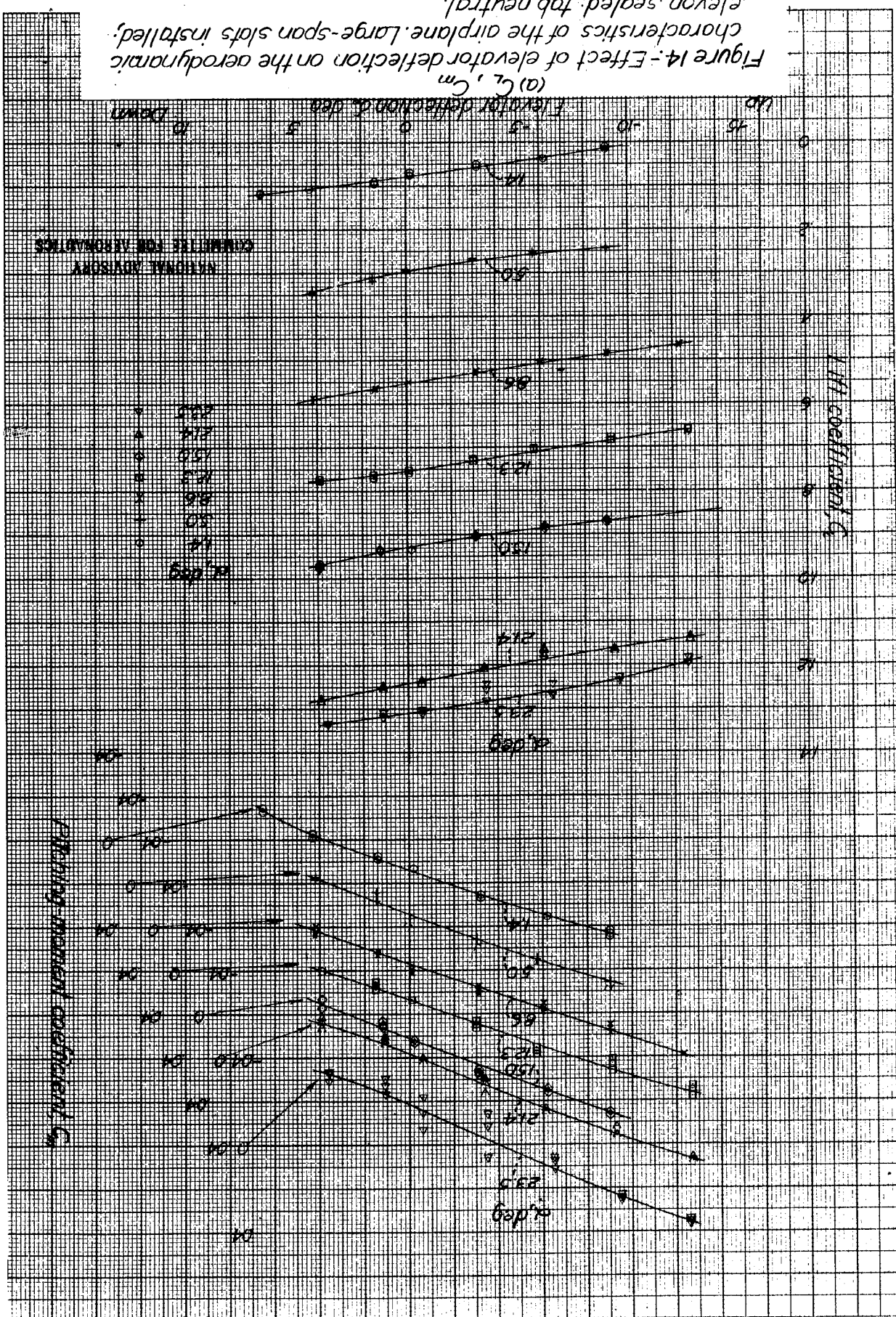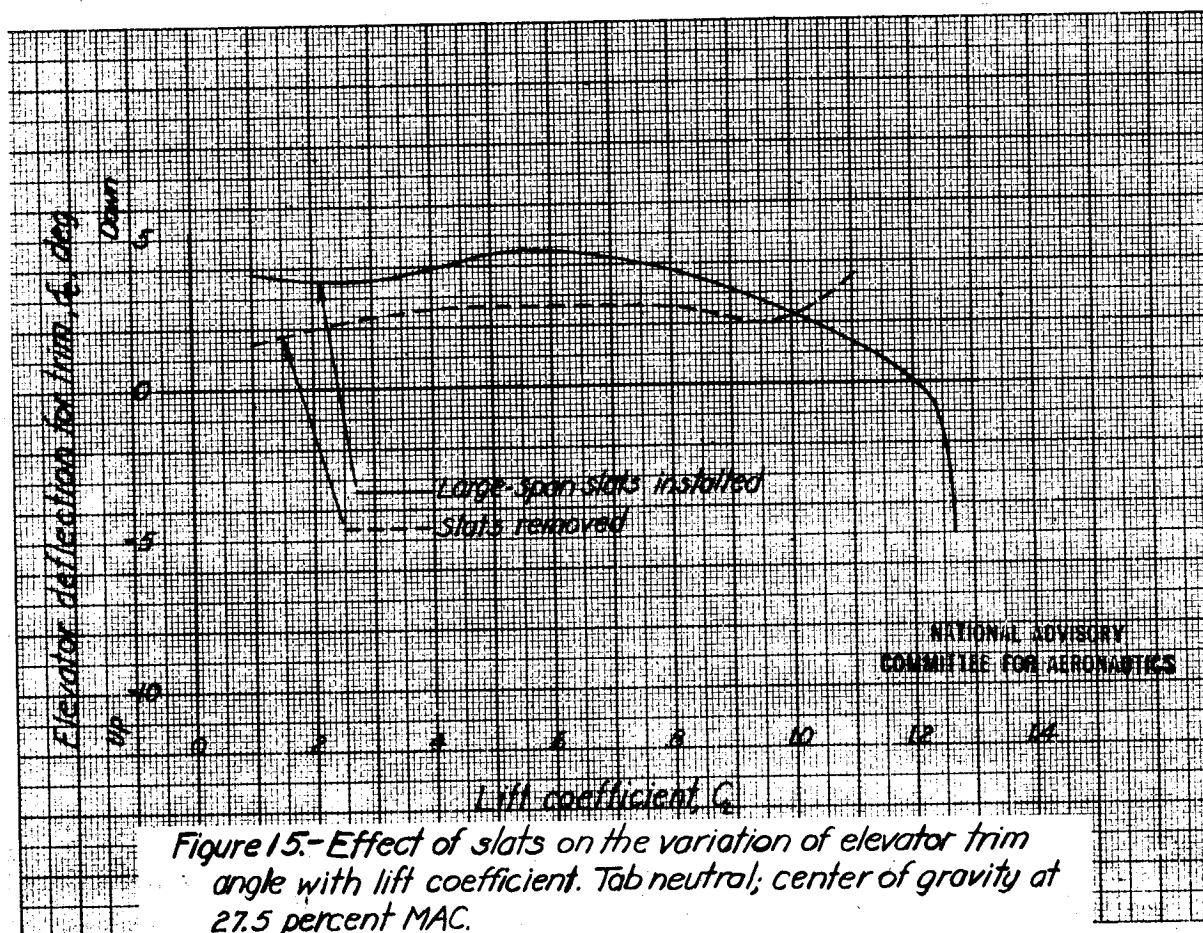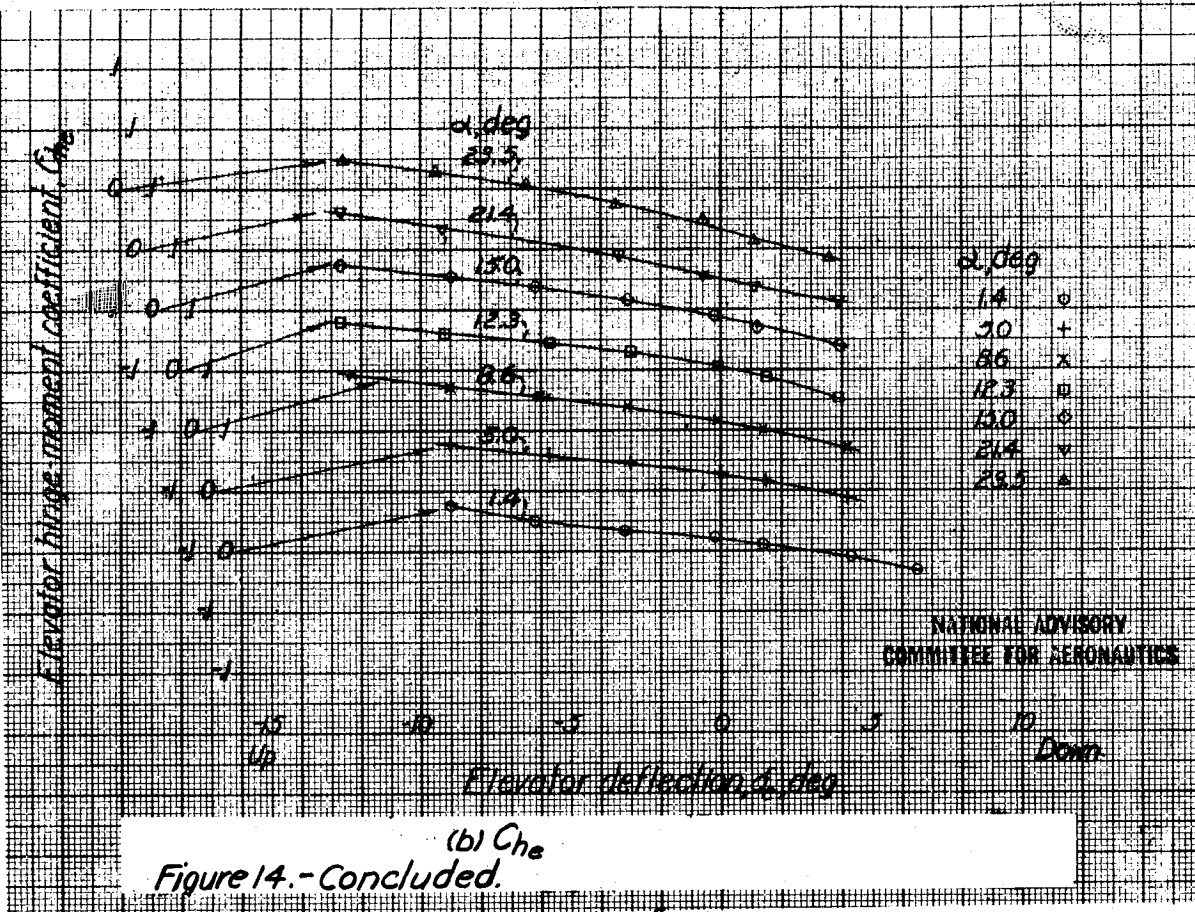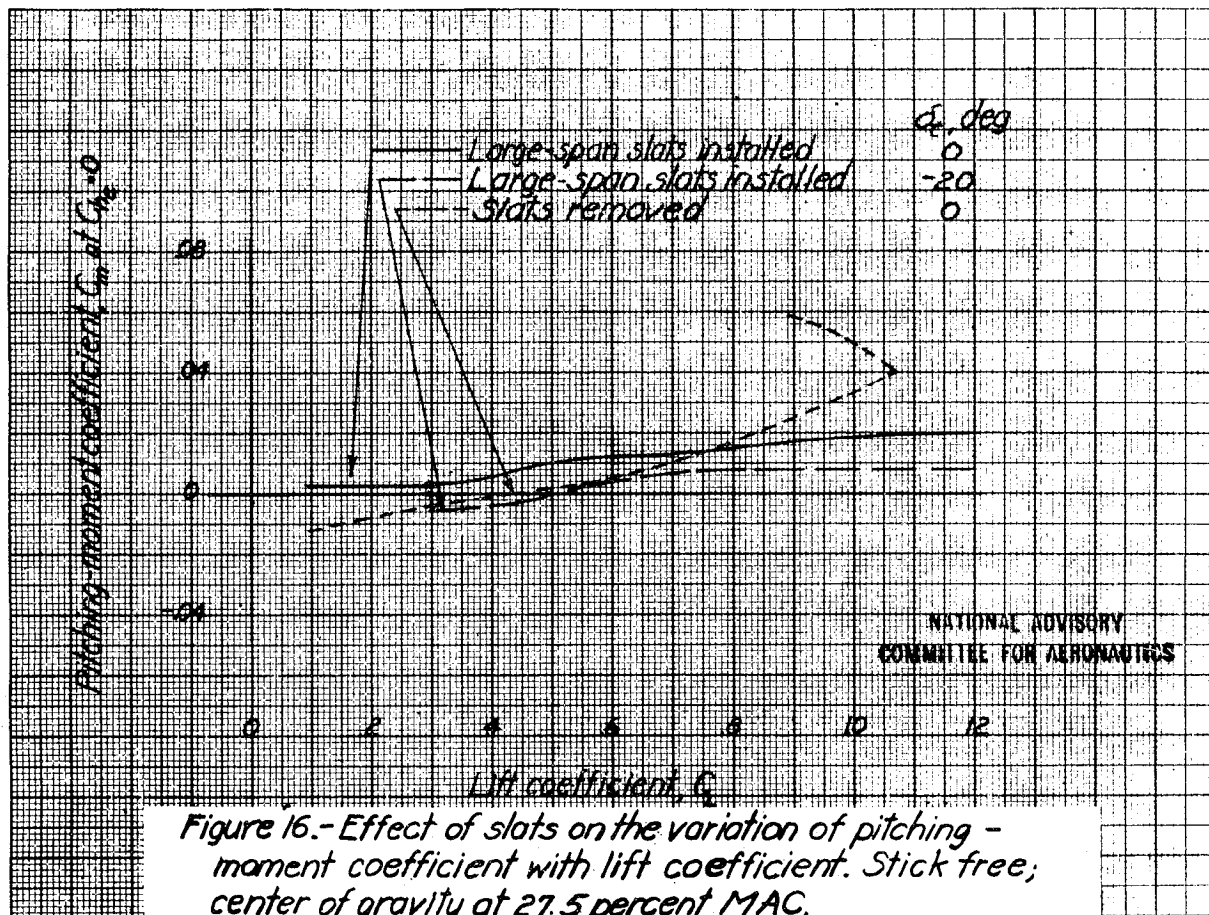
Figure 16.- Effect of slats on the variation of pitching - moment coefficient with lift coefficient. Stick free; center of gravity at 27.5 percent MAC.
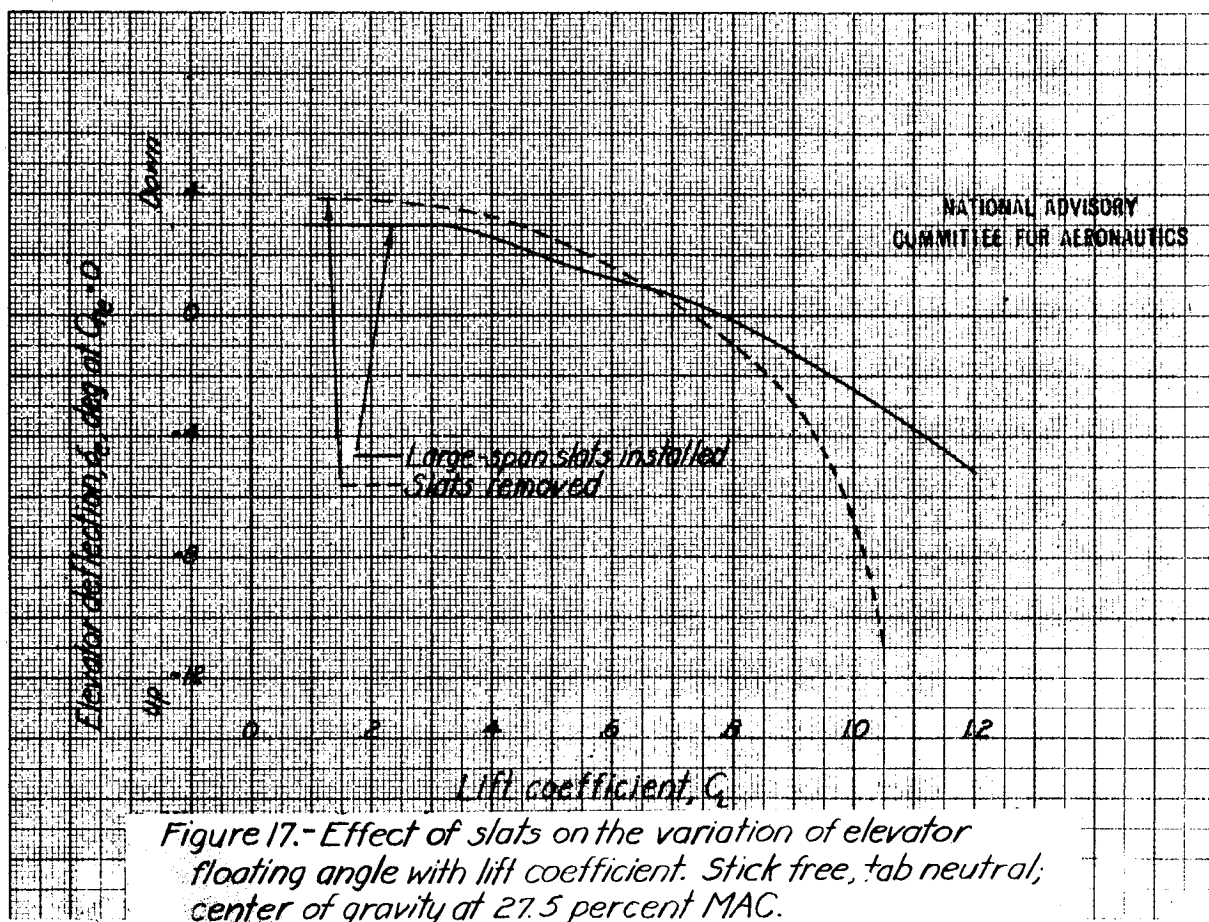
Figure 17.- Effect of slats on the variation of elevator floating angle with lift coefficient. Stick free, tab neutral; center of gravity at 27.5 percent MAC.
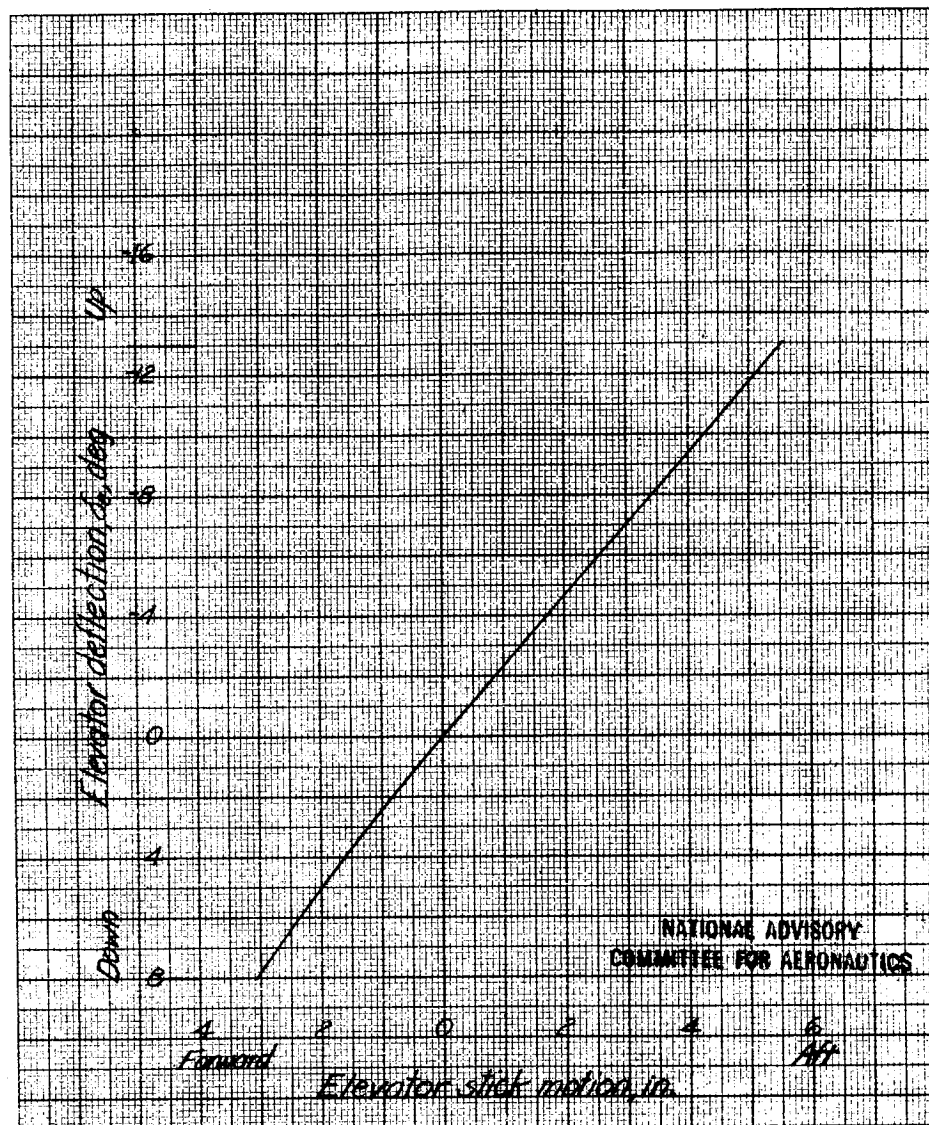
Figure 18.- Variation of stick travel with elevator deflection for the MX-334 airplane.
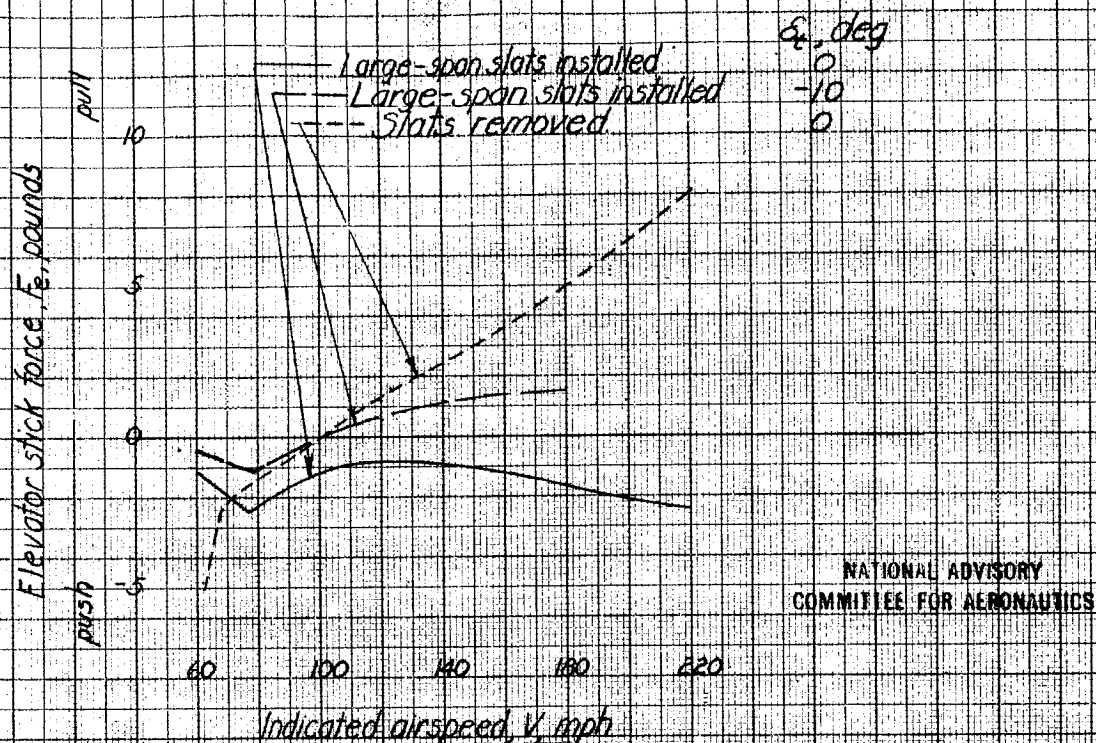
Figure 19.- Effect of slats on the variation of elevator stick
force for trim with indicated airspeed at sea level.
Center of gravity at 27.5 MAC; W/S, 11.85.
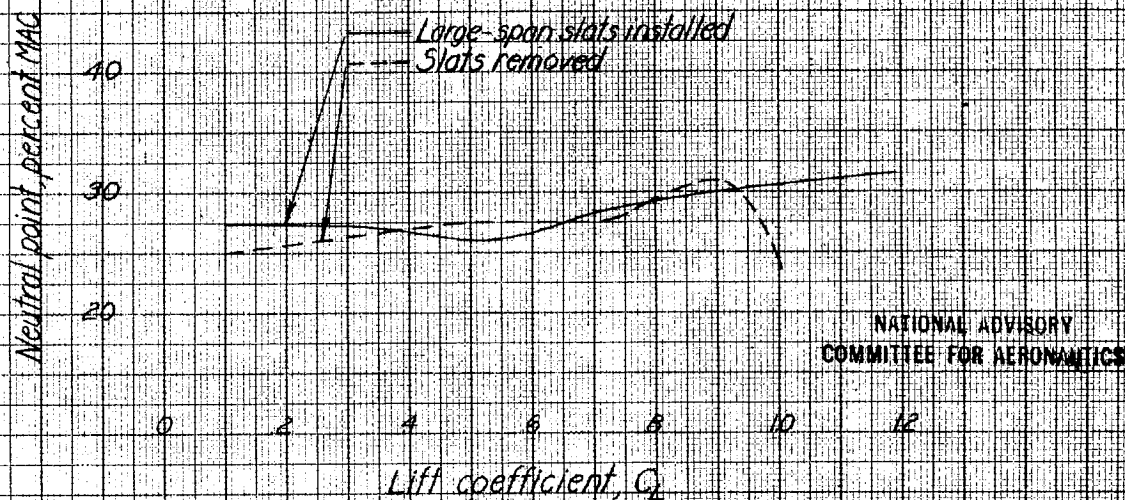
Figure 20.- Variation of neutral point with lift coefficient
for the airplane with and without slats.

Pitching-moment coefficient, C_m

C_m

δ_t, deg

C_{m_e}

Elevator-hinge-moment coefficient, C_{h_e}

δ_t, deg

	δ_t, deg
	0 ... 10
	-10
	-20
	-30

Lift coefficient, C_L

C_L

α, deg

NATIONAL ADVISORY
COMMITTEE FOR AERONAUTICS

Elevator deflection, δ_e, deg

Up   Down
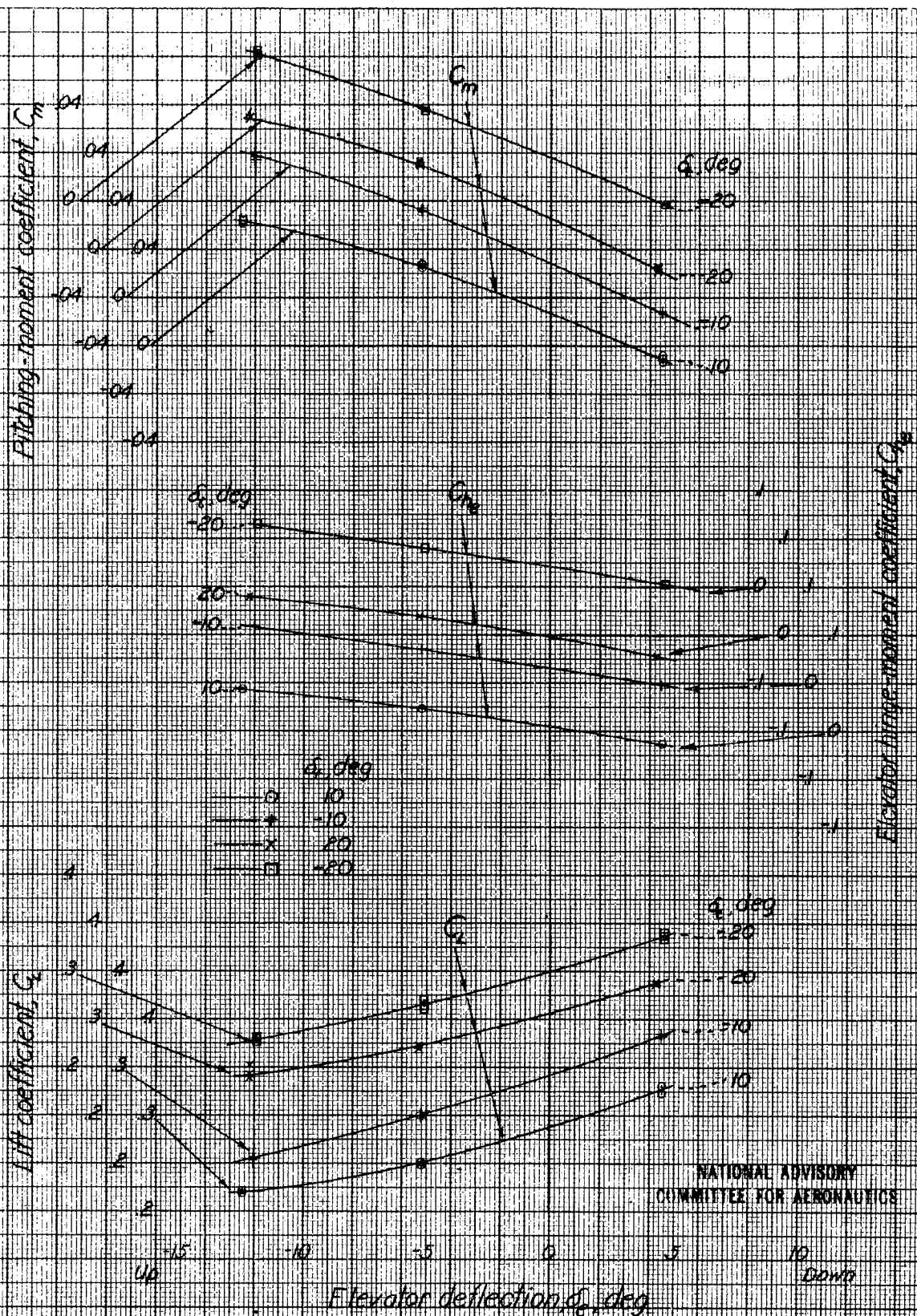
(a) α, 5.1°

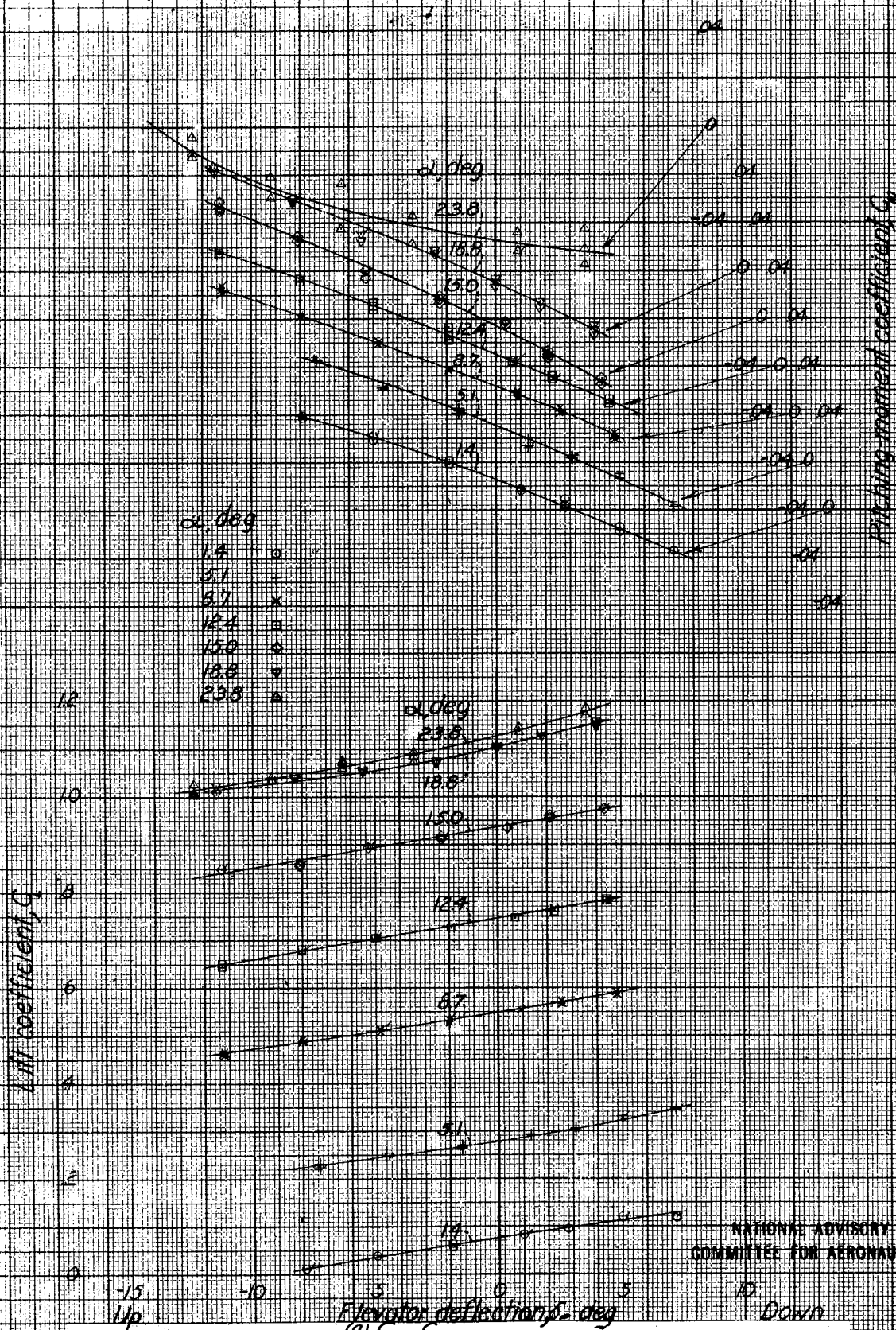Figure 21.- Effect of elevator deflection and elevator tab
setting on the aerodynamic characteristics of the
airplane. Large-span slats installed; elevon sealed.

(b) α, 12.4°

Figure 21.- Continued.

Pitching-moment coefficient, C_m

.04

.04

0 .04

0 .04

0 .04

0 -.04

-.04

-.04

δ_e, deg
-20

-20

-10

10

δ_e, deg
-20

-20

-10

10

δ_e, deg
○ 10
+ -10
× 20
□ -20

Lift coefficient, C_L

1.3

1.3

1.2 1.3

1.2 1.3

1.1 1.2

1.1 1.2

1.1

δ_e, deg
-20

-20

-10

10
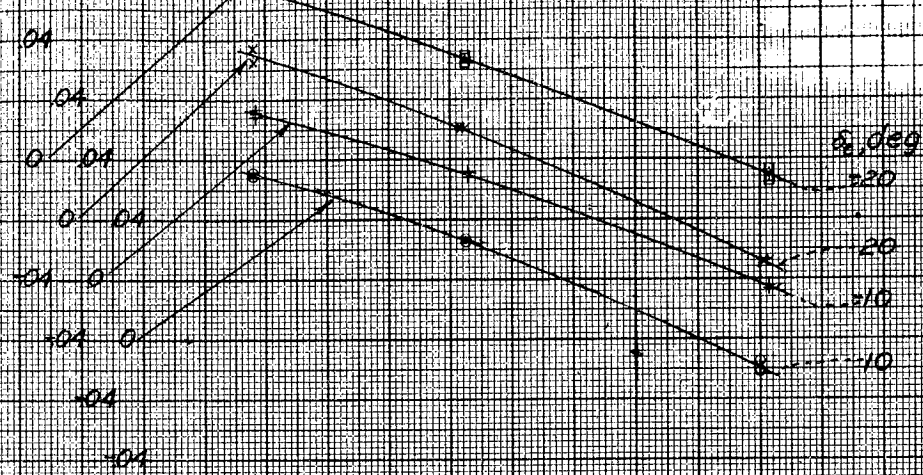
Elevator hinge-moment coefficient, C_{he}
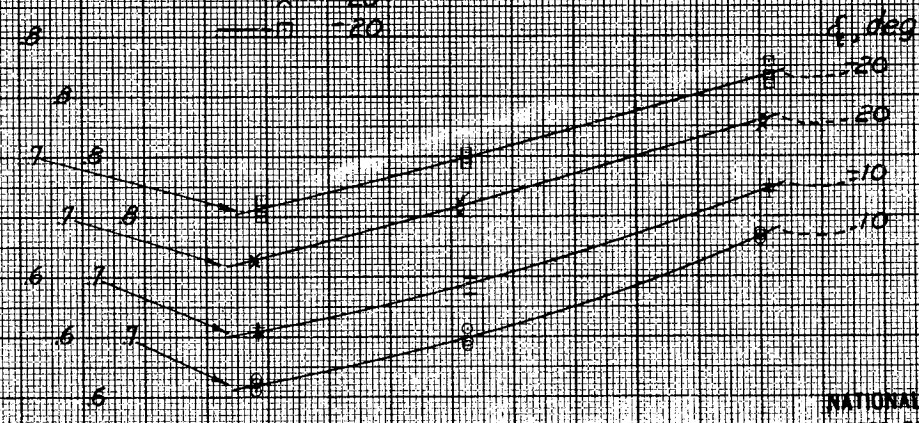
-15
Up

-10

-5

0

.5

10
Down

Elevator deflection, δ_e, deg

(c) α, 21.6°

Figure 21.- Concluded.
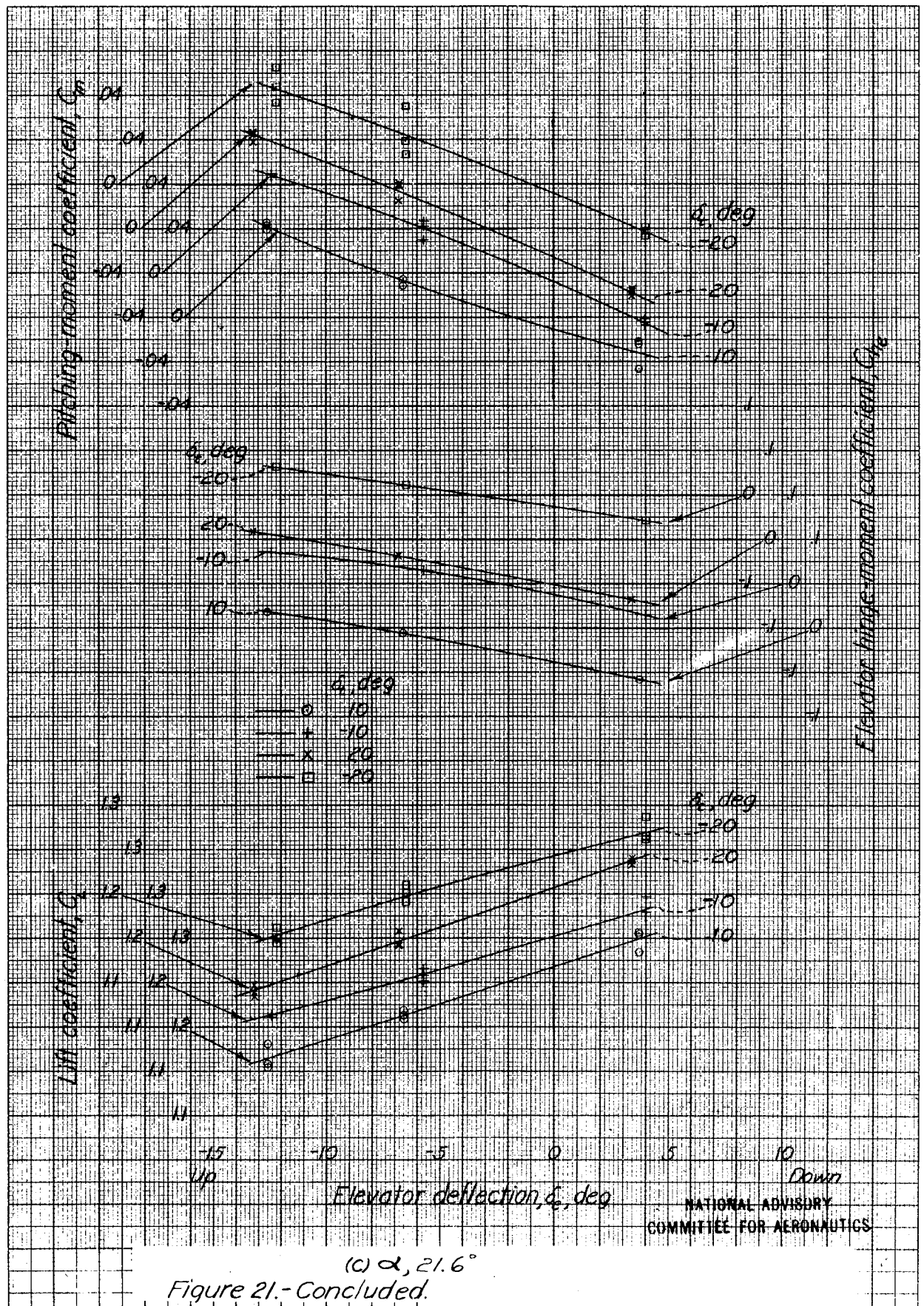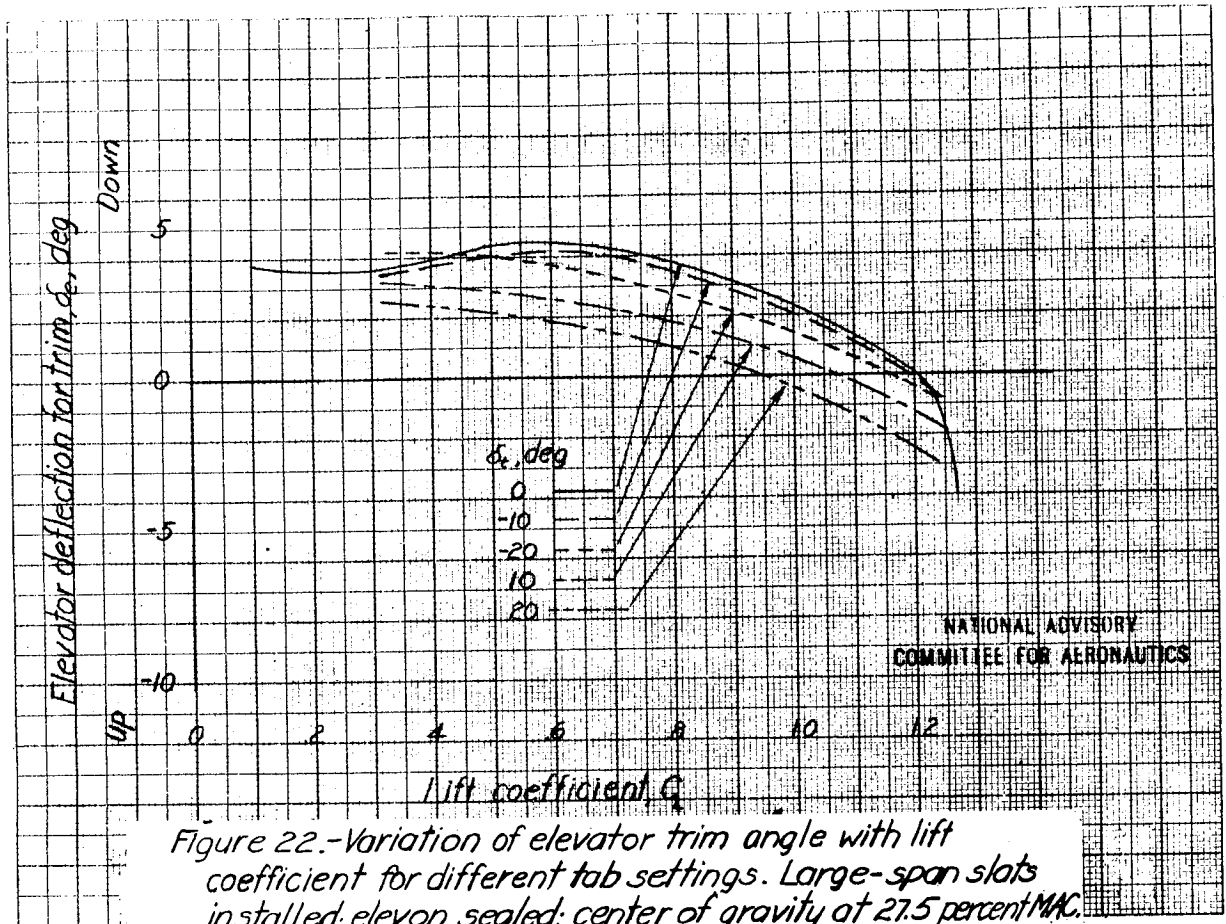
Figure 22.-Variation of elevator trim angle with lift
coefficient for different tab settings. Large-span slats
installed; elevon sealed; center of gravity at 27.5 percent MAC.
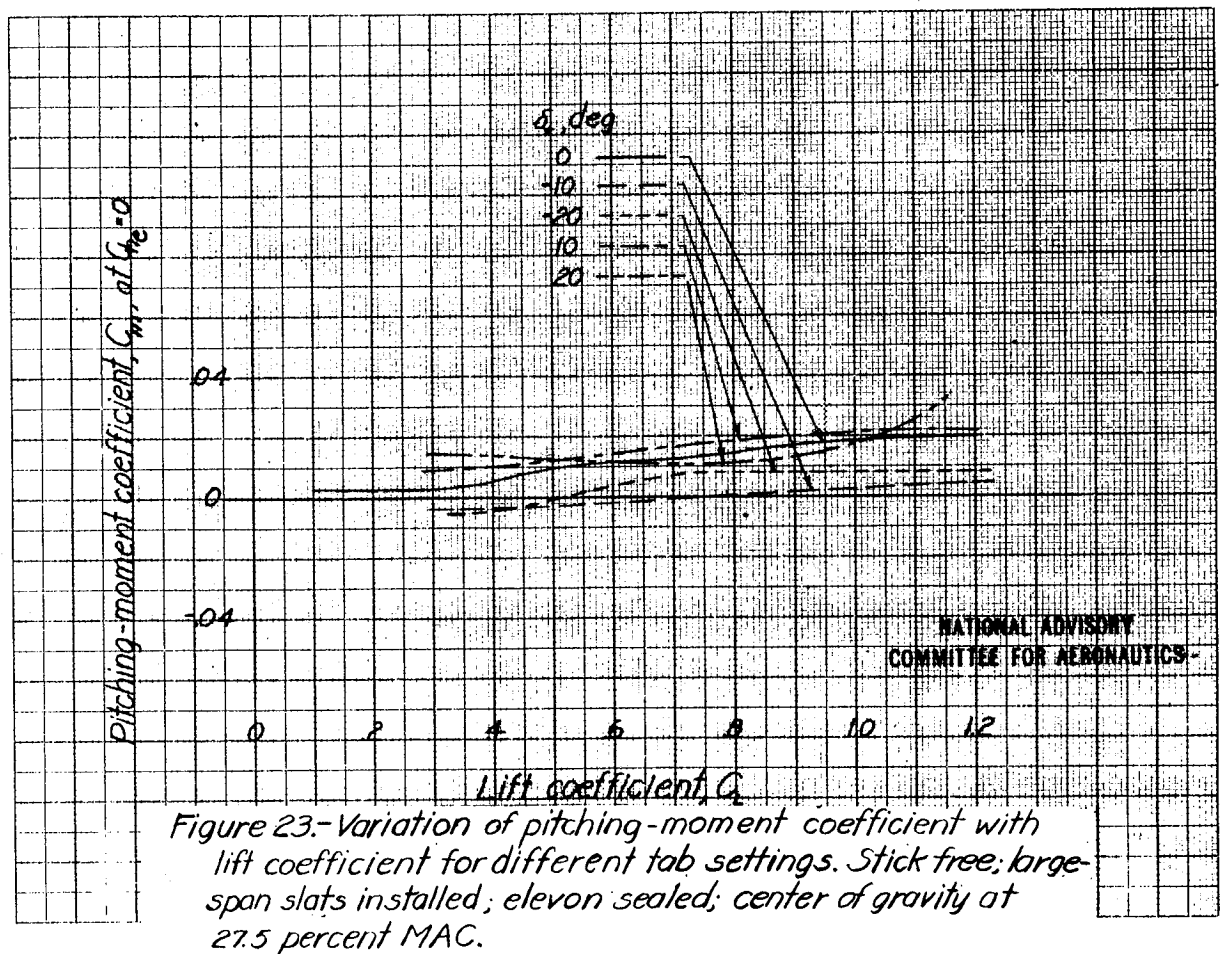
Figure 23.- Variation of pitching-moment coefficient with
lift coefficient for different tab settings. Stick free; large-
span slats installed; elevon sealed; center of gravity at
27.5 percent MAC.
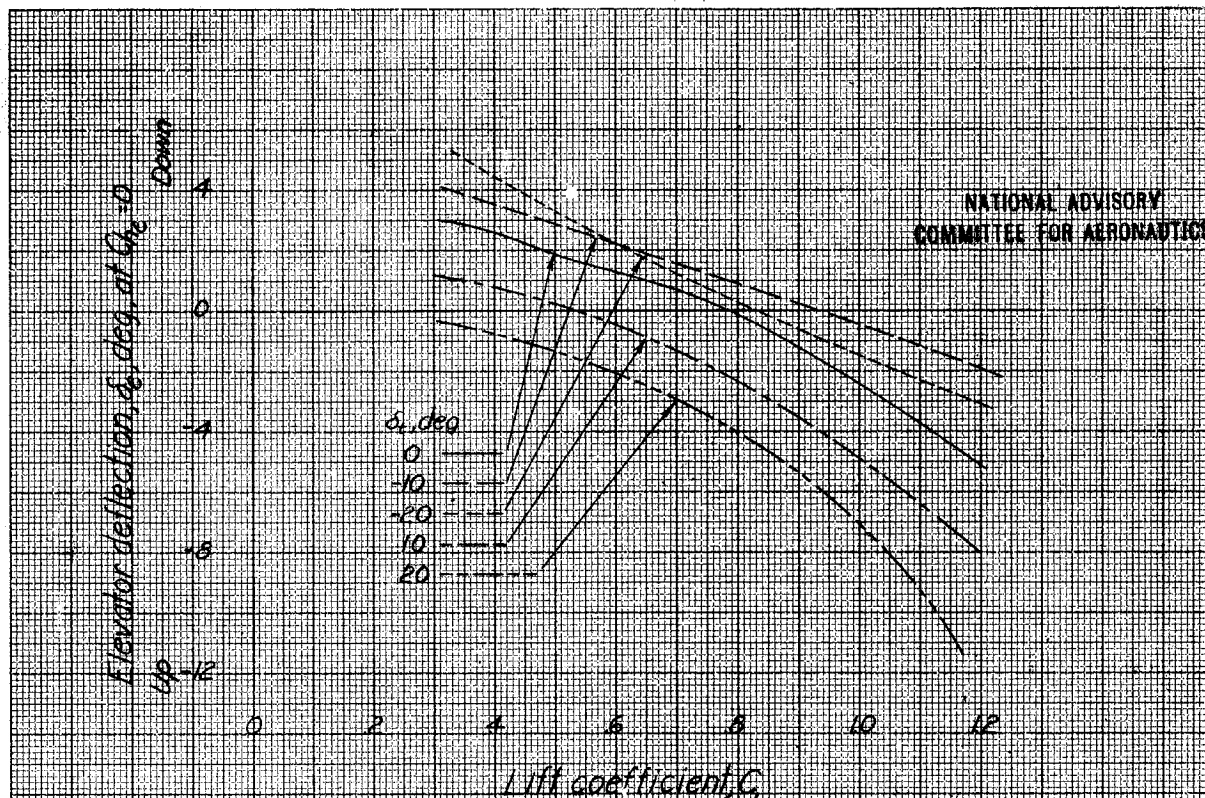
Figure 24.-Variation of elevator floating angle with lift
coefficient for different tab settings. Stick free; large-
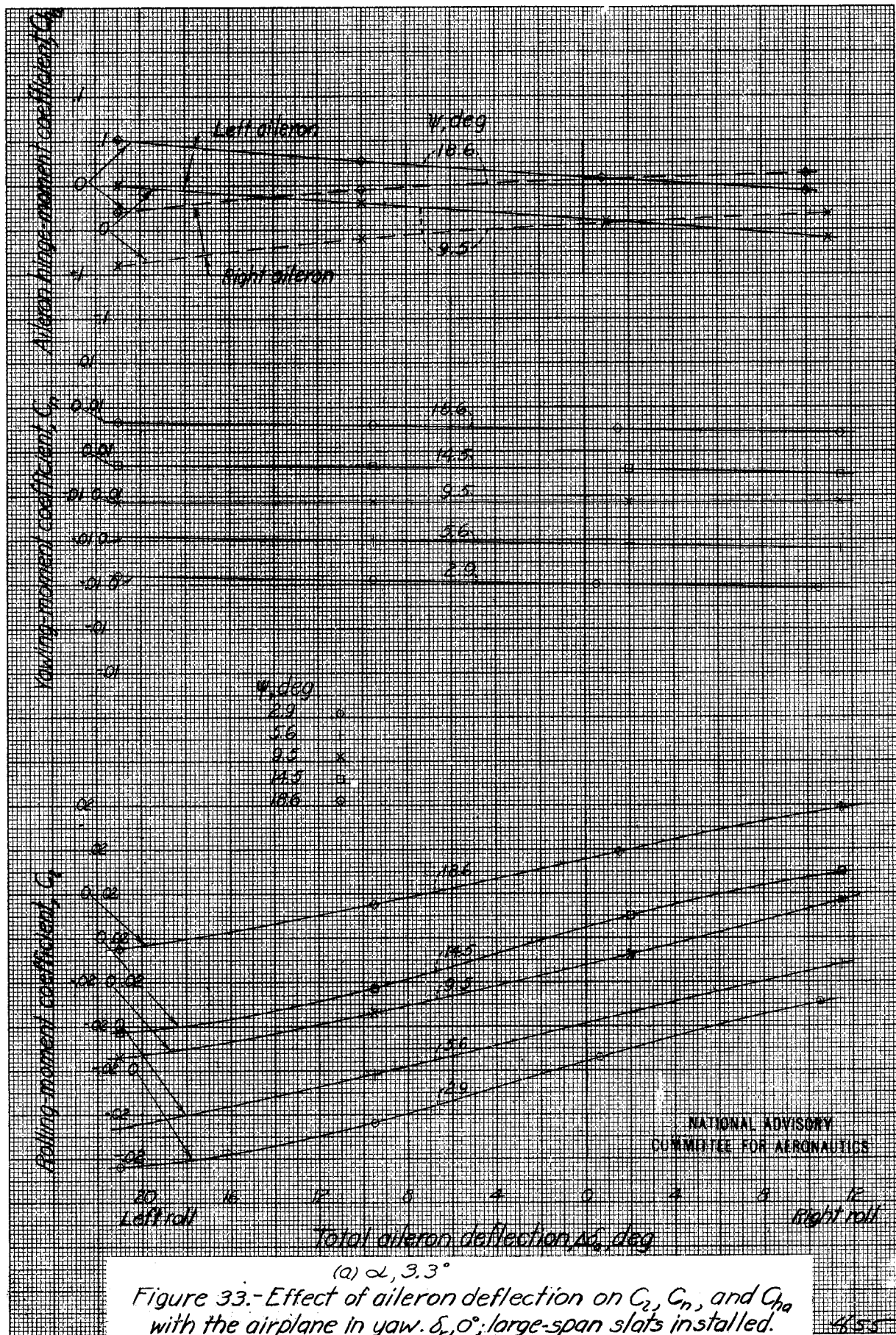span slats installed; elevon sealed; center of gravity at
27.5 percent MAC.
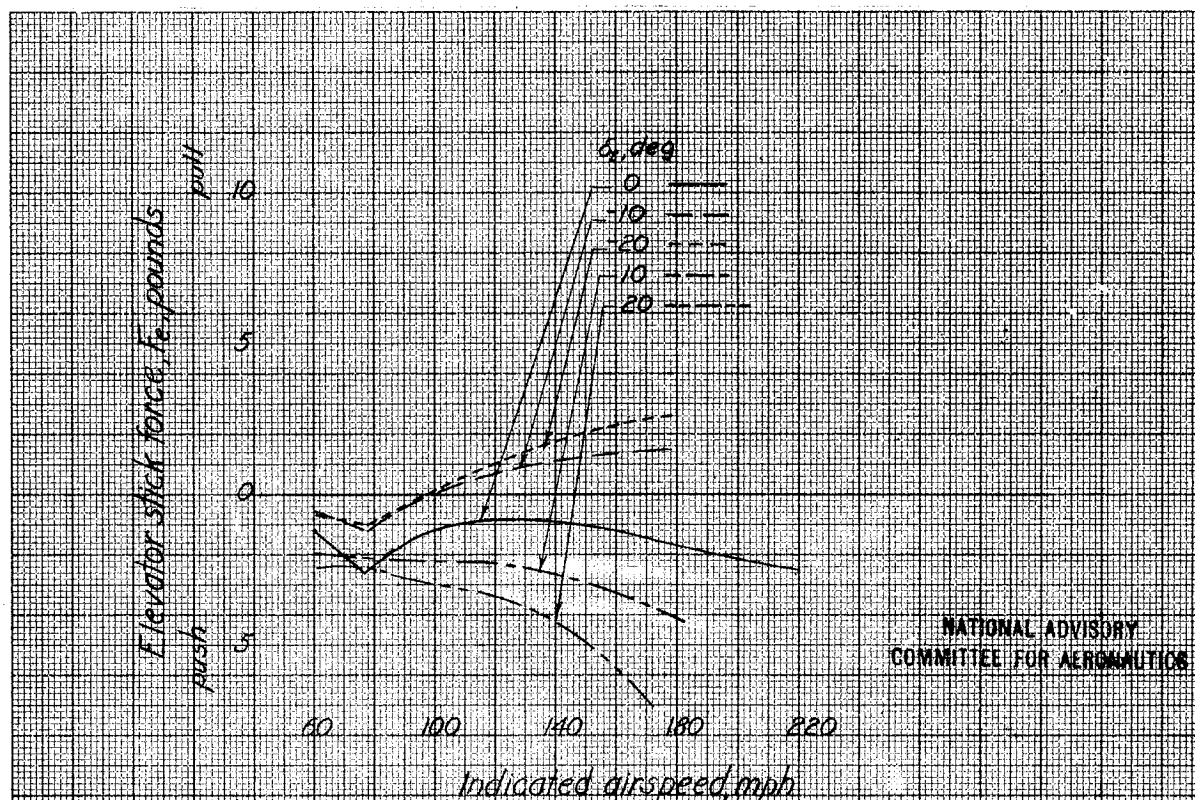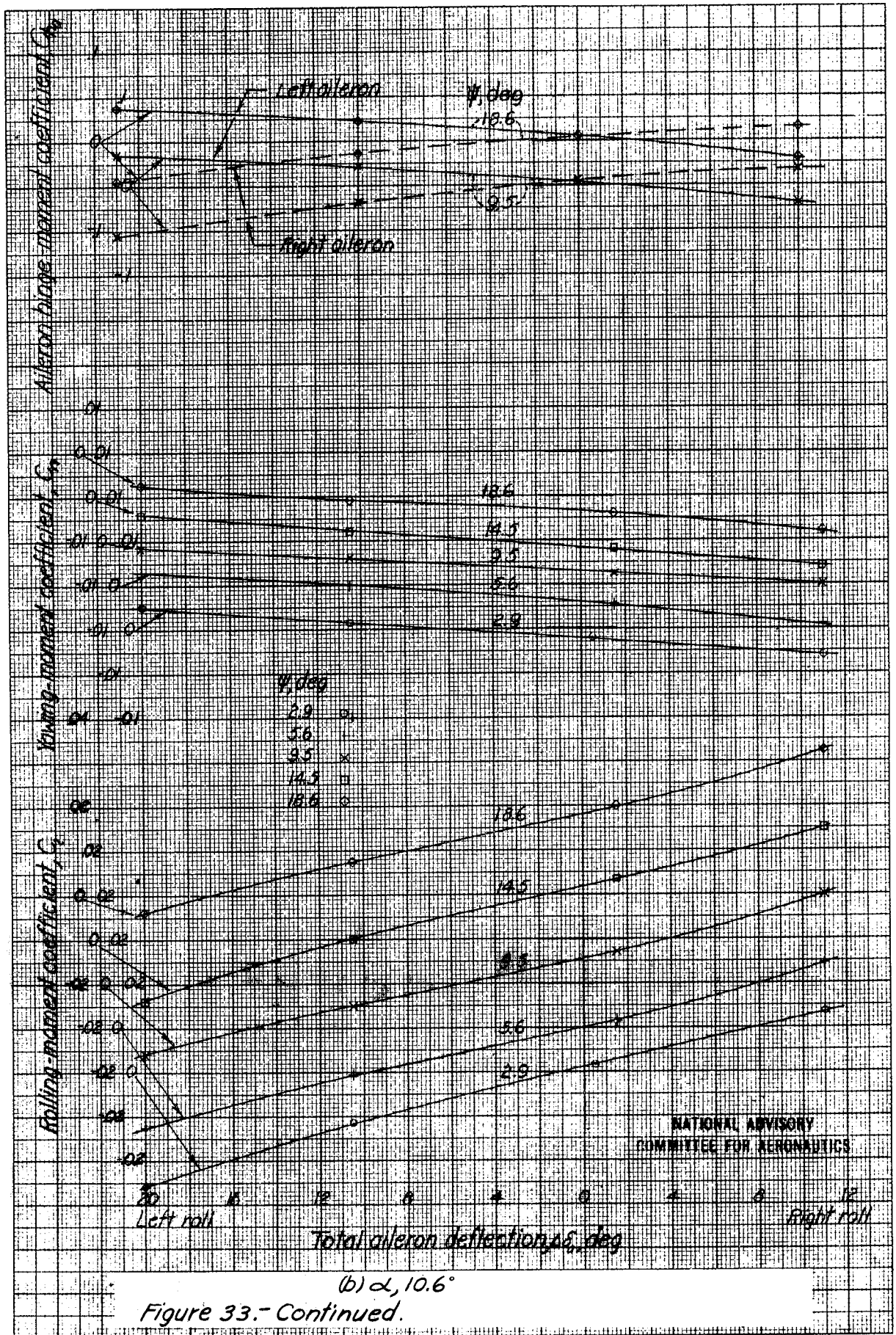

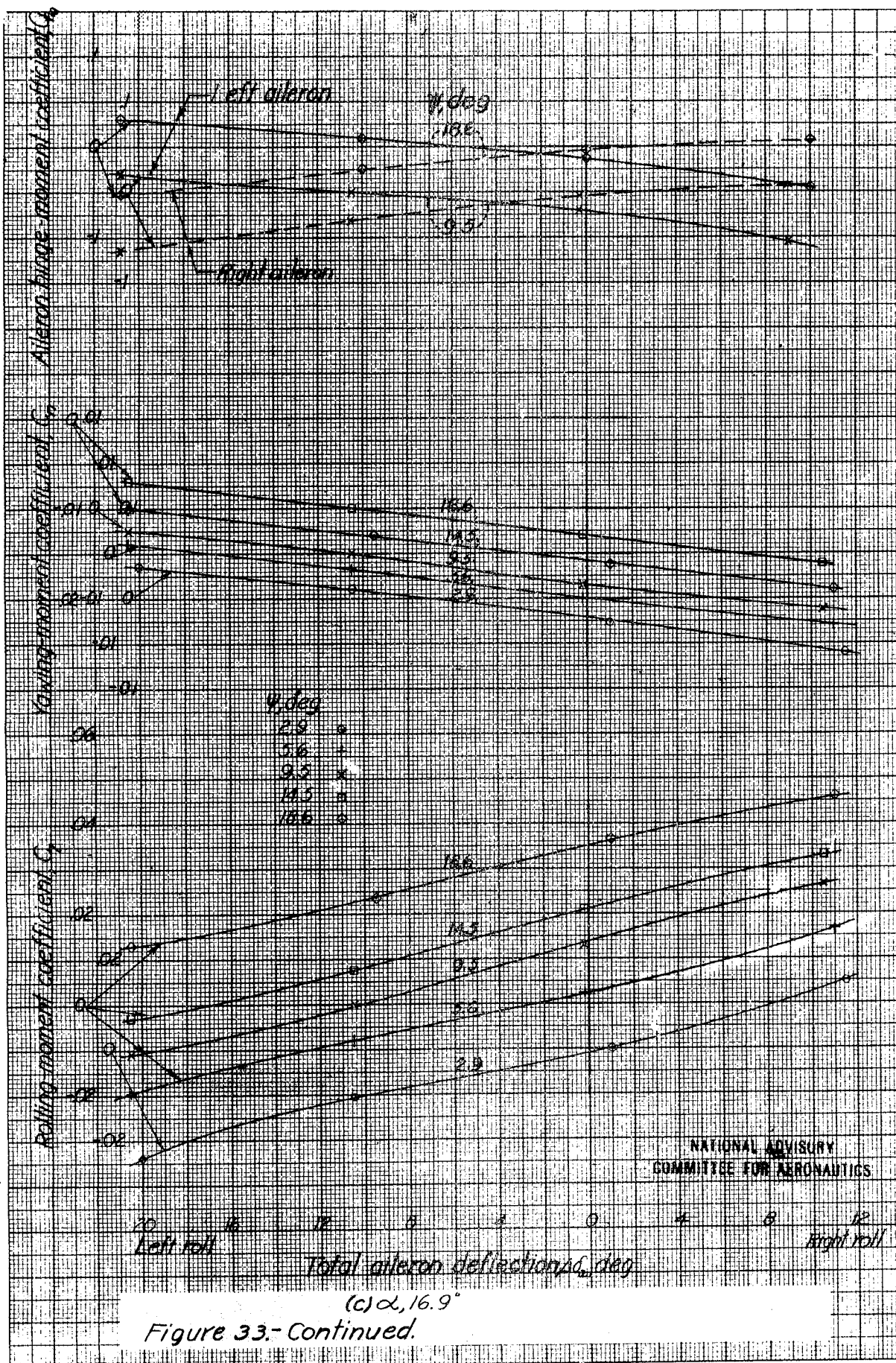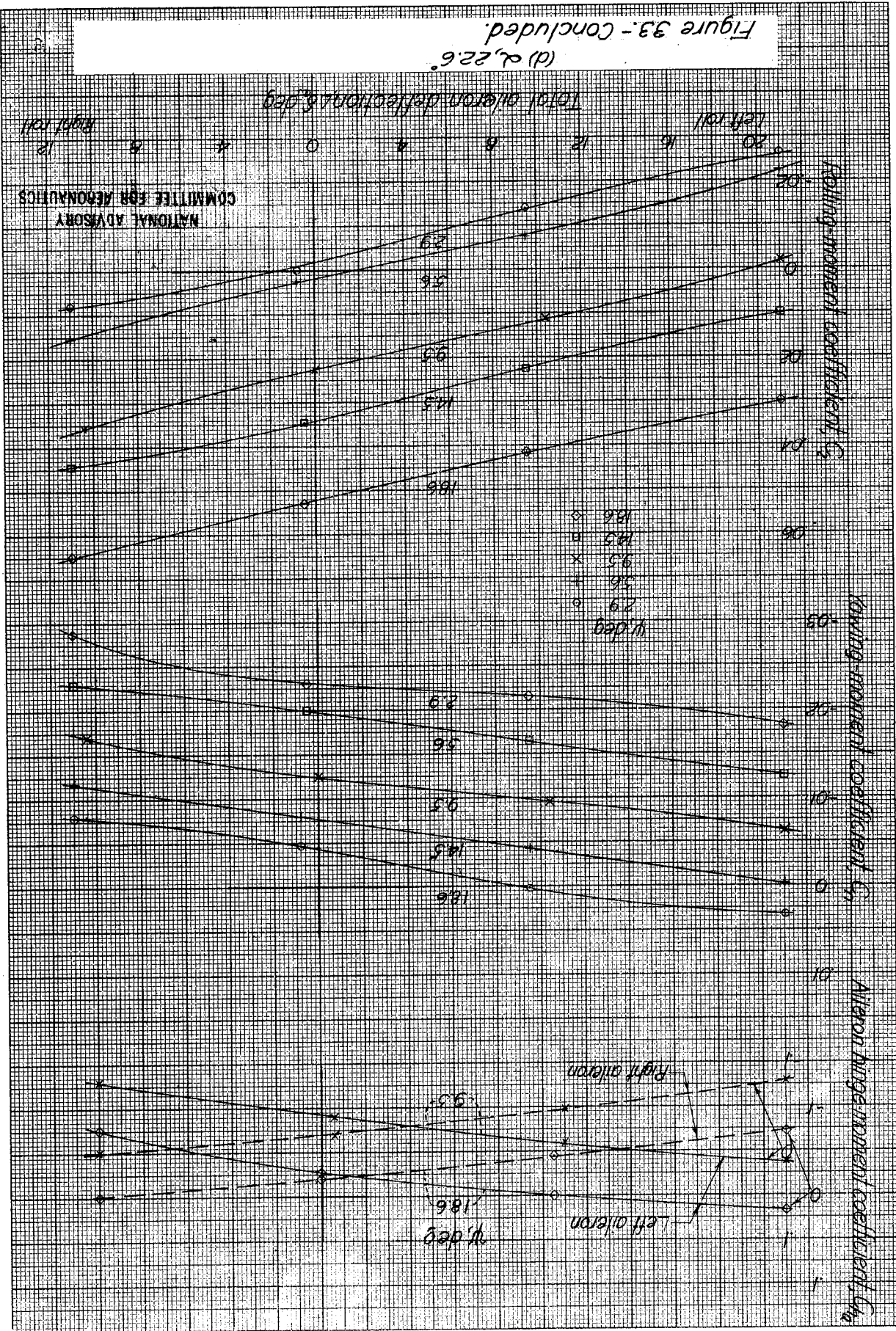Figure 25.-Variation of elevator stick force for trim with
indicated airspeed at sea level for different tab settings.
Large-span slats installed; elevon sealed; center of gravity
at 27.5 percent MAC.
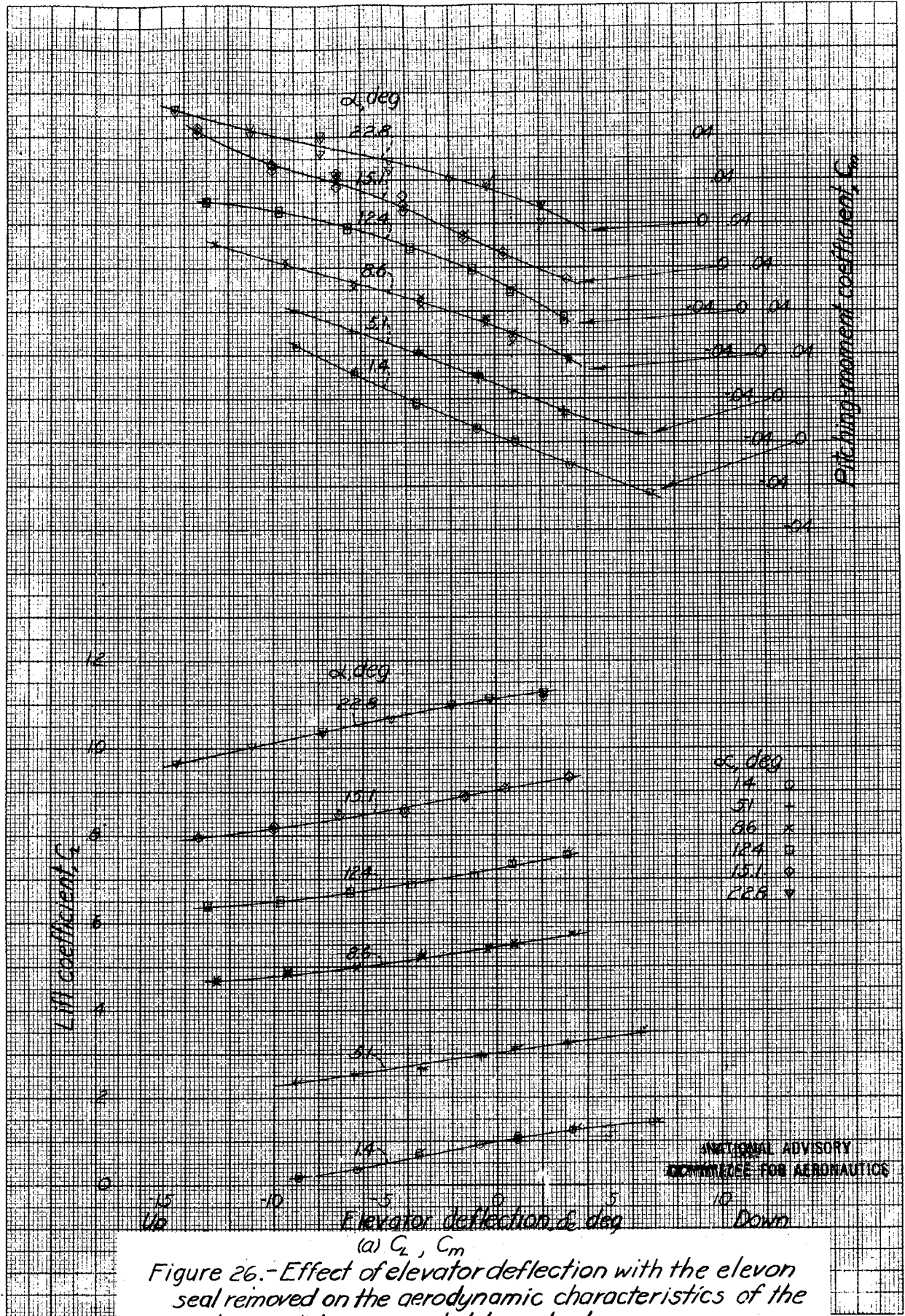
Figure 26.- Effect of elevator deflection with the elevon seal removed on the aerodynamic characteristics of the airplane. Slats removed; tab neutral.

(a) C_L, C_m
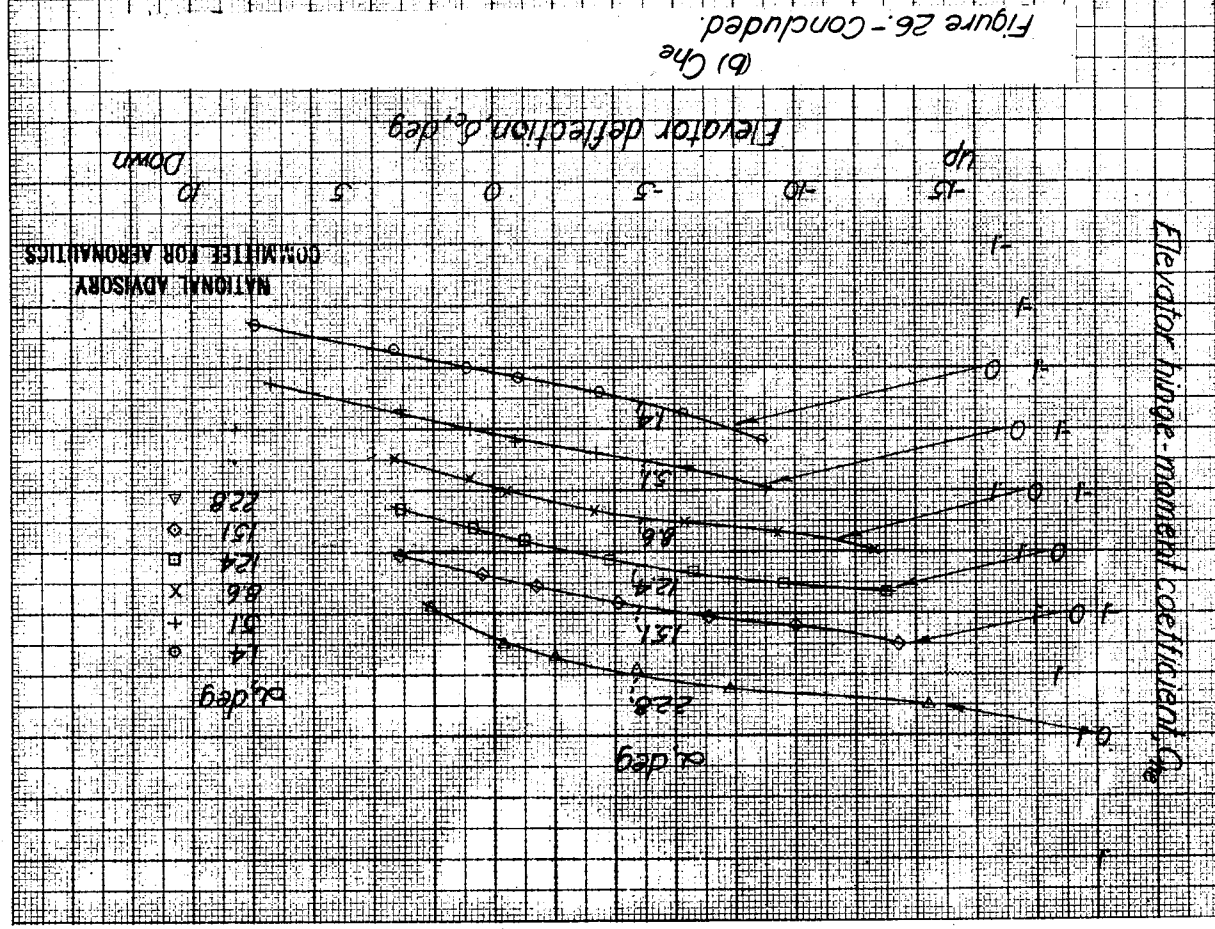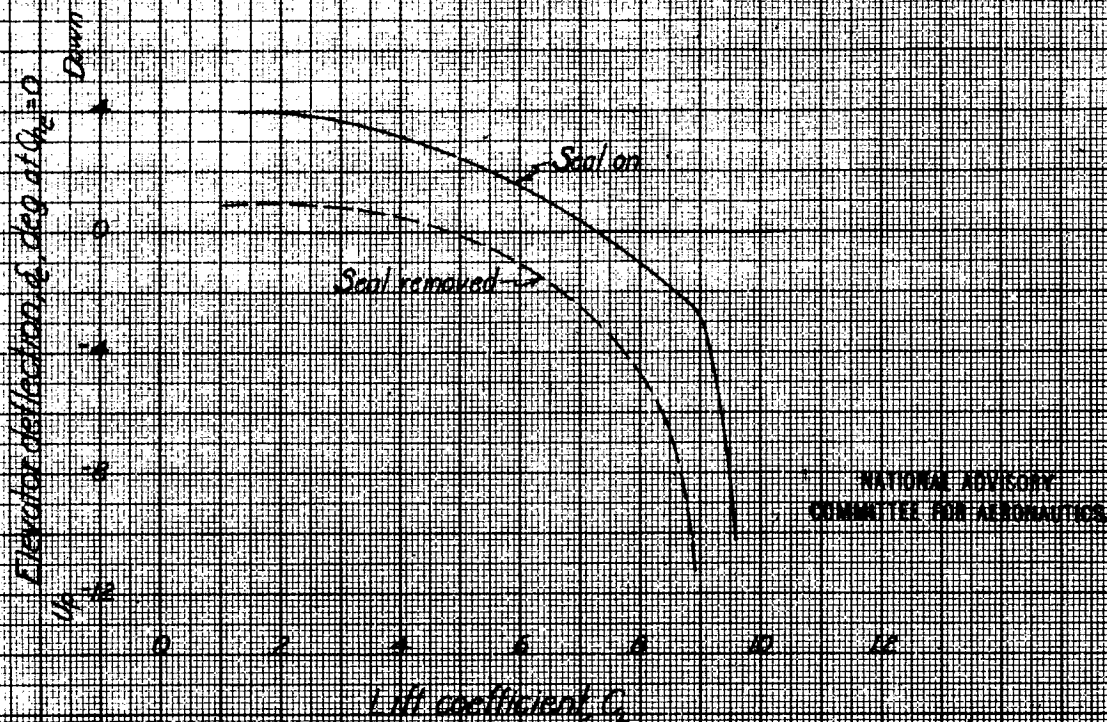
Figure 27.- Effect of the elevon seal on the elevator floating
angle. Stick free; slats removed; tab neutral; center of
gravity at 27.5 percent MAC.
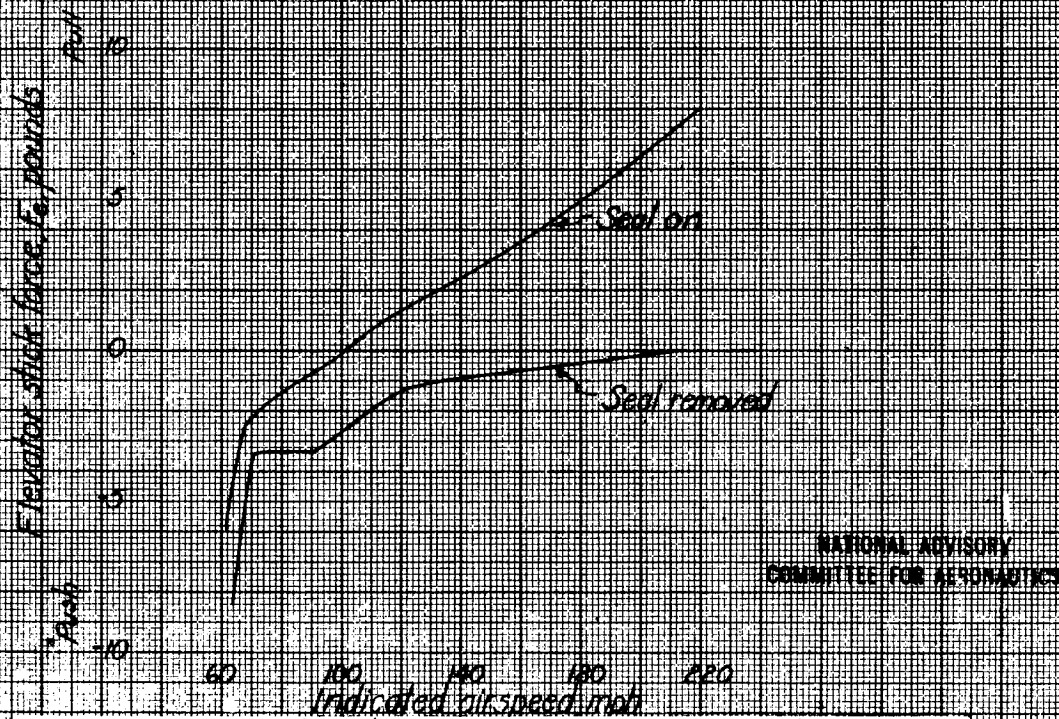
Figure 28.- Effect of the elevon seal on the variation of
elevator stick force for trim with indicated airspeed at
sea level. Slats removed; tab neutral; center of gravity
at 27.5 percent MAC.

Figure 29.- Effect of elevator deflection with the elevon seal removed on the aerodynamic characteristics of the airplane. Large-span slats installed; tab neutral; beveled elevon installed.
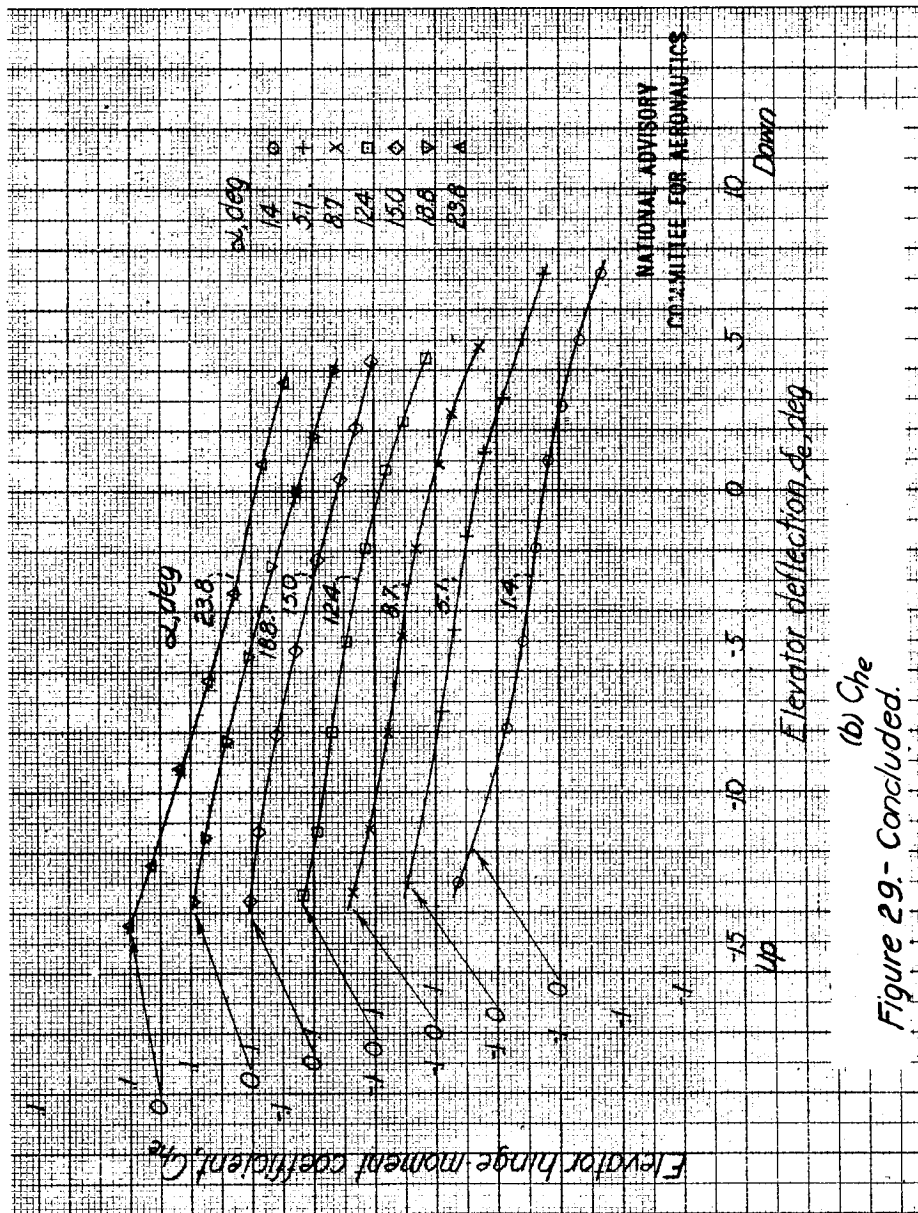
(b) C_{h_e}.

Figure 29.- Concluded.
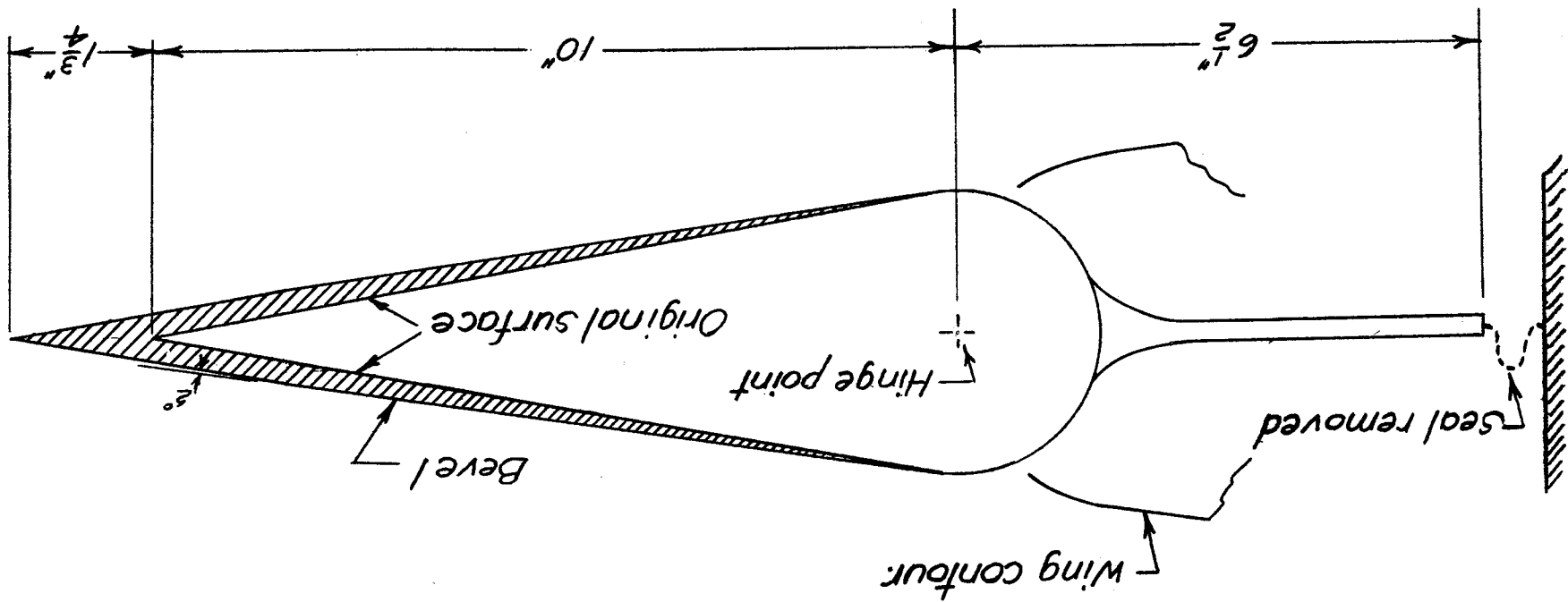
Figure 30.- Sketch of the beveled elevon for the MX-334 airplane.

NATIONAL ADVISORY
COMMITTEE FOR AERONAUTICS
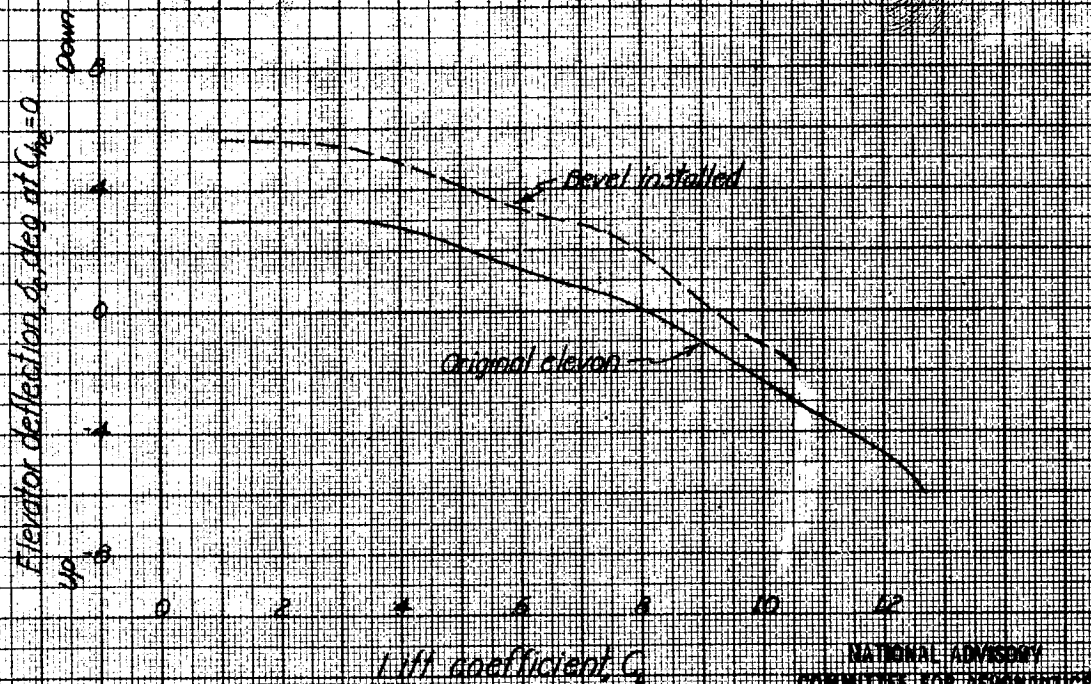
Figure 31.- Effect of the bevel on the elevon floating angle. Large-span slats installed; elevon seal on; tab neutral; center of gravity at 27.5 percent MAC.
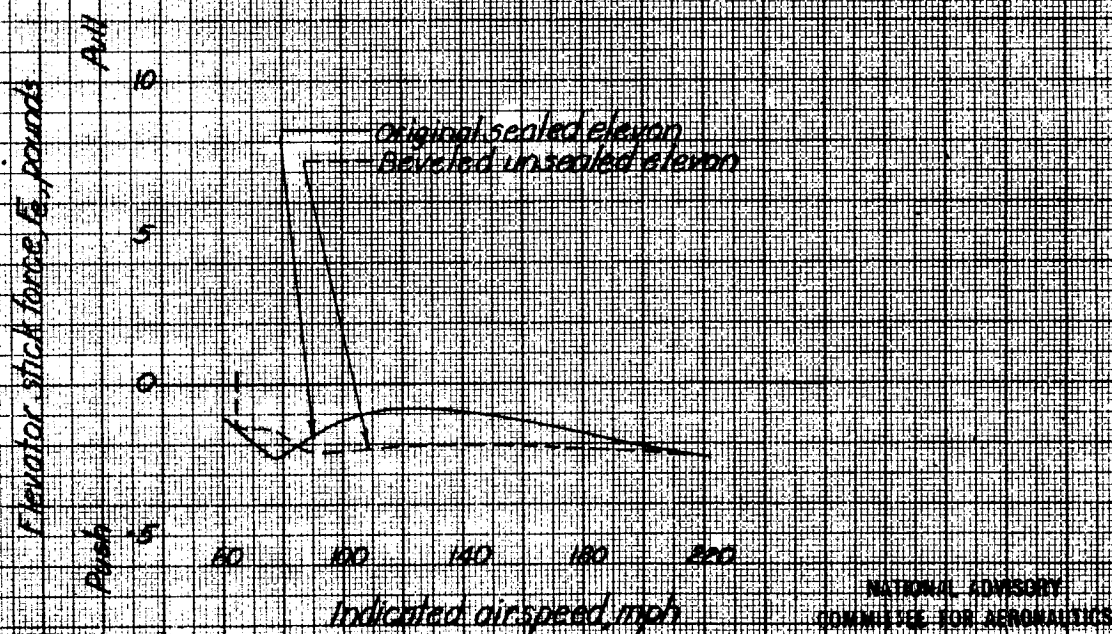
Figure 32.- Variation of elevator stick force for trim with indicated airspeed at sea level for the beveled and original elevon. Large-span slats installed; tab neutral; center of gravity at 27.5 percent MAC; W/S, 11.85.

(a) α, 3.3°

Figure 33.- Effect of aileron deflection on C_l, C_n, and C_{h_a} with the airplane in yaw. δ_r, 0°; large-span slats installed.

(b) α, 10.6°

Figure 33.- Continued.

(c) α, 16.9°

Figure 33.- Continued.

Figure 33.- Concluded.

(d) α, 22.6°.

NATIONAL ADVISORY
COMMITTEE FOR AERONAUTICS

Total aileron deflection, δ_a, deg

Right roll   Left roll

Rolling-moment coefficient, C_l

Yawing-moment coefficient, C_n

Aileron hinge-moment coefficient, C_{ha}

Right aileron

Left aileron

ψ, deg

Figure 34.- Effect of aileron deflection on the lateral-force coefficient of the airplane in yaw. δ_r,0°; large-span slats installed.
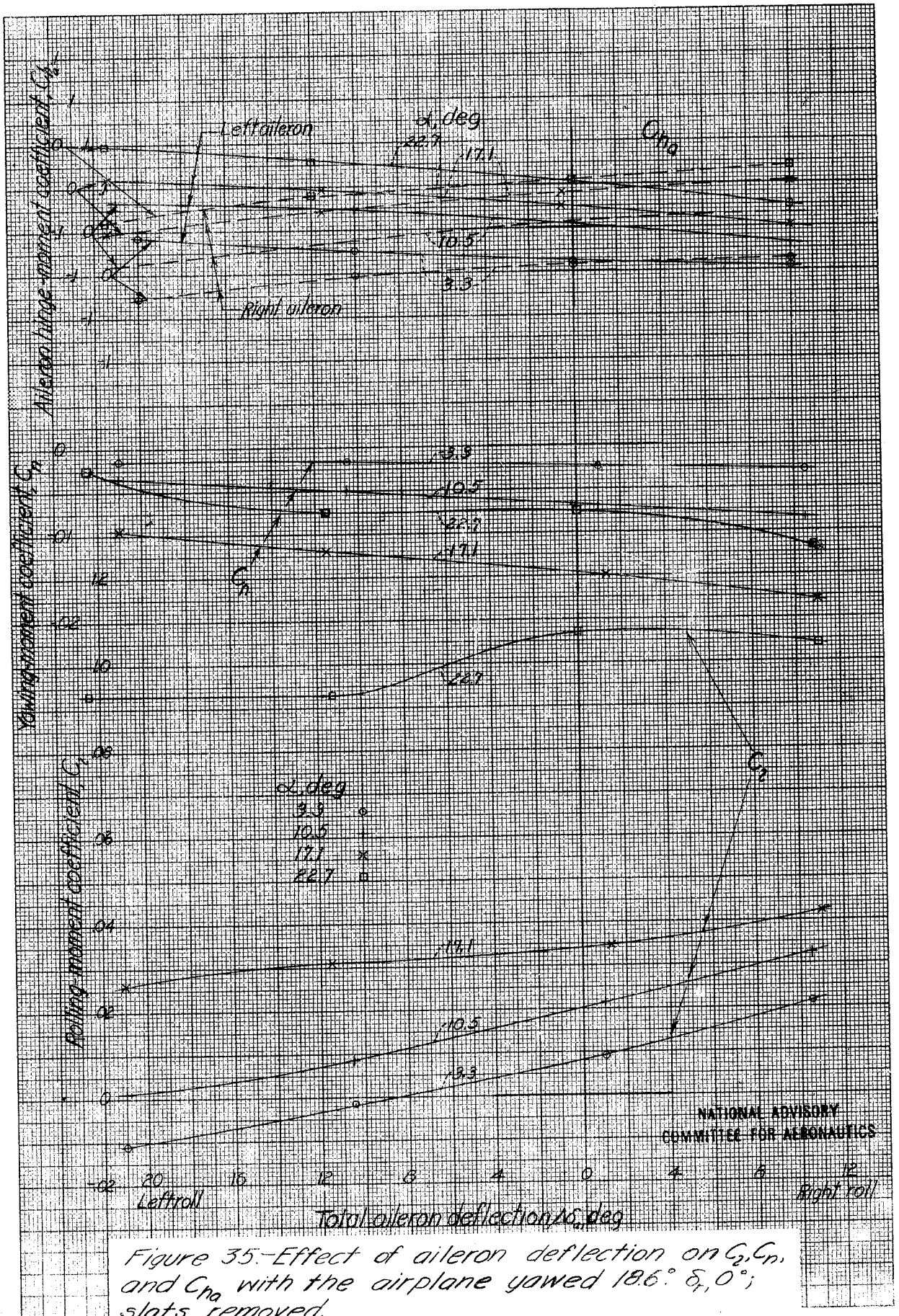
Figure 35.-Effect of aileron deflection on C_l, C_n, and C_{h_a} with the airplane yawed 18.6°; δ_r, 0°; slats removed.
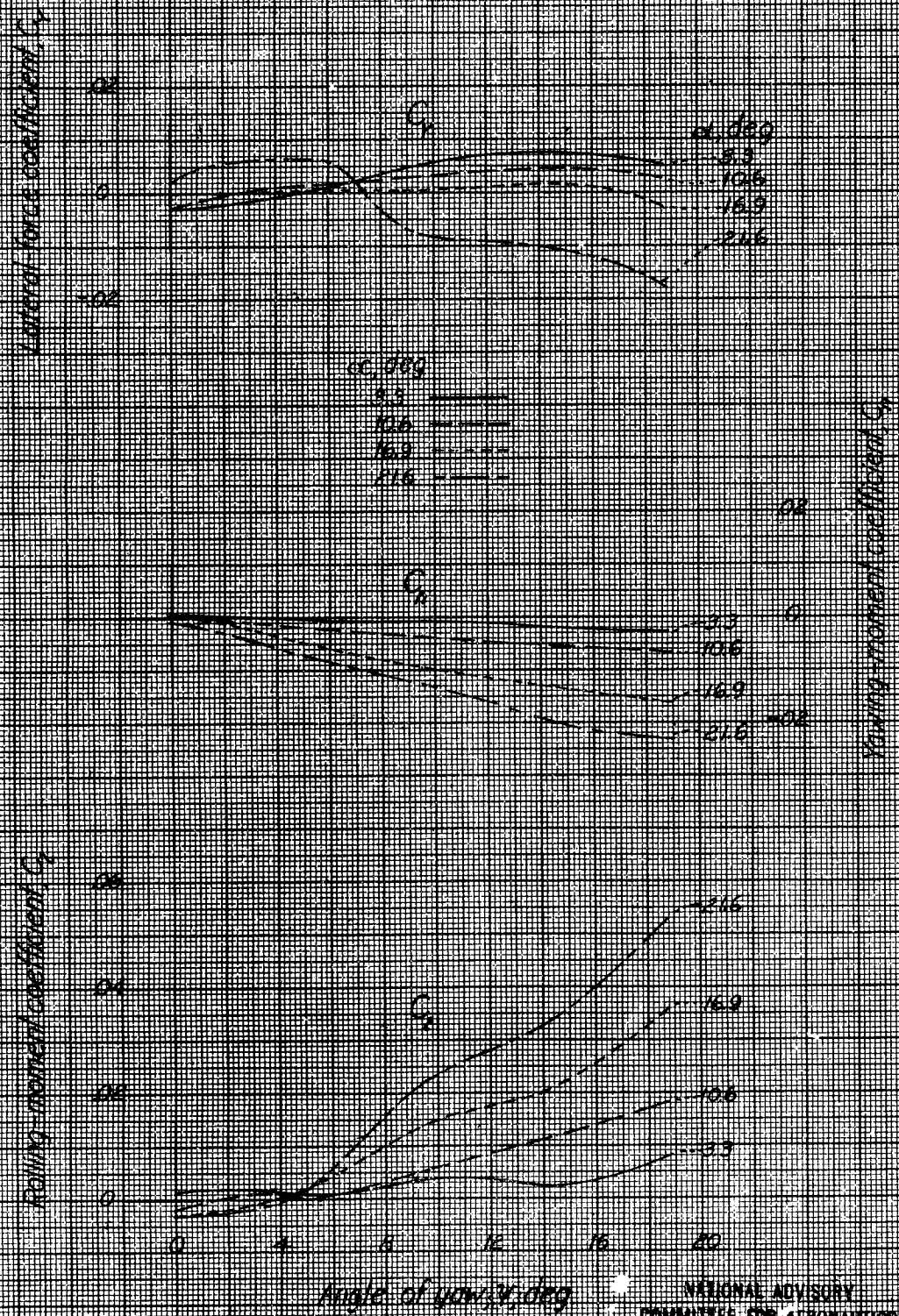
Figure 36.—Effect of yaw on the aerodynamic characteristics of the airplane. δ_0, 0°; large-span slats installed.
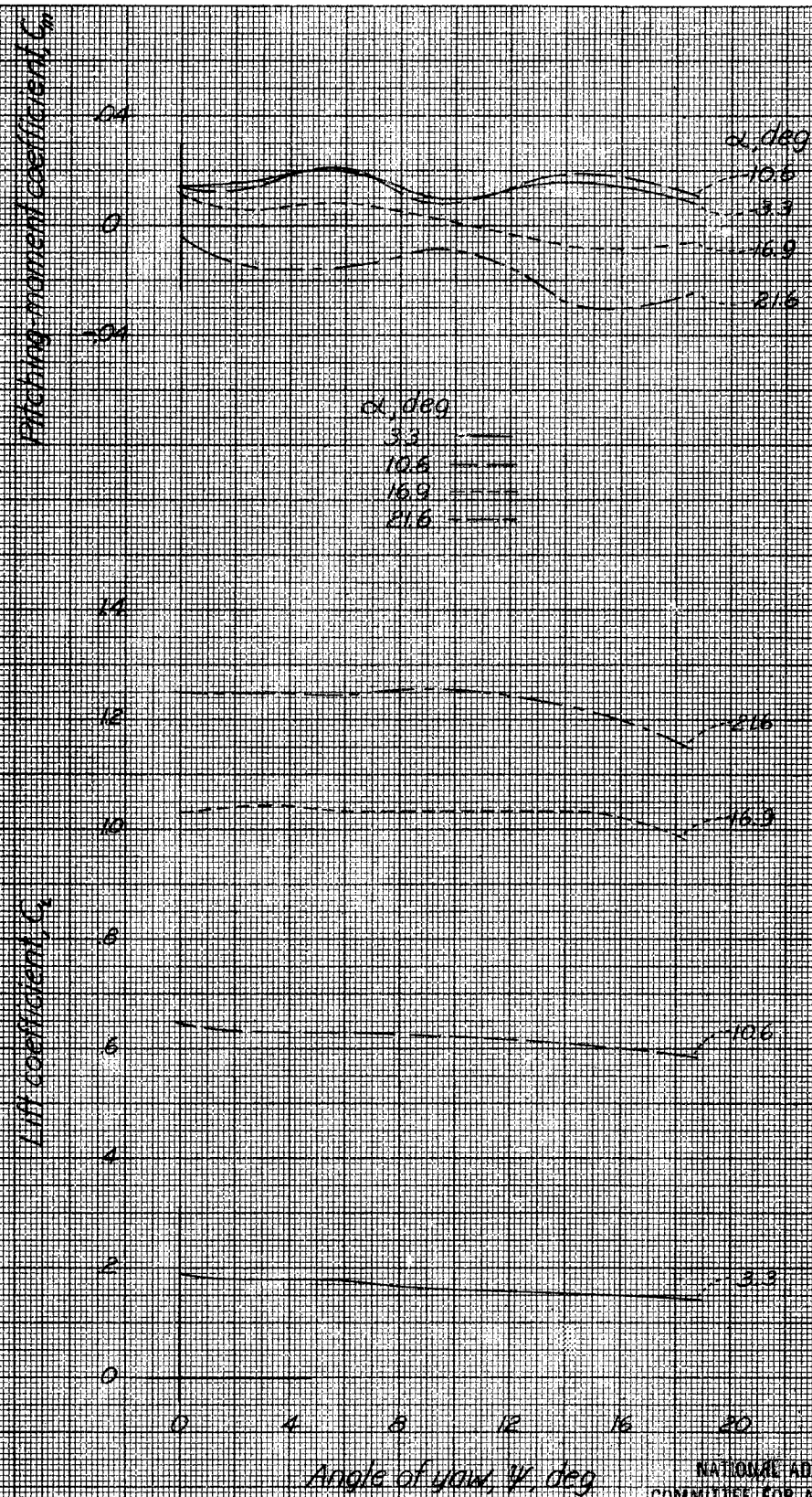
Figure 37.- Variation of lift coefficient and pitching-moment coefficient with angle of yaw. δ_a, 0°; δ_r, 0°; large-span slats installed.
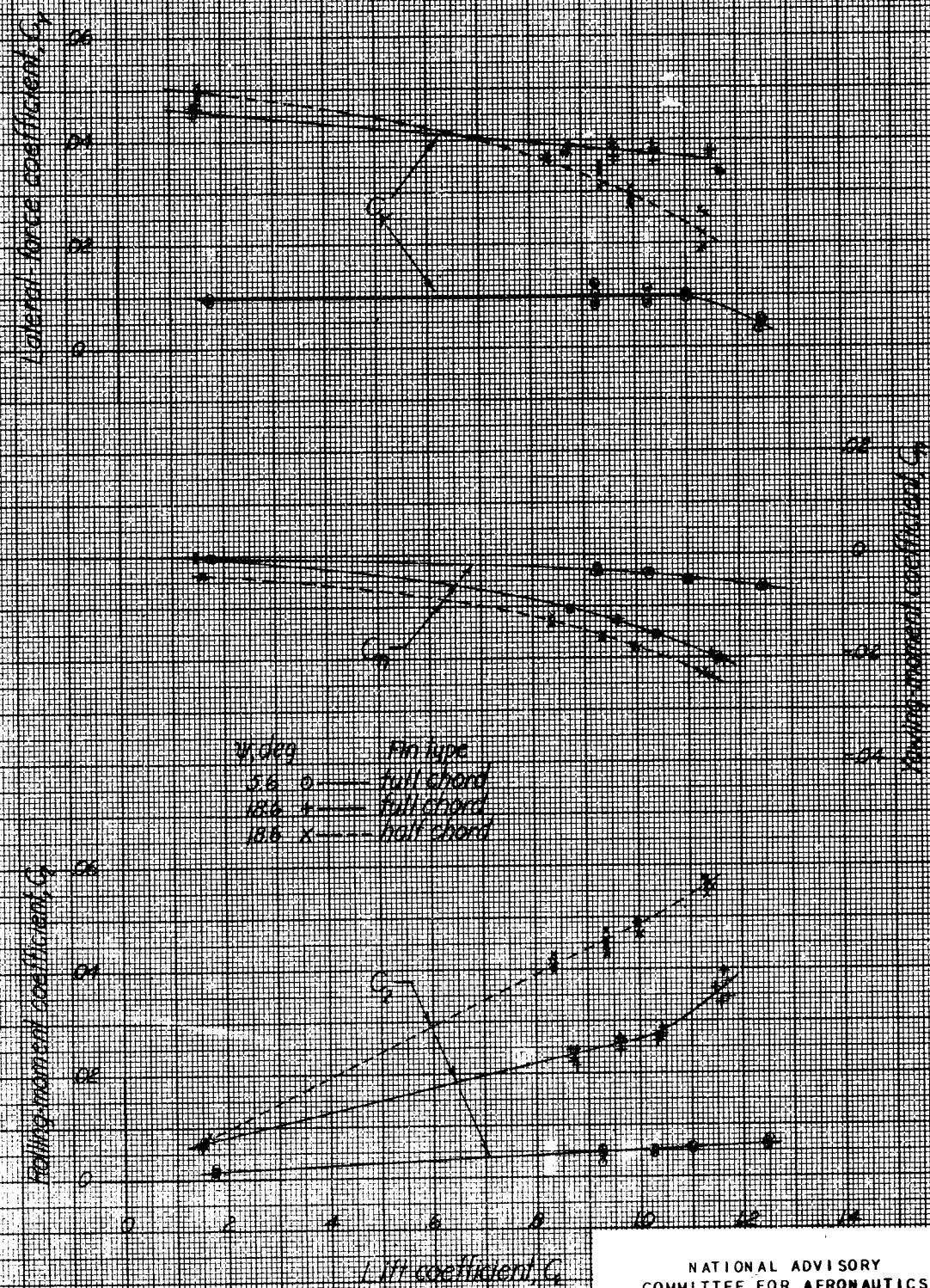
Figure 38.- Effect of fins on the variations of C_l, C_n, C_Y with C_L with the airplane yawed. δ_a, 0°; δ_r, 0°; large-span slots installed.
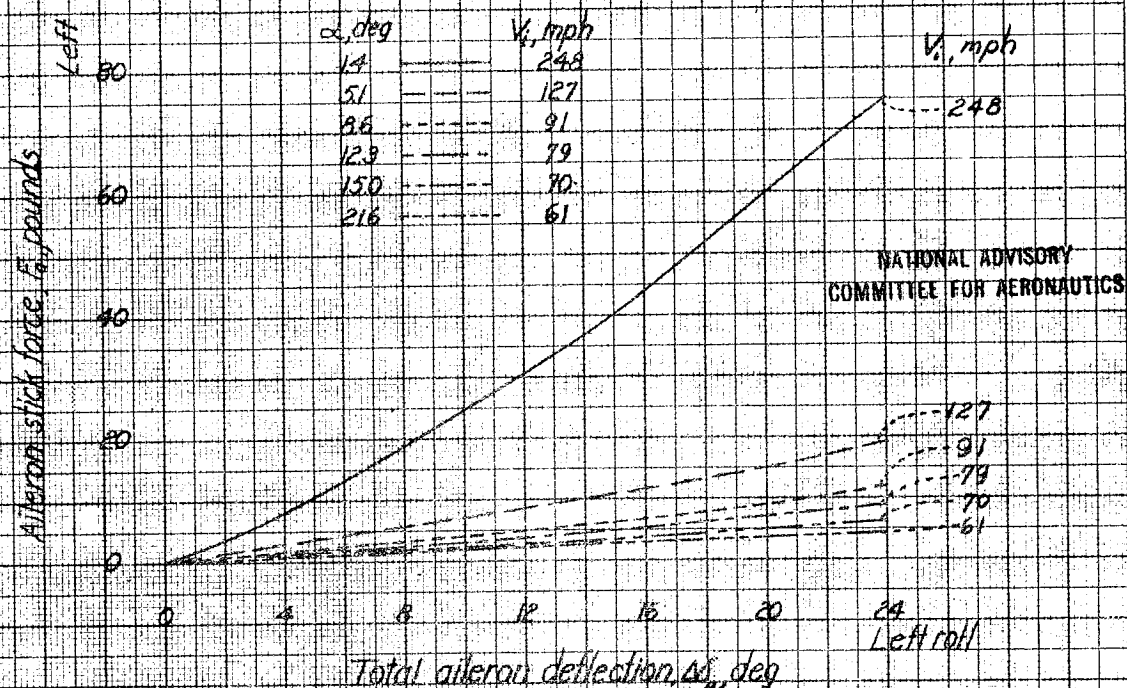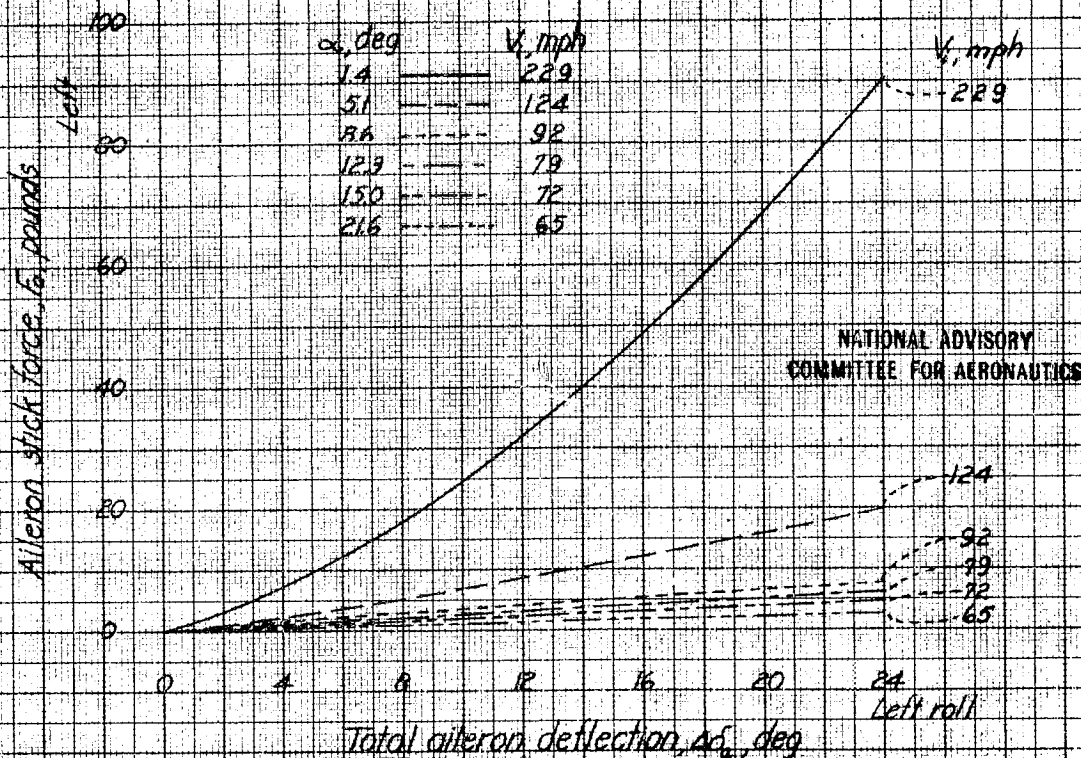
Figure 39.-The aerodynamic characteristics of the airplane yawed 14.5° Controls neutral; large-span slots installed.

(a) Large-span slats installed.
Figure 40.—Effect of aileron deflection on the aerodynamic characteristics of the airplane. ψ, 0°; δr, 0°.
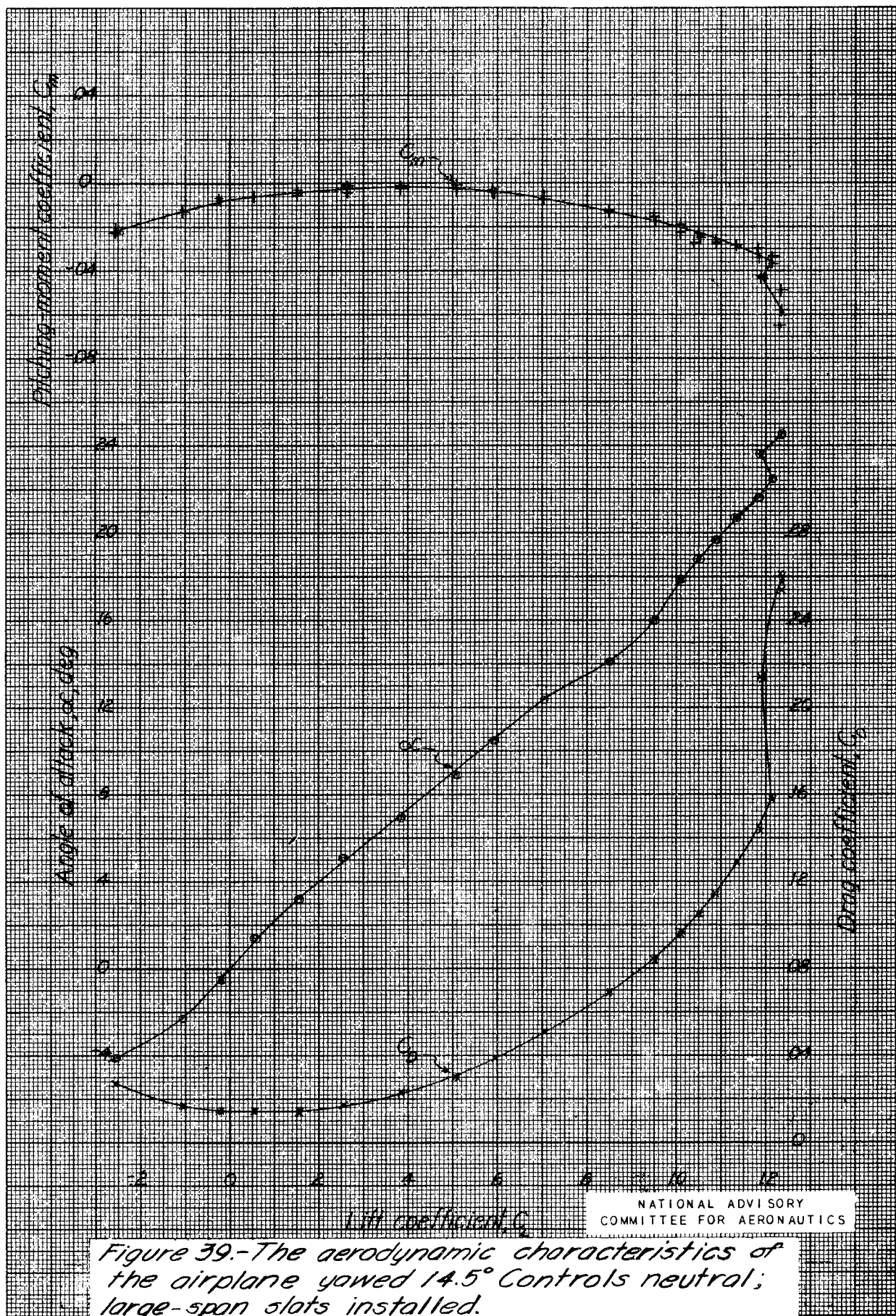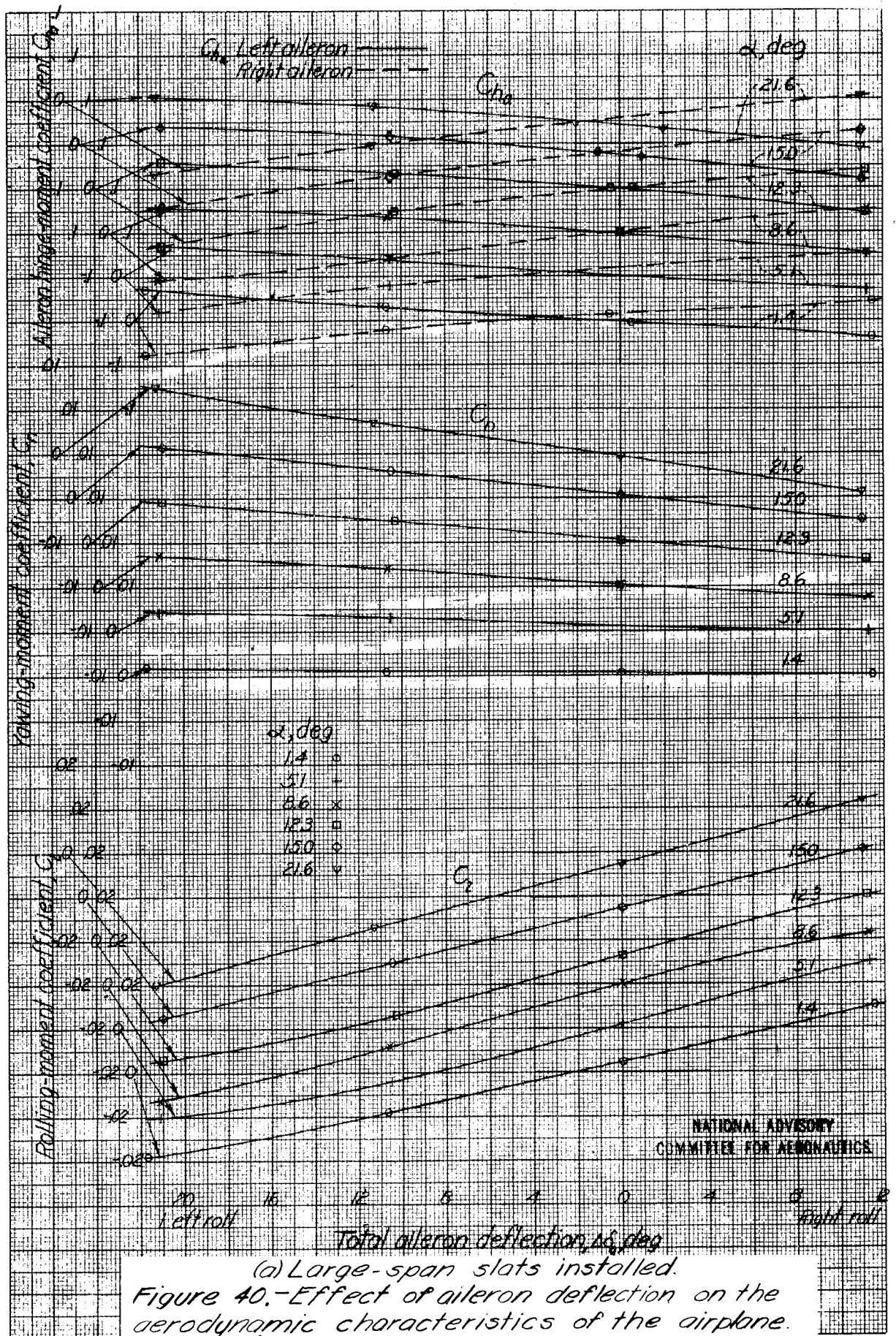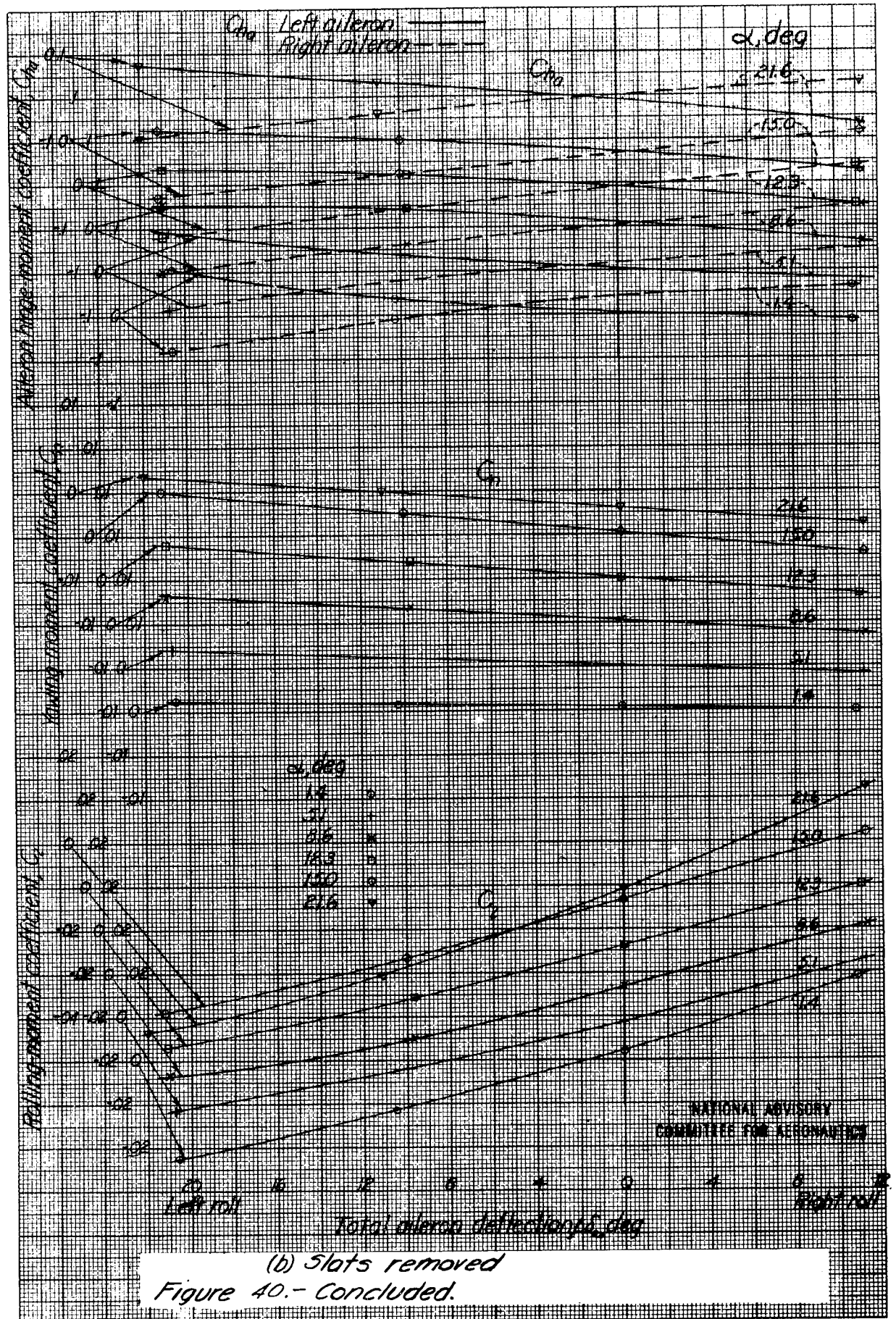
(b) Slats removed

Figure 40.— Concluded.

(a) Large-span slats installed

Figure 41.-Variation of helix angle with aileron
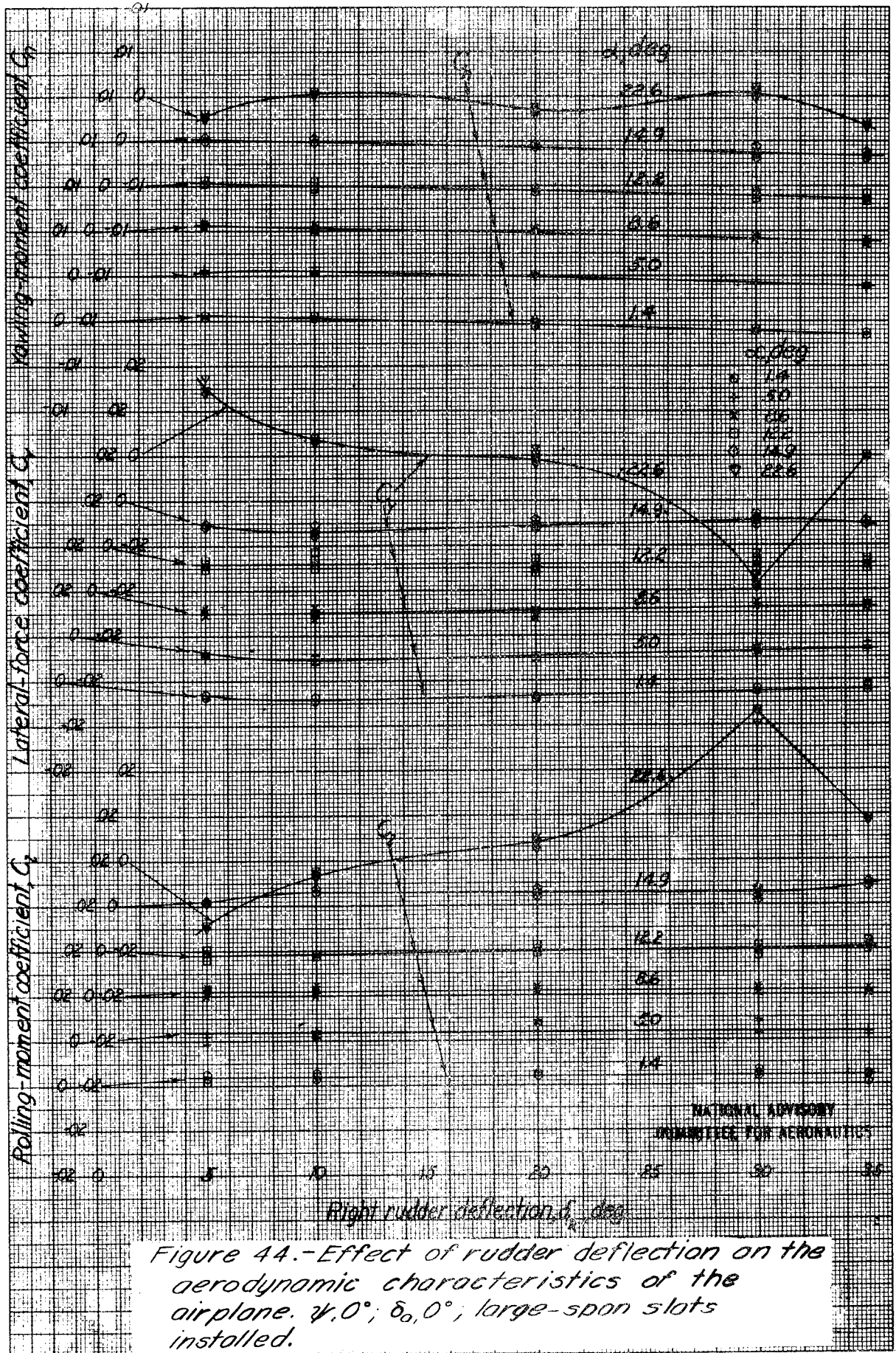deflection at different sea level indicated
airspeeds.

(b) Slots removed

Figure 41.- Concluded.
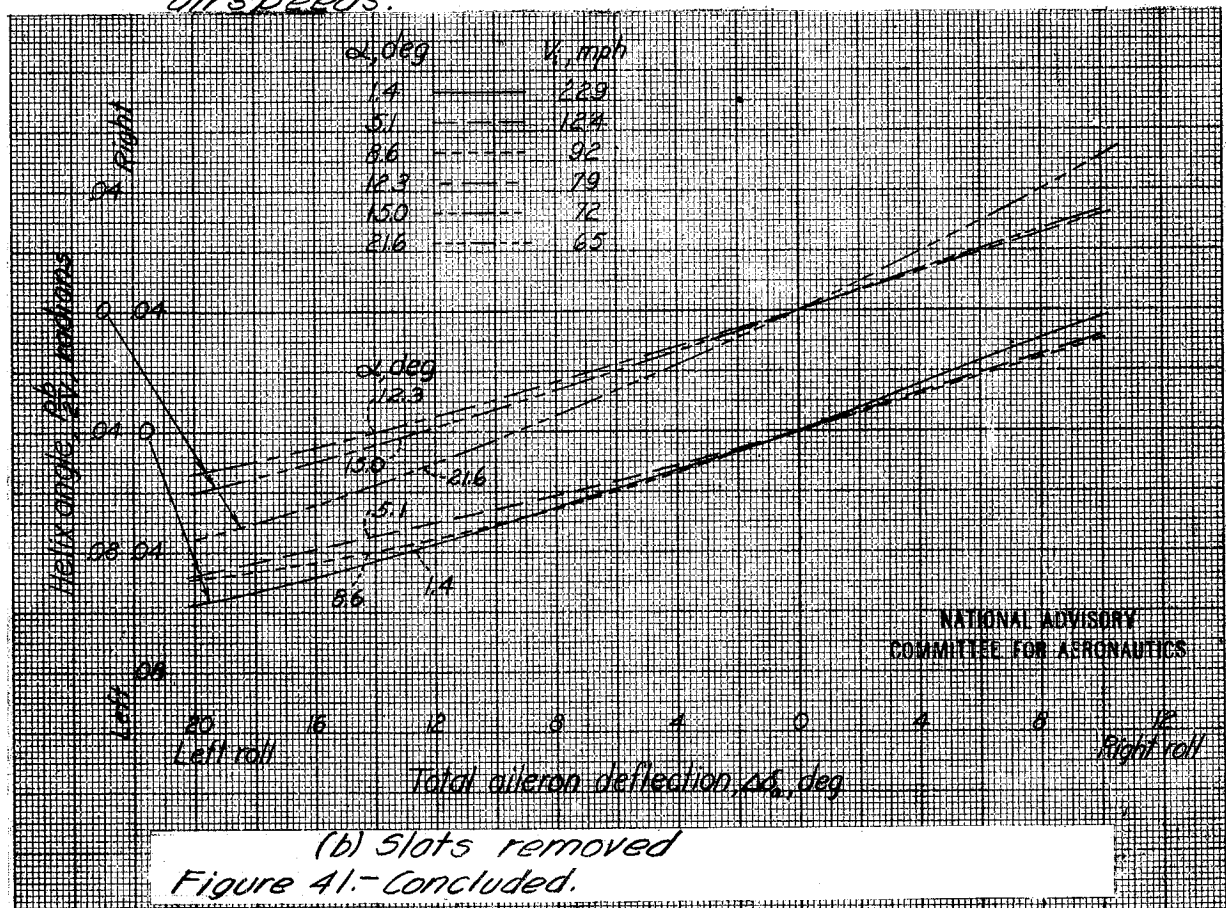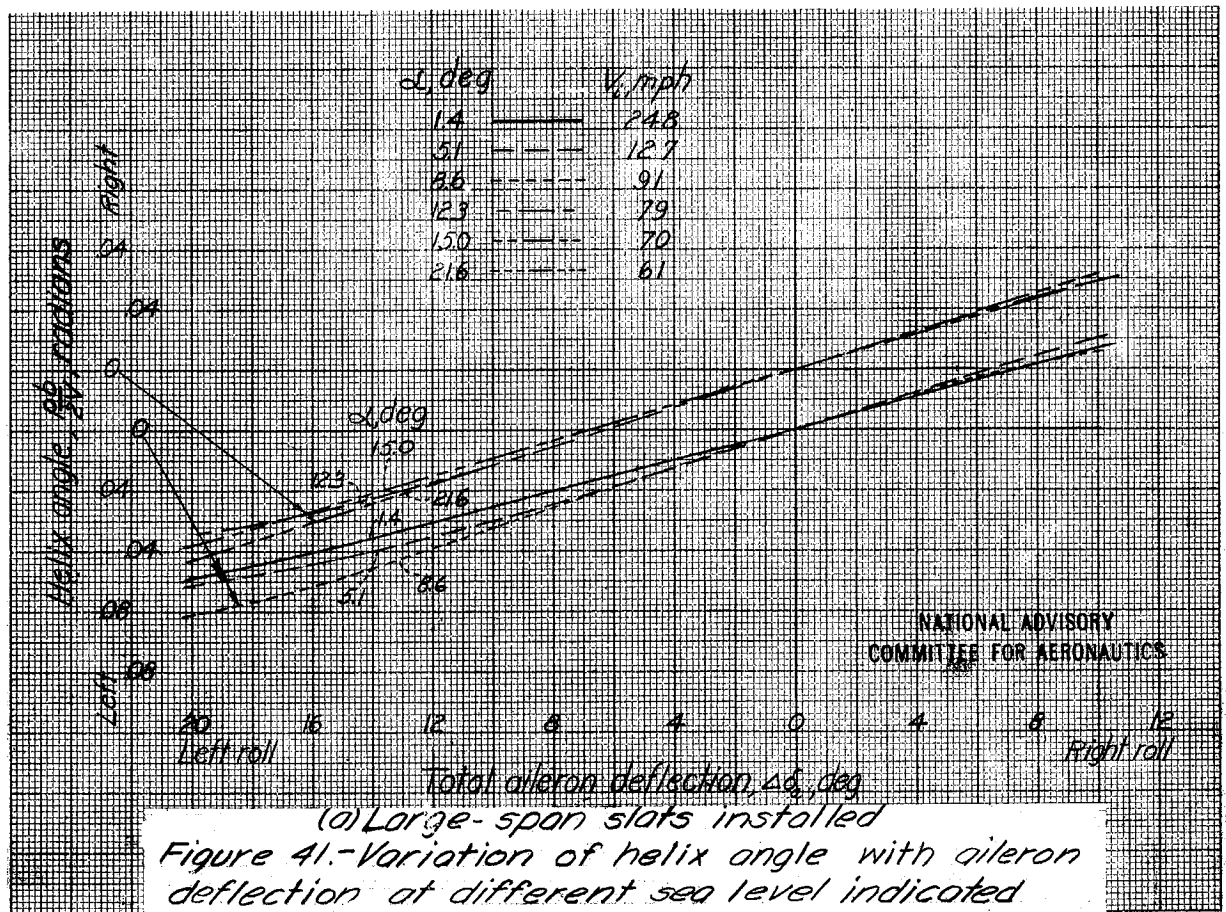
(a) Large-span slats installed

Figure 42.-Variation of aileron stick force with aileron deflection at different sea-level indicated air speed.

(b) Slats removed

Figure 42.-Concluded.

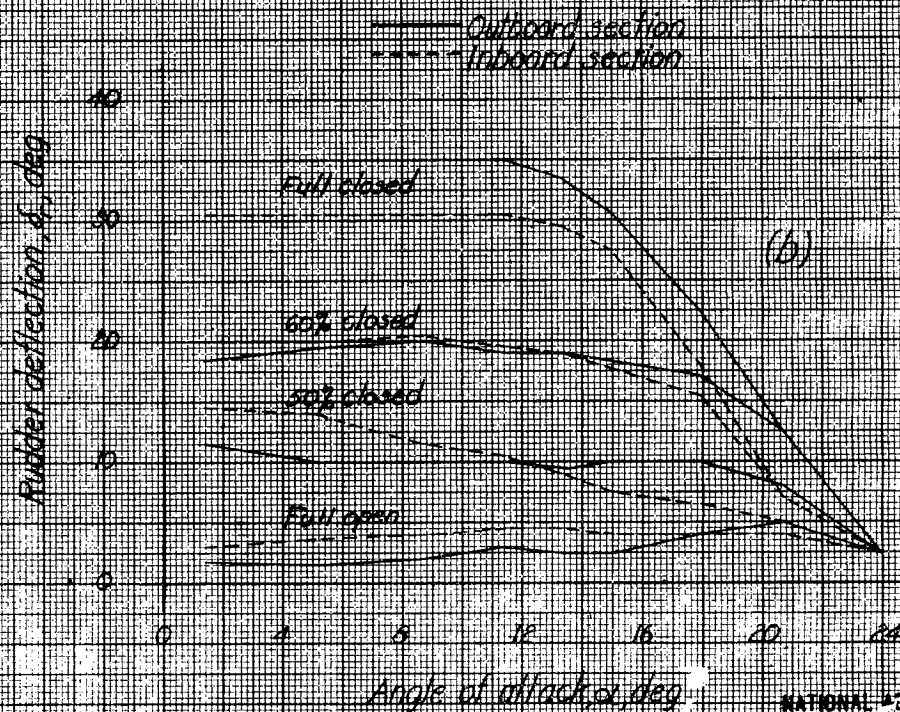Figure 43.- Variation of stick angle with aileron deflection for the MX-334 airplane.

Figure 44.- Effect of rudder deflection on the
aerodynamic characteristics of the
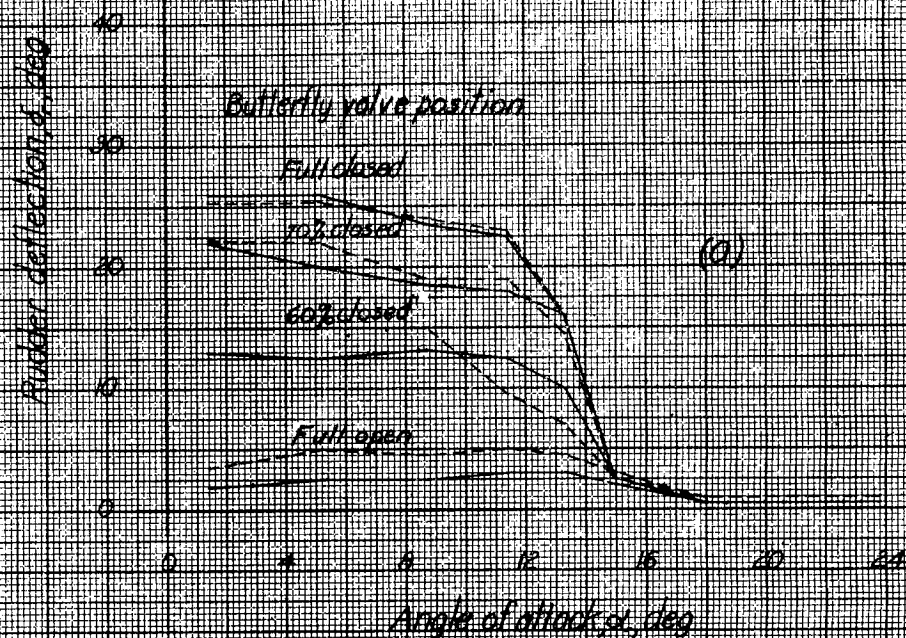airplane. $\psi, 0°; \delta_o, 0°;$ large-span slots
installed.
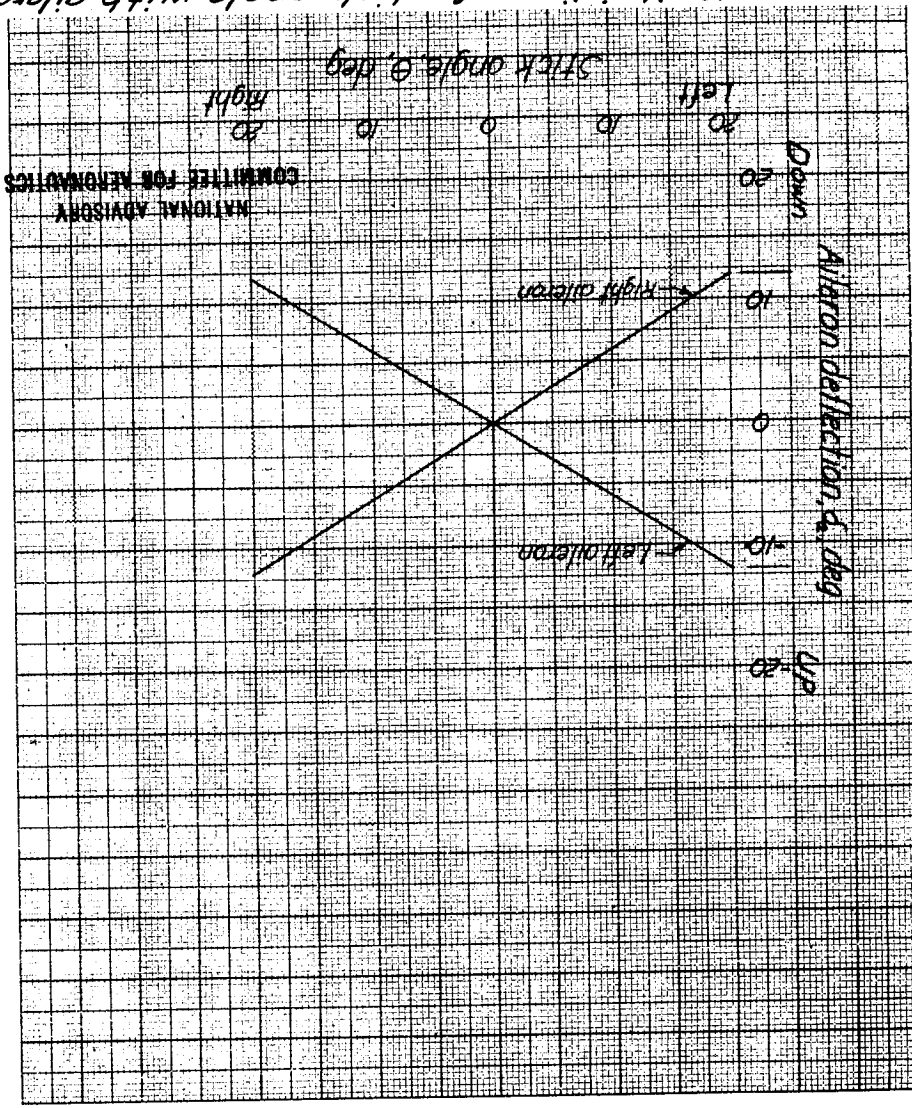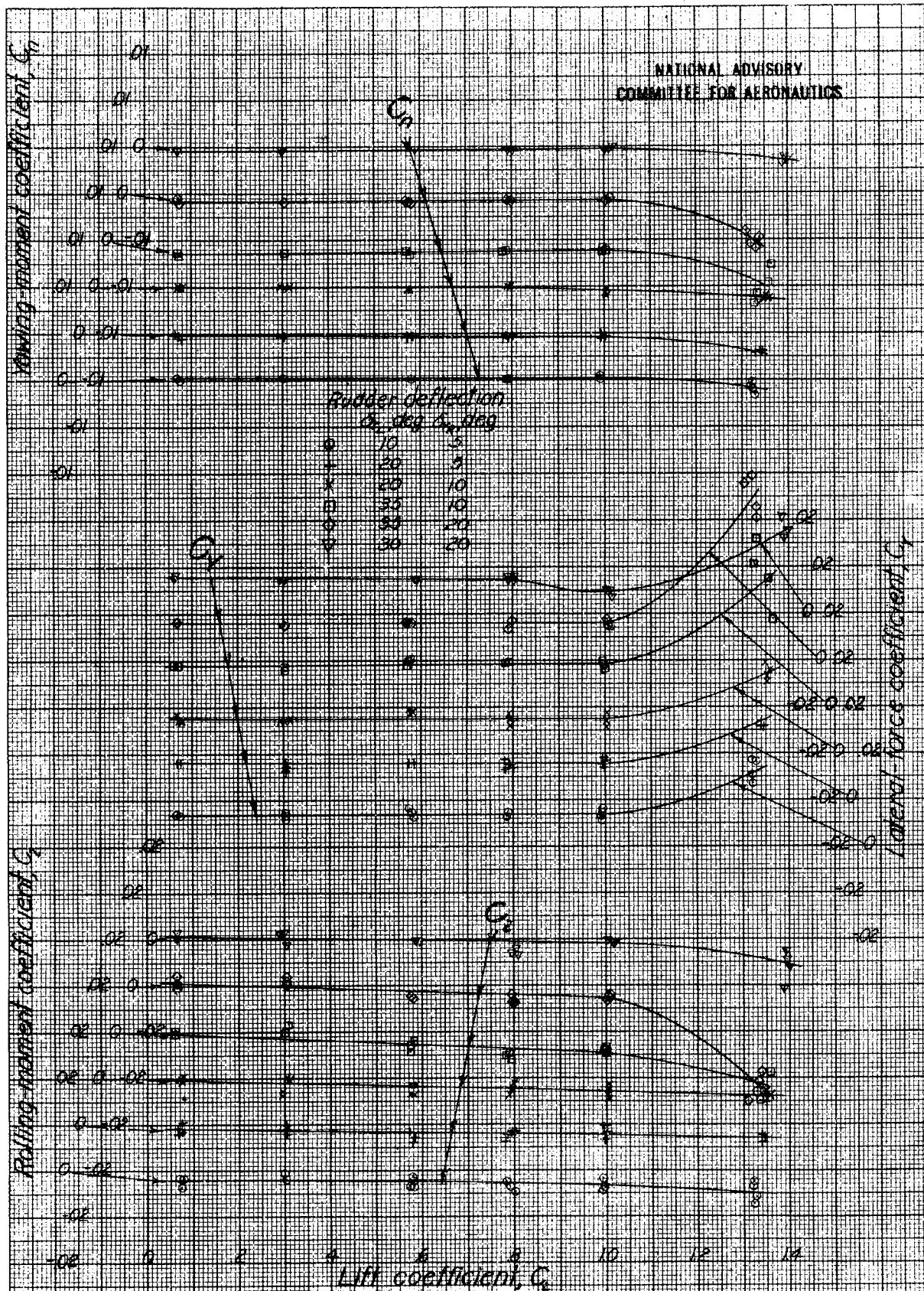
Figure 45.—Effect of rudder and brake deflection on the aerodynamic characteristics of the airplane. ψ, 0°; δ_a, 0°; large-span slots installed.

(a) Original inlet (b) Modified inlet

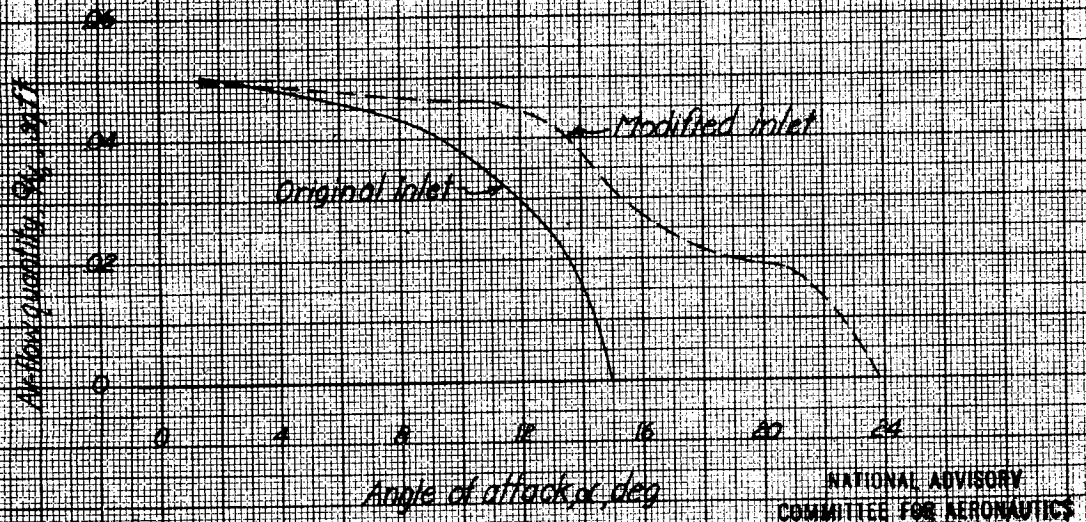Figure 46.- Effect of inlet design on rudder deflection for four butterfly valve positions.

Figure 47.- Effect of inlet design on the air flow quantity. δ_r, 0°.
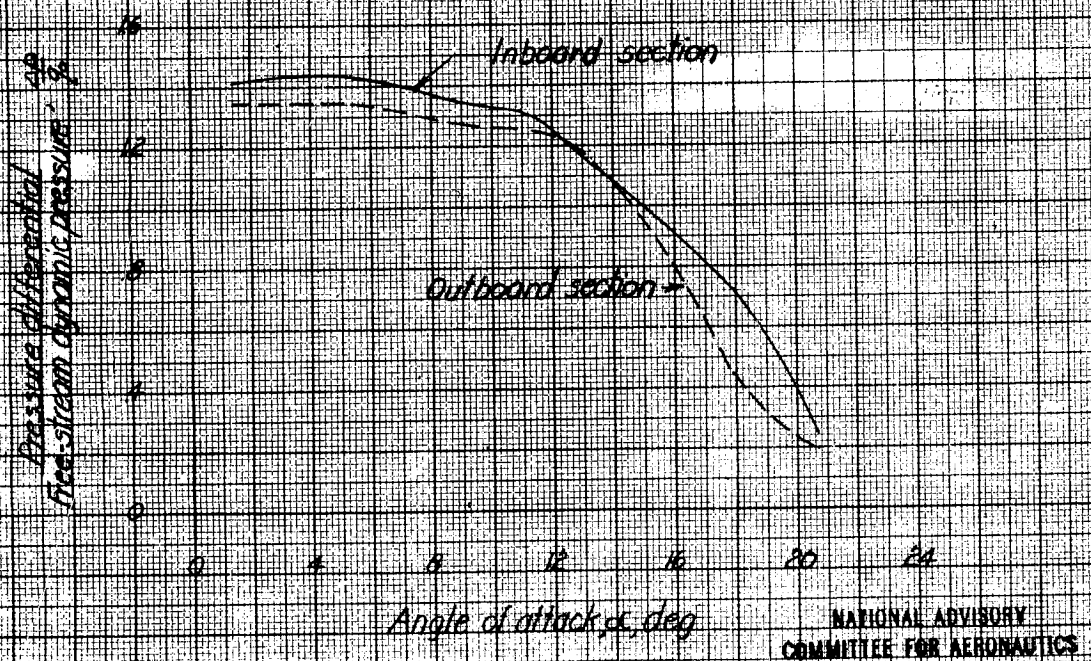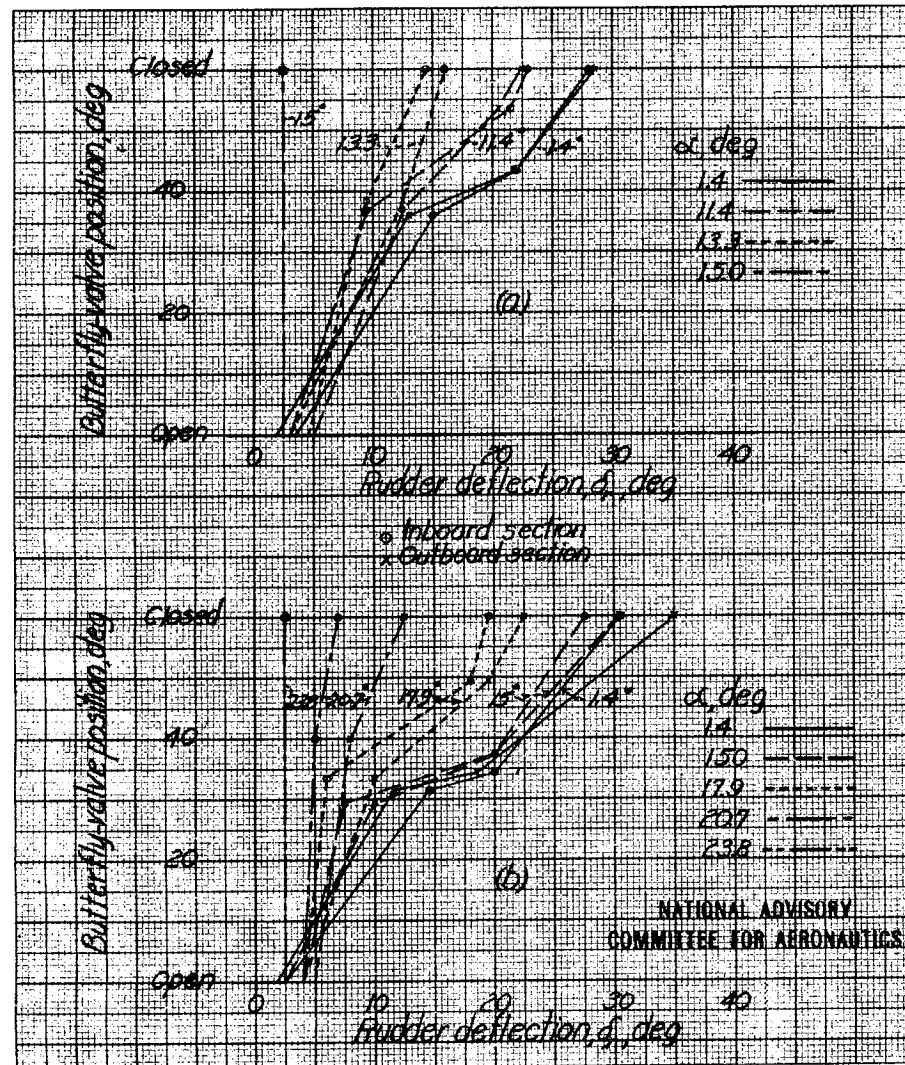

Figure 48.- Variation of bellows pressure with angle of attack. Butterfly valve closed; modified inlet installed.

(a) Original inlet   (b) Modified inlet

Figure 49.- Variation of butterfly-valve position with rudder deflection at several angles of attack.